UNCLASSIFIED

AD NUMBER
AD858093
LIMITATION CHANGES
TO: **Approved for public release; distribution is unlimited. Document partially illegible.**
FROM: **Distribution authorized to U.S. Gov't. agencies only; Administrative/Operational Use; 22 AUG 1969. Other requests shall be referred to Department of Defense, Attn: Public Affairs Office, Washington, DC 20301. Document partially illegible.**
AUTHORITY
DoD per DTIC form 55

THIS PAGE IS UNCLASSIFIED

AD-858093

REV LTR

THE BOEING COMPANY

CODE IDENT. NO. 81205

NUMBER D2-113222-3

TITLE: INCIPIENT FAILURE DETECTION: INCIPIENT FAILURE DETECTION IN BALL BEARINGS

ORIGINAL RELEASE DATE _____. FOR THE RELEASE DATE OF SUBSEQUENT REVISIONS, SEE THE REVISIONS SHEET. FOR LIMITATIONS IMPOSED ON THE DISTRIBUTION AND USE OF INFORMATION CONTAINED IN THIS DOCUMENT, SEE THE LIMITATIONS SHEET.

MODEL All ASG

ISSUE NO. _____

ISSUE TO _____

PREPARED UNDER:

☐ CONTRACT NO.

☒ IR&D

☐ OTHER

A

Edited by C. R. James 8/22/69
C. R. James

PREPARED BY H. L. Balderston
H. L. Balderston

SUPERVISED BY R. C. Schneider
R. C. Schneider

APPROVED BY H. F. Eppenstein
H. F. Eppenstein

APPROVED BY R. C. Schneider 8/24/69
R. C. Schneider

Distribution limited to U.S. Gov't. agencies only; Other requests for this document must be referred to Boeing, Seattle, Wash. 98124

SHEET 1

U3 4802 1430 REV. 9/68

ACTIVE SHEET RECORD

SHEET NUMBER	REV LTR	ADDED SHEETS				SHEET NUMBER	REV LTR	ADDED SHEETS			
		SHEET NUMBER	REV LTR	SHEET NUMBER	REV LTR			SHEET NUMBER	REV LTR	SHEET NUMBER	REV LTR
1						46					
2						47					
3						48					
4						49					
5						50					
6						51					
7						52					
8						53					
9						54					
10						55					
11						56					
12						57					
13						58					
14						59					
15						60					
16						61					
17						62					
18						63					
19						64					
20						65					
21						66					
22						67					
23						68					
24						69					
25						70					
26						71					
27						72					
28						73					
29						74					
30						75					
31						76					
32						77					
33						78					
34						79					
35						80					
36						81					
37						82					
38						83					
39						84					
40						85					
41						86					
42						87					
43						88					
44						89					
45						90					

ACTIVE SHEET RECORD

SHEET NUMBER	REV LTR	ADDED SHEETS				SHEET NUMBER	REV LTR	ADDED SHEETS			
		SHEET NUMBER	REV LTR	SHEET NUMBER	REV LTR			SHEET NUMBER	REV LTR	SHEET NUMBER	REV LTR
91											
92											
93											
94											
95											
96											
97											
98											
99											
100											
101											
102											
103											
104											
105											
106											
107											
108											
109											
110											
111											
112											
113											
114											
115											
116											
117											
118											

REVISIONS			
LTR	DESCRIPTION	DATE	APPROVAL

U3 4802 1432 ORIG. 4/65

LIMITATIONS

All U. S. Government agencies may obtain copies directly from DDC. [redacted] requested to route all other requests to Boeing for approval. Seattle, Wash. 98124

This document is controlled by Reliability, System Safety and Value Engineering

All revisions to this document shall be approved by the above noted organization prior to release.

USE FOR TYPEWRITTEN MATERIAL ONLY

ABSTRACT AND KEY WORDS

This document reports the results of an investigation of incipient failure detection in ball bearings by means of acoustic monitoring techniques. The change of acoustic emanation strength with bearing condition was studied to determine if changes within the frequency spectrum monitored would manifest the onset of a bearing failure. This investigation showed that the acoustic energy emitted from bearings is very sensitive to bearing condition and provides a clear indication of the onset of bearing failure.

INCIPIENT FAILURE
BEARING FAILURE
FAILURE DETECTION
ULTRASONIC MONITORING
BEARING MAINTENANCE
BEARING INSPECTION

TABLE OF CONTENTS

		Page
	ILLUSTRATIONS	7-33
1.0	INTRODUCTION	34
	1.1 Objective	34
	1.2 Scope	34
	1.3 Method	34
2.0	SUMMARY	35
3.0	CONCLUSIONS AND RECOMMENDATIONS	35
4.0	DISCUSSION	36
	4.1 Techniques Employed	36
	4.1.1 Test Description	36
	4.1.2 Instrumentation	37
	4.1.3 Data Analysis	38
	4.2 Rotational Frequencies	40
	4.3 Resonant Frequencies	42
	4.4 Acoustic Emission	43
5.0	DEFINITIONS	47
6.0	REFERENCES	48
7.0	BIBLIOGRAPHY	49
8.0	APPENDICES	50
	8.1 Rotational Frequency Calculations	51
	8.2 Resonant Frequency Calculations	55
	8.3 Raw Data	60

USE FOR TYPEWRITTEN MATERIAL ONLY

U3 4802 1434 REV. 8-65

ILLUSTRATIONS

The following several pages are illustrations which pertain to the textual discussion in Section 4.0. There are twenty-six such illustrations. These have been gathered here for two reasons. Firstly, their logical position within the text itself would be awkward for the reader, since continuity would suffer. Secondly, their inclusion in the Appendices would be equally confusing, because the Appendices contain more than fifty additional pages of plotted raw data.

Accordingly, we hope for the readers' indulgence in referring forward to this area when any of the illustrations gathered here are mentioned in Section 4.0. If reader reaction is adverse, however, we will rearrange these pages at the first revision to the document.

USE FOR TYPEWRITTEN MATERIAL ONLY

U3 4802 1434 REV. 8-65

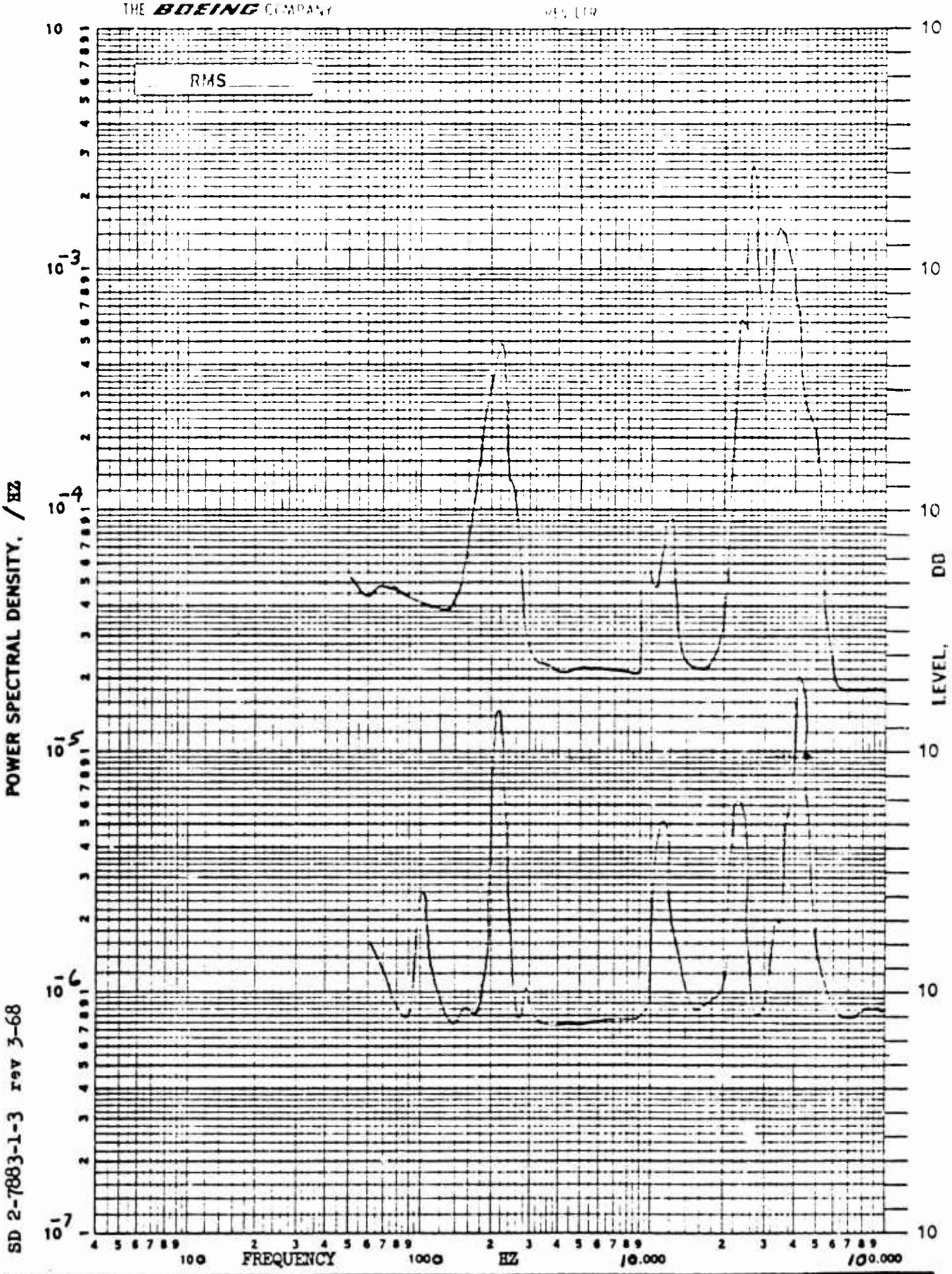

CALC.		D	RANGE OF ENERGY DIRECT BEARINGS 1,2,3,5 - NEW, LUBED 5000 RPM	Figure 1
CHECK		A		D2-113029-3
APP'D		T		
APP'D		E		PAGE: 3

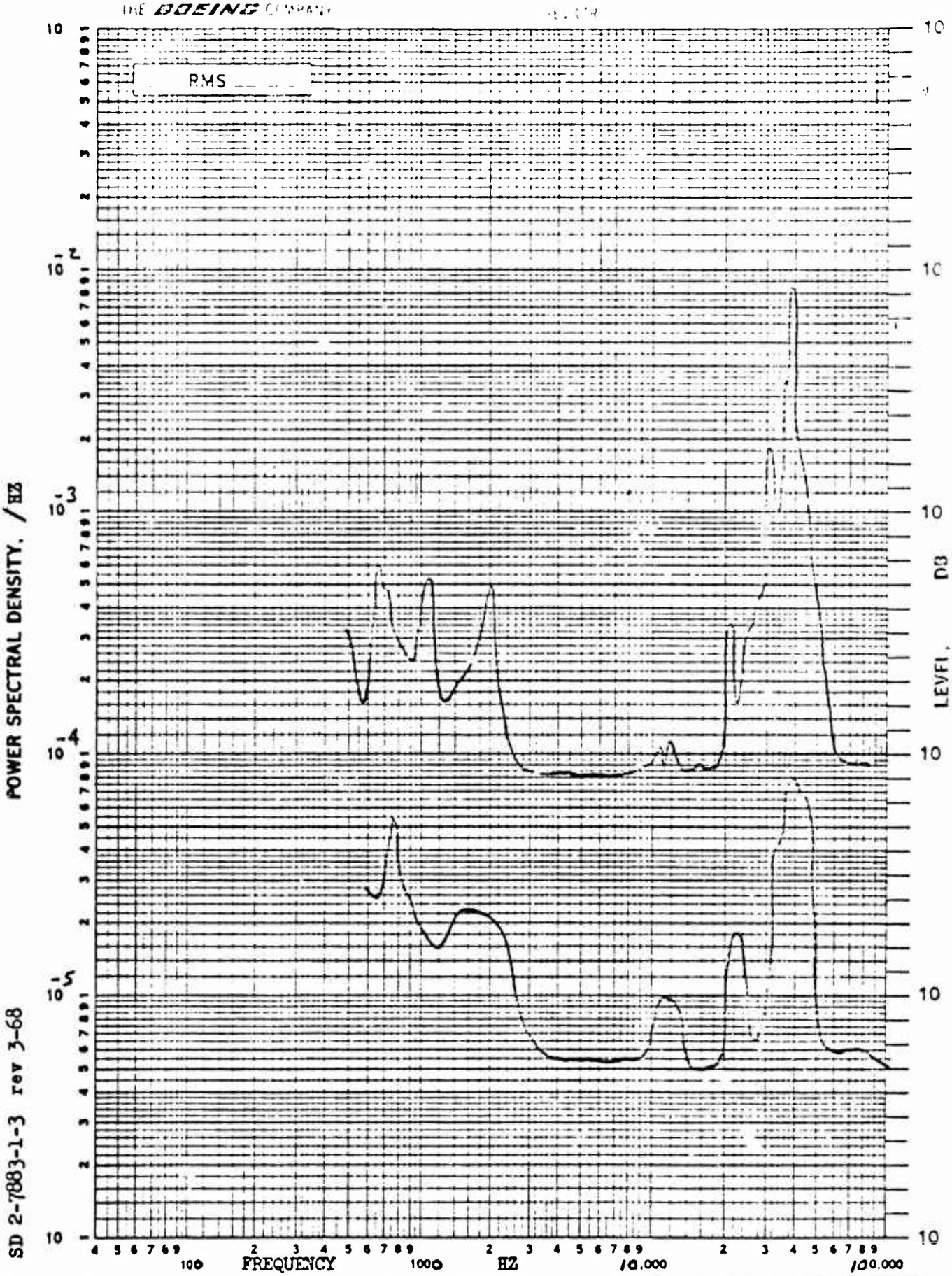

SD 2-7883-1-3 rev 3-68

CALC.		D	RANGE OF ENERGY DIRECT BEARINGS 1,2,3,5 - NEW, LUBED 10,000 RPM	Figure 2
CHECK		A		D2-113029-3
APP'D		T		
APP'D		E		PAGE: 9

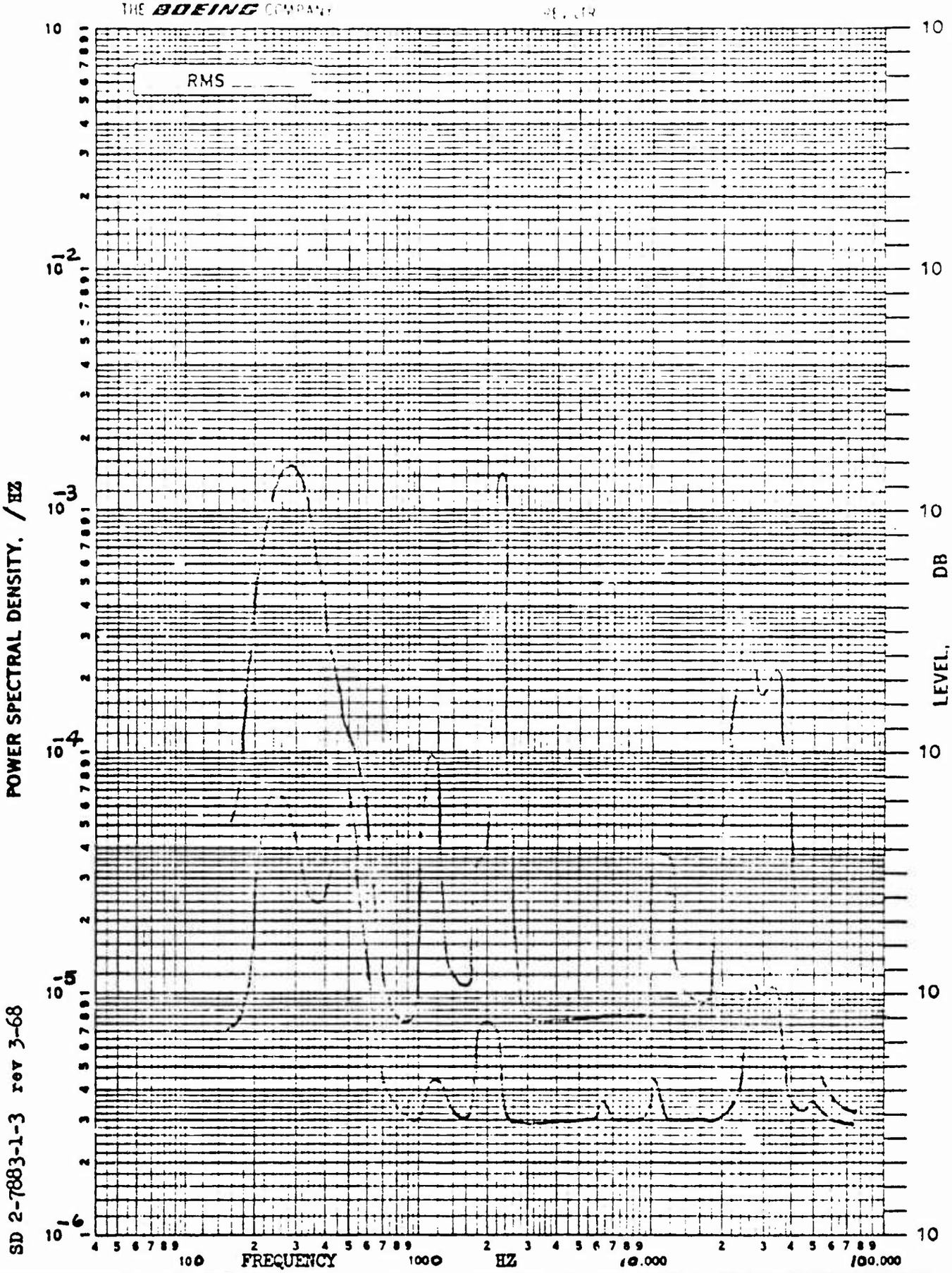

CALC.		D	RANGE OF ENERGY DIRECT	Figure 3
CHECK		A	BEARINGS 4, 6, 7 - NEW LUBED	D2-113039-3
APP'D		T	5000 RPM	
APP'D		E		PAGE: 10

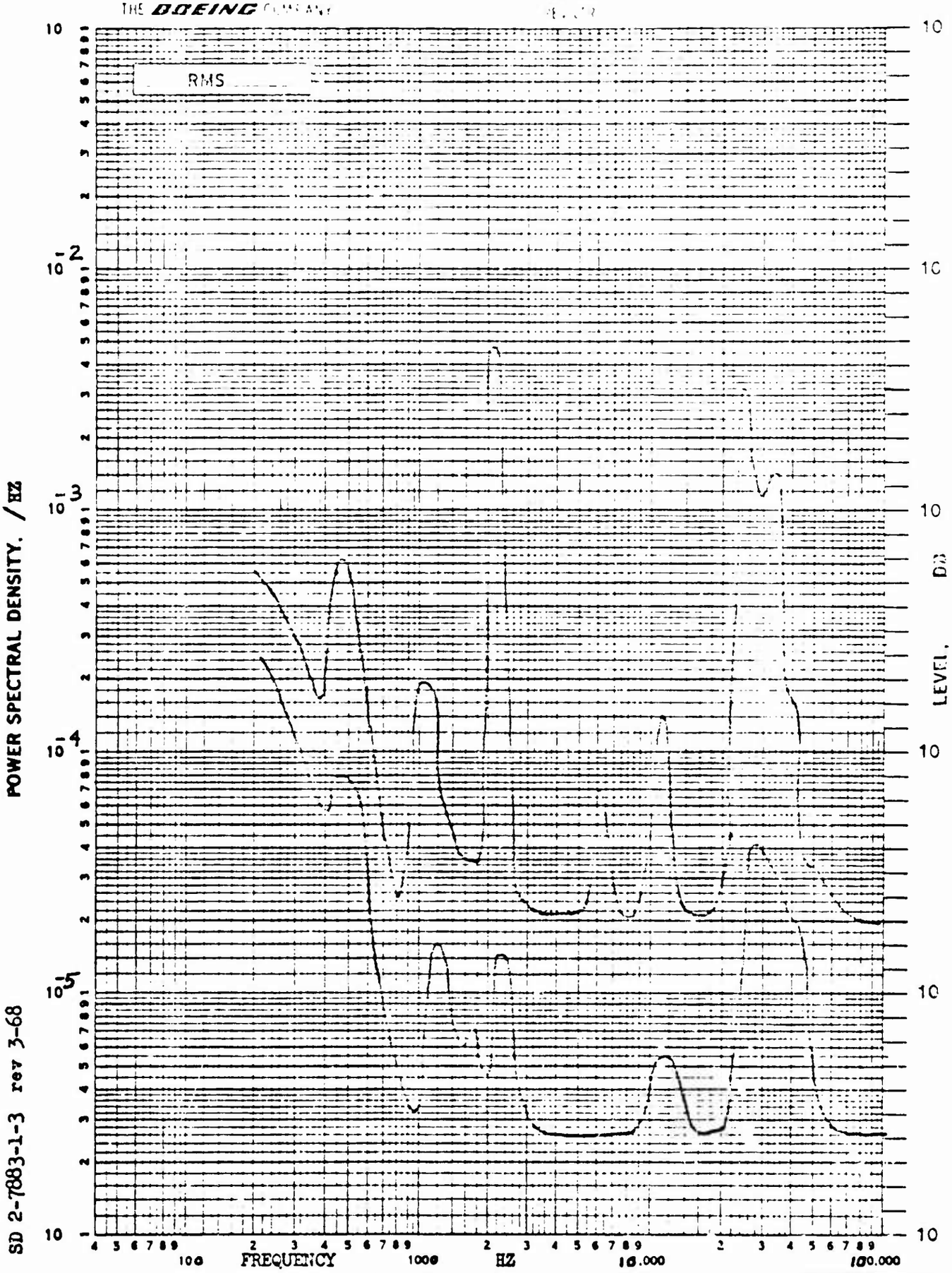

CALC.		D	RANGE OF ENERGY DIRECT BEARINGS 4, 6, 7 – NEW LUBED 10,000 RPM
CHECK		A	
APP'D		T	
APP'D		E	

Figure 4
D2-113020-3
PAGE: 11

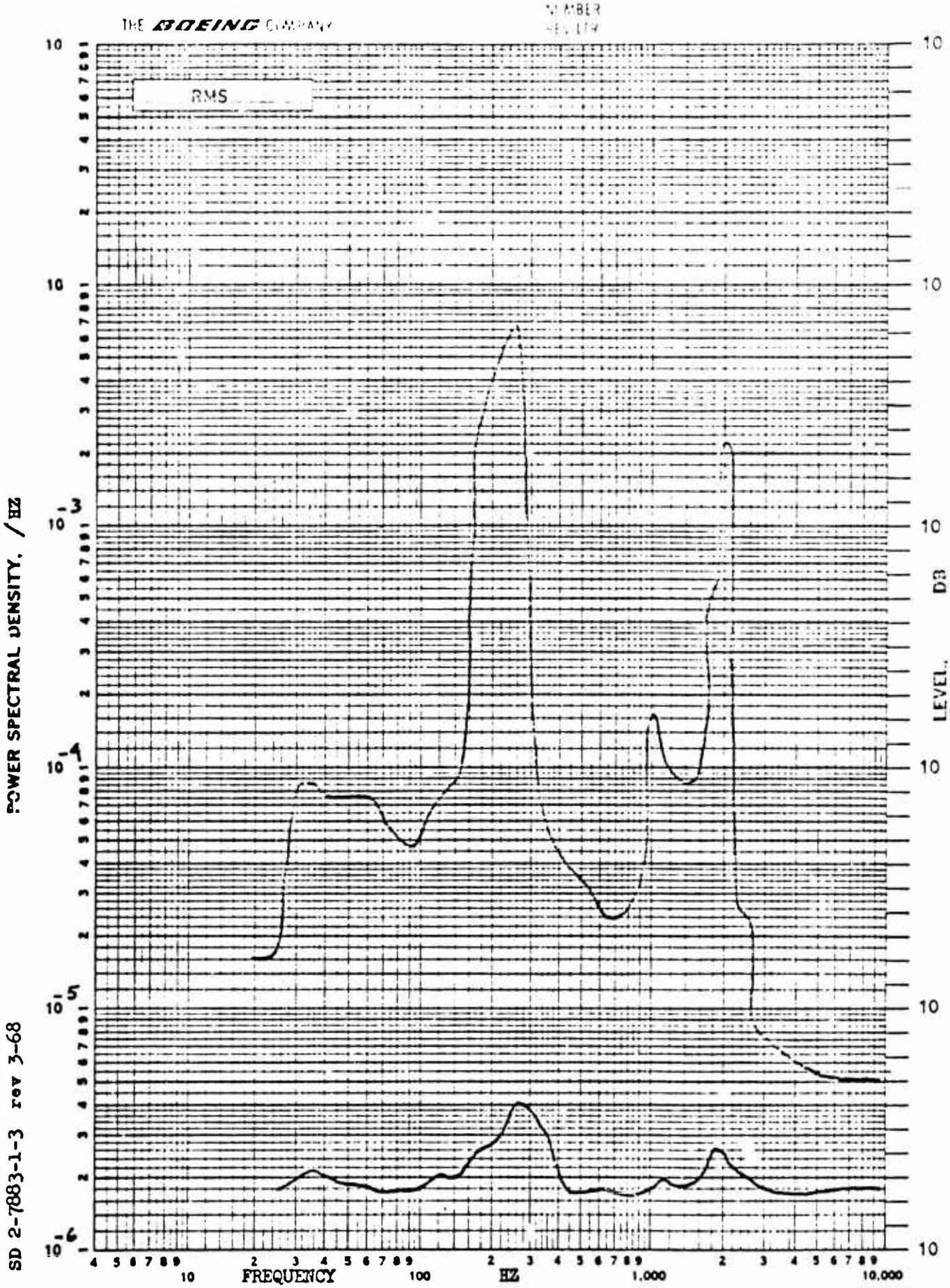

SD 2-7883-1-3 rev 3-68

CALC.		D	RANGE OF ENERGY FM BEARINGS 4,6&7 NEW LUBED 5000 RPM
CHECK		A	
APP'D		T	
APP'D		E	

Figure 5
LP-113029-3
PAGE 12

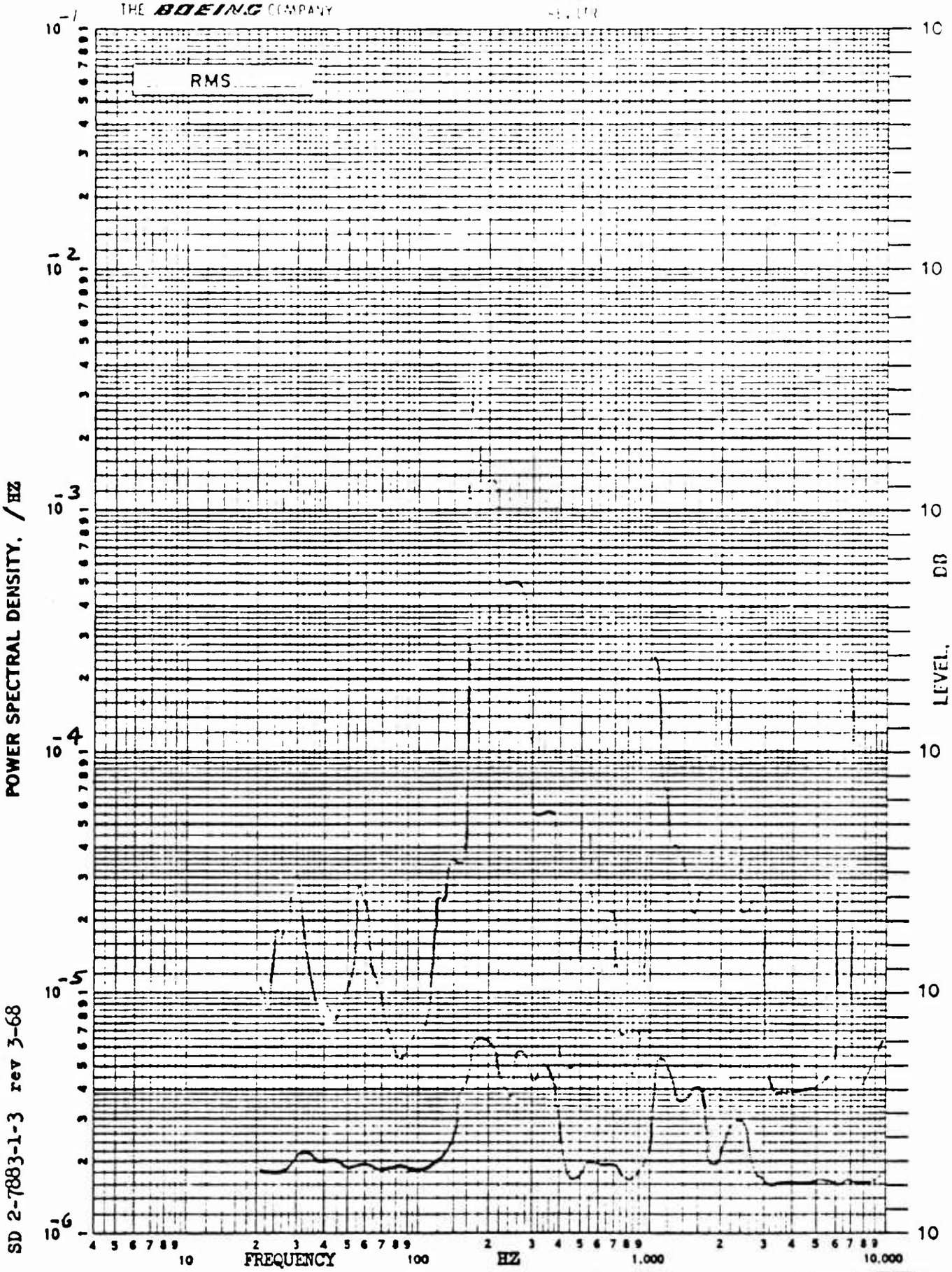

CALC.		D	RANGE OF ENERGY FM	Figure 6
CHECK		A	BEARINGS 4, 6, 7 — NEW LUBED	D2-113029-3
APP'D		T	10,000 RPM	
APP'D		E		PAGE: 13

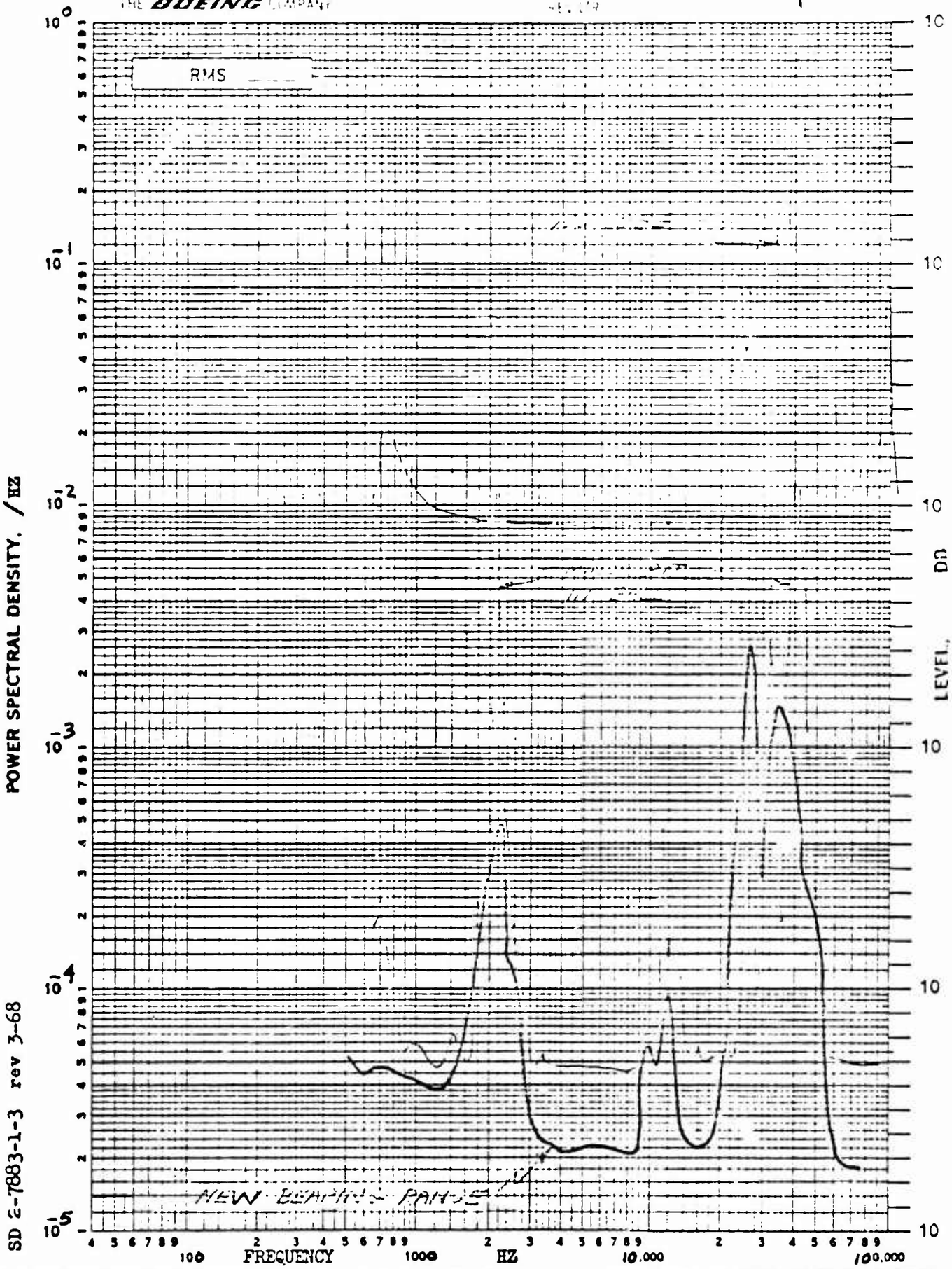

SD 2-7883-1-3 rev 3-68

CALC.		D	BEARING NO. 1 FAULT EFFECTS
CHECK		A	
APP'D		T	5000 RPM
APP'D		E	

Figure 7

D2-113029-3

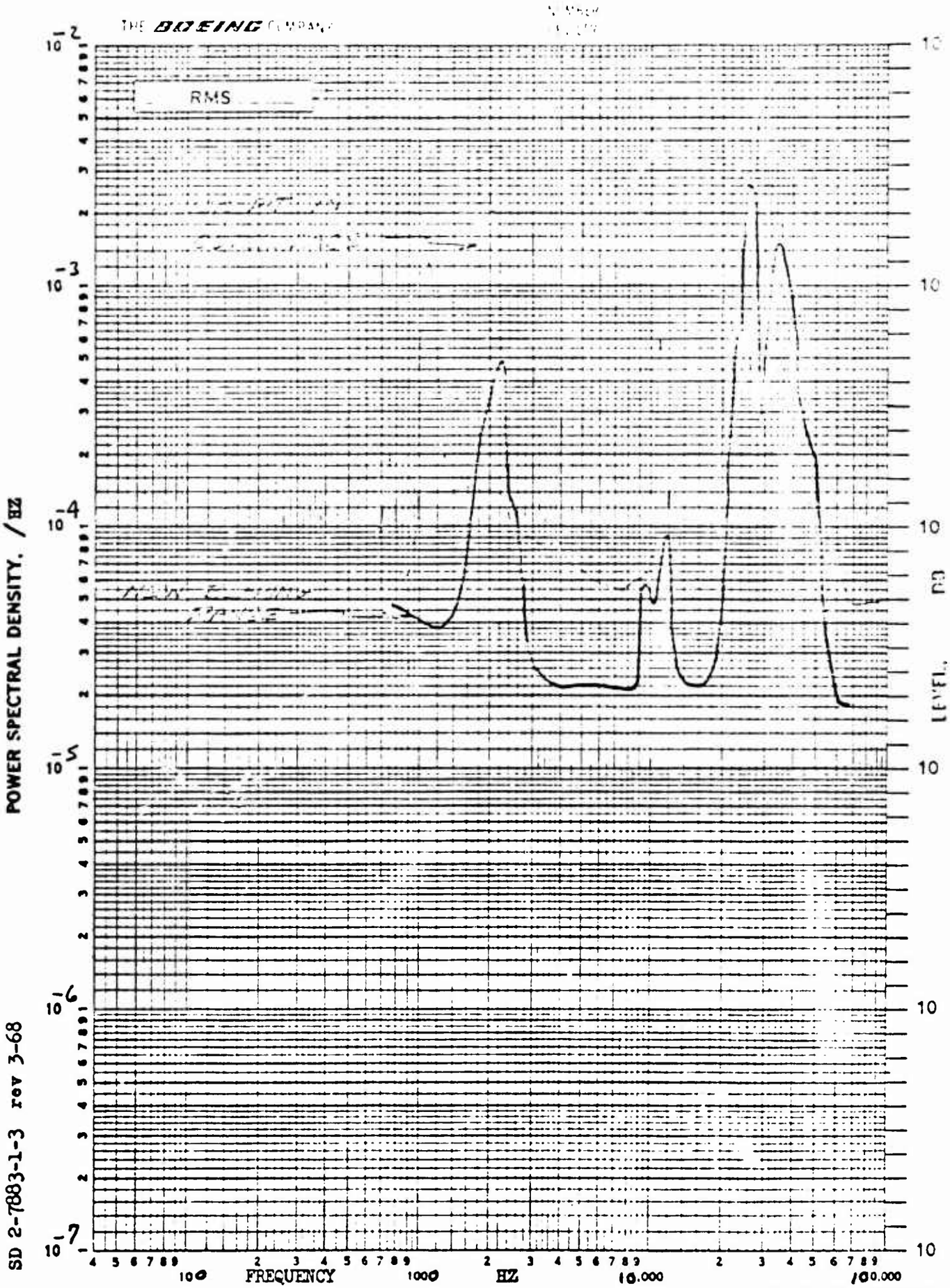

CALC.		D	BEARING NO. 2 FAULT EFFECTS	Figure 3
CHECK		A		D2-113029-3
APP'D		T	5000 RPM	
APP'D		E		PAGE: 15

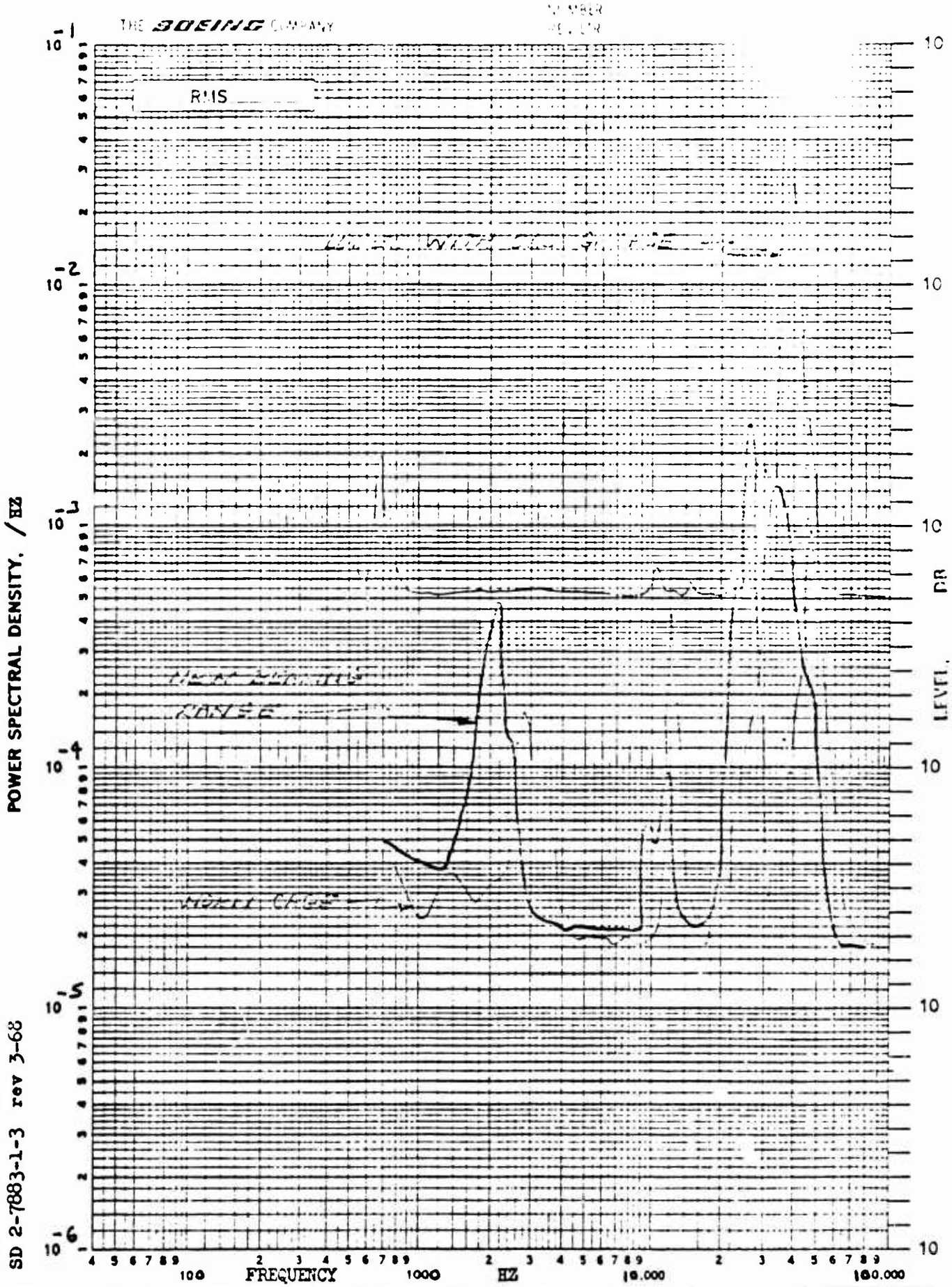

CALC.		D	BEARING NO. 3 FAULT EFFECTS	Figure 9
CHECK		A		D2-113029-3
APP'D		T		
APP'D		E	5000 RPM	PAGE: 16

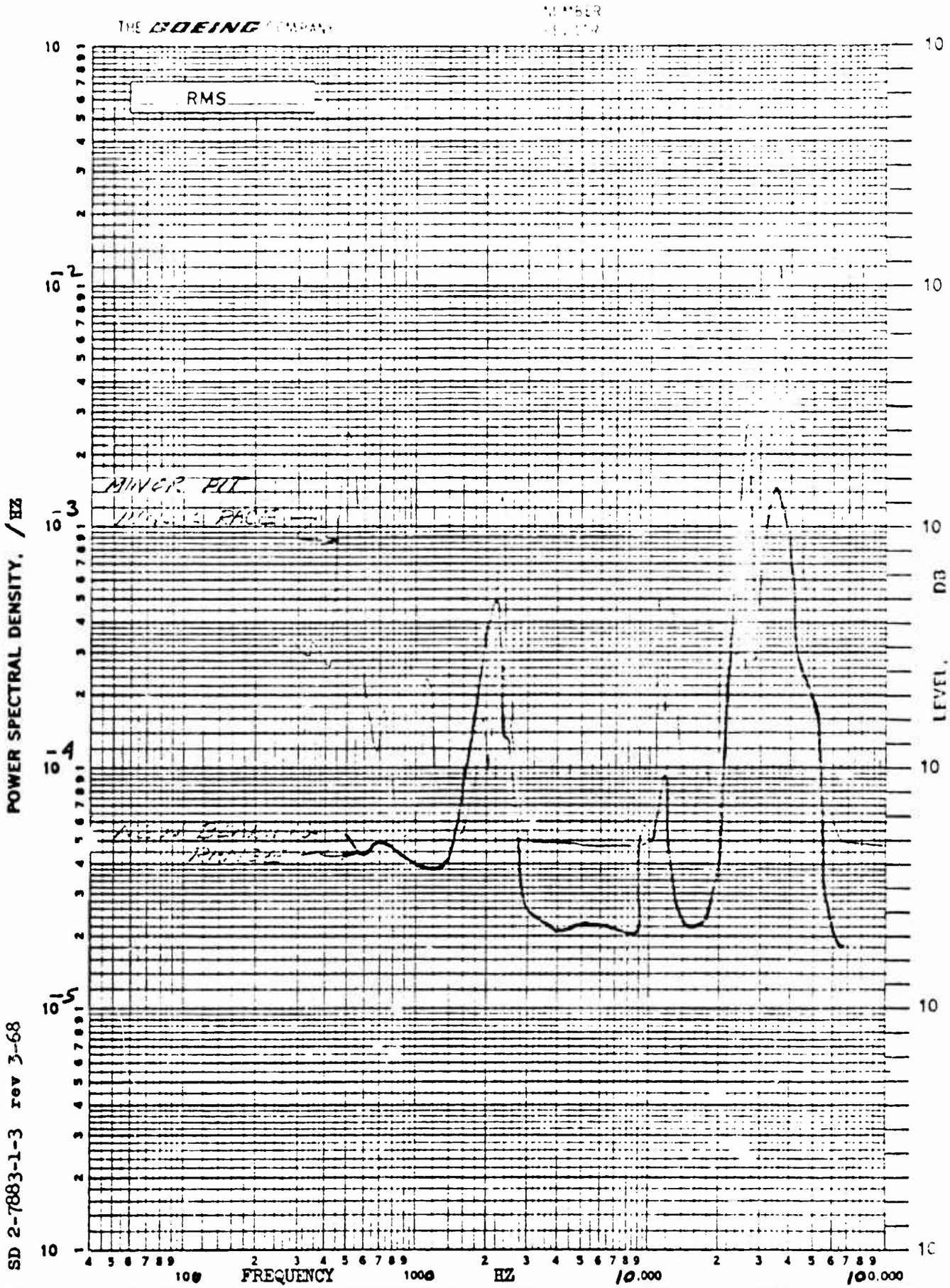

CALC.		D	BEARING NO. 5 FAULT EFFECTS 5000 RPM
CHECK		A	
APP'D		T	
APP'D		E	

Figure 10
D2-113099-3
PAGE: 17

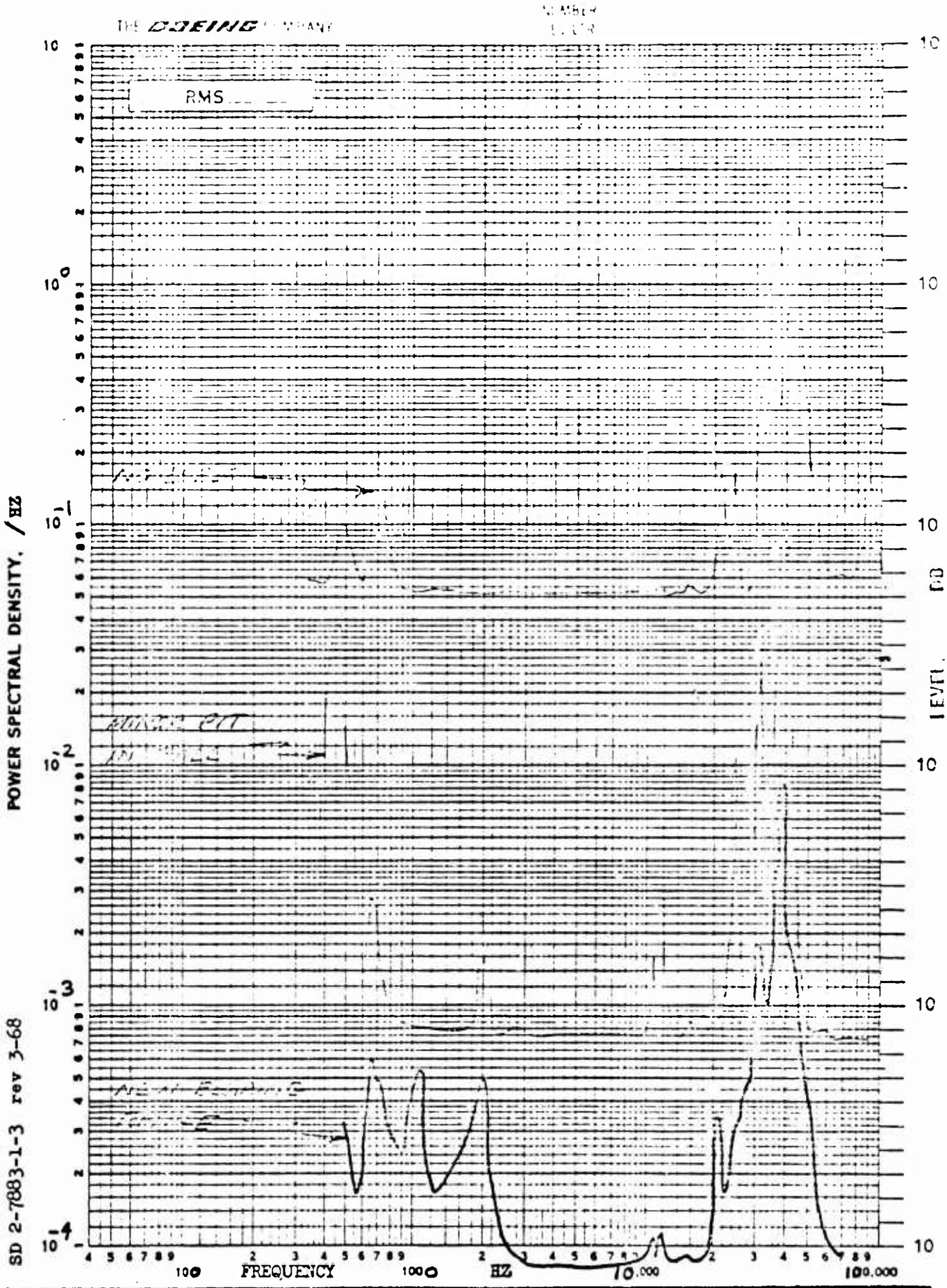

CALC.		D	BEARING NO. 1 FAULT EFFECTS
CHECK		A	
APP'D		T	
APP'D		E	10,000 RPM

Figure 11

D2-113029-3

PAGE: 18

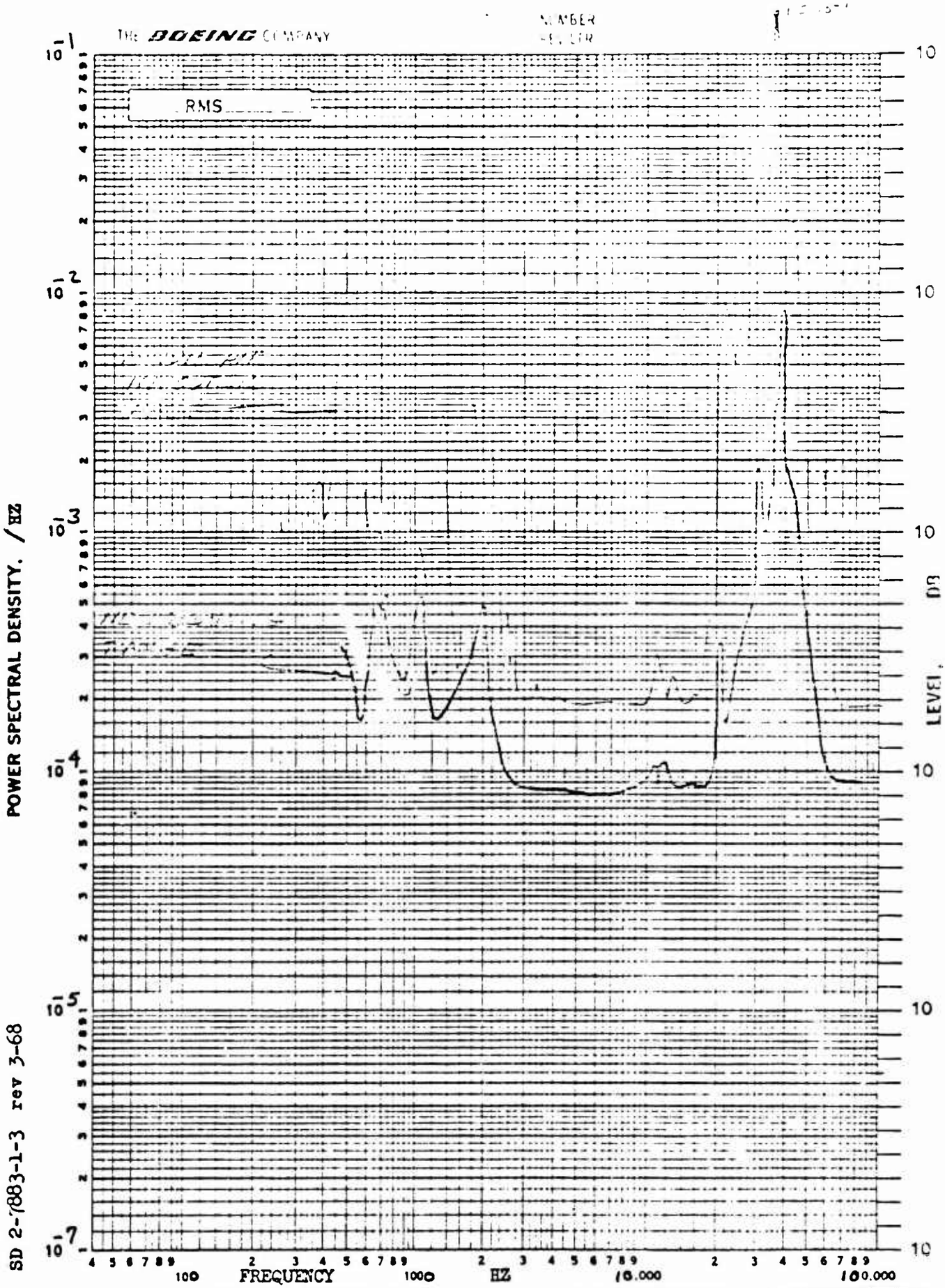

CALC.		D	BEARING NO. 2 FAULT EFFECTS	Figure 12
CHECK		A		D2-113020-3
APP'D		T	10,000 RPM	
APP'D		E		PAGE: 19

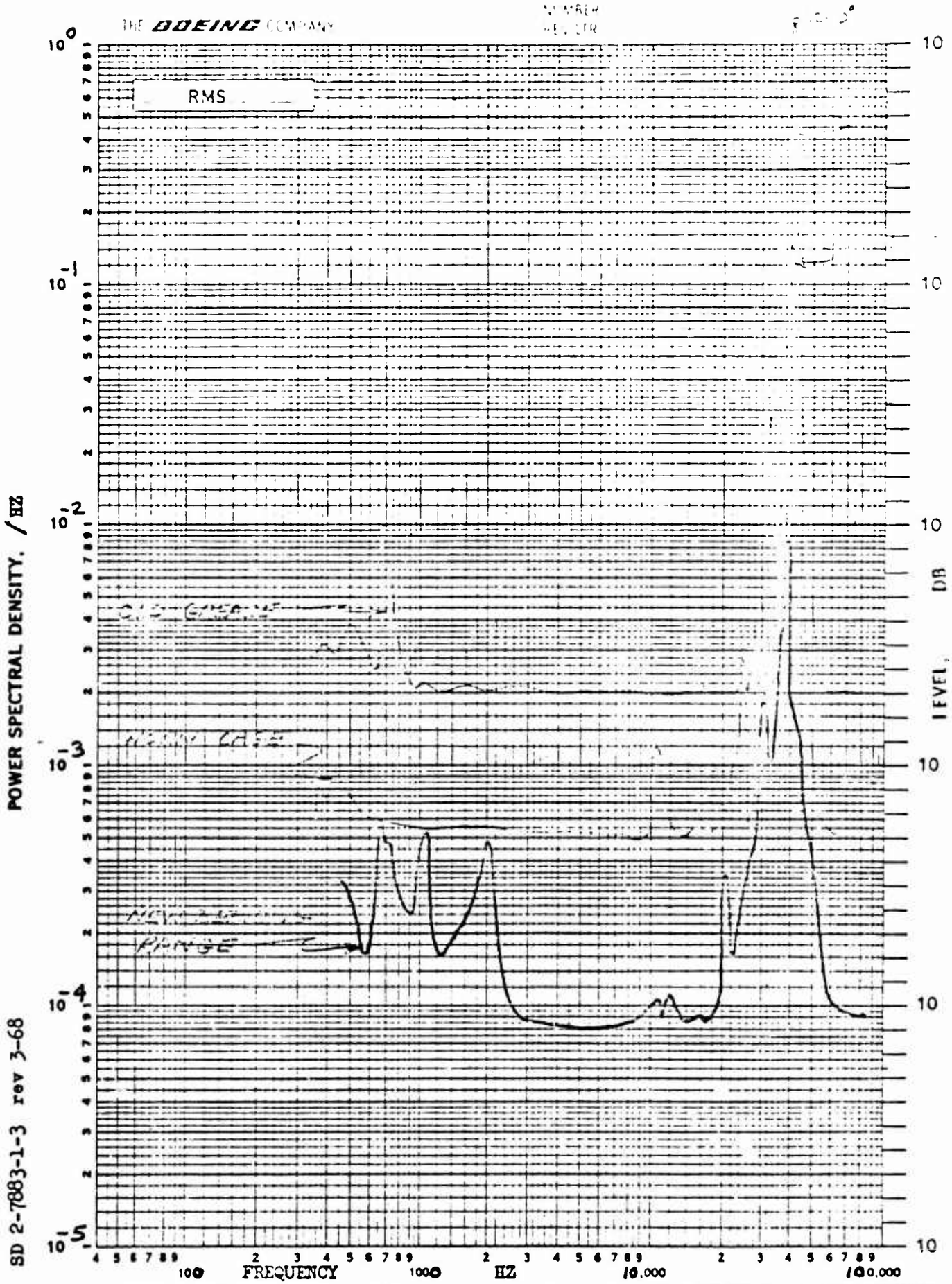

CALC.		D	BEARING NO. 3 FAULT EFFECTS	Figure 13
CHECK		A		D2-113069-3
APP'D		T	10,000 RPM	
APP'D		E		PAGE: 20

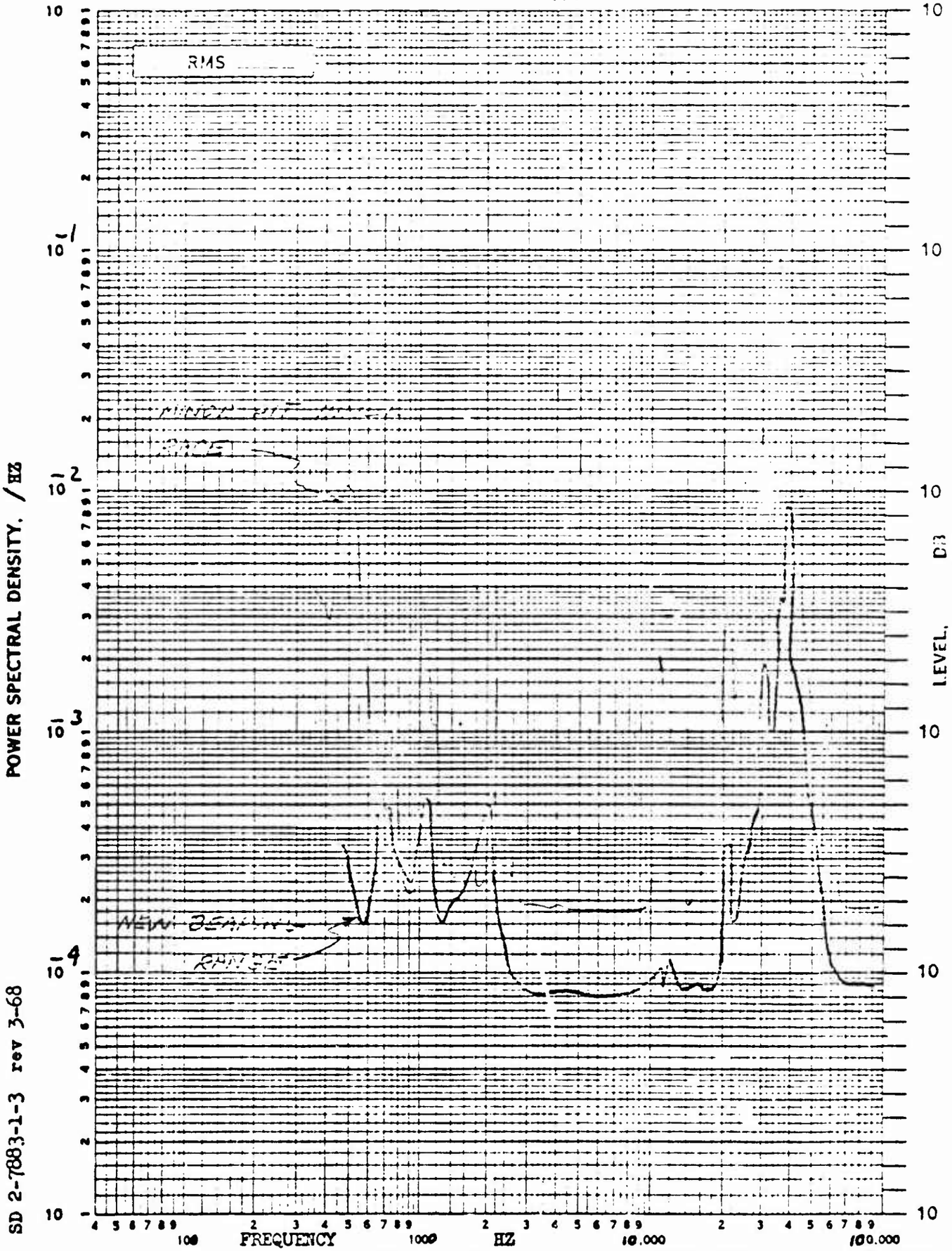

CALC.		D	BEARING NO. 5 FAULT EFFECTS	Figure 14
CHECK		A		D2-113029-3
APP'D		T	10,000 RPM	
APP'D		E		PAGE: 21

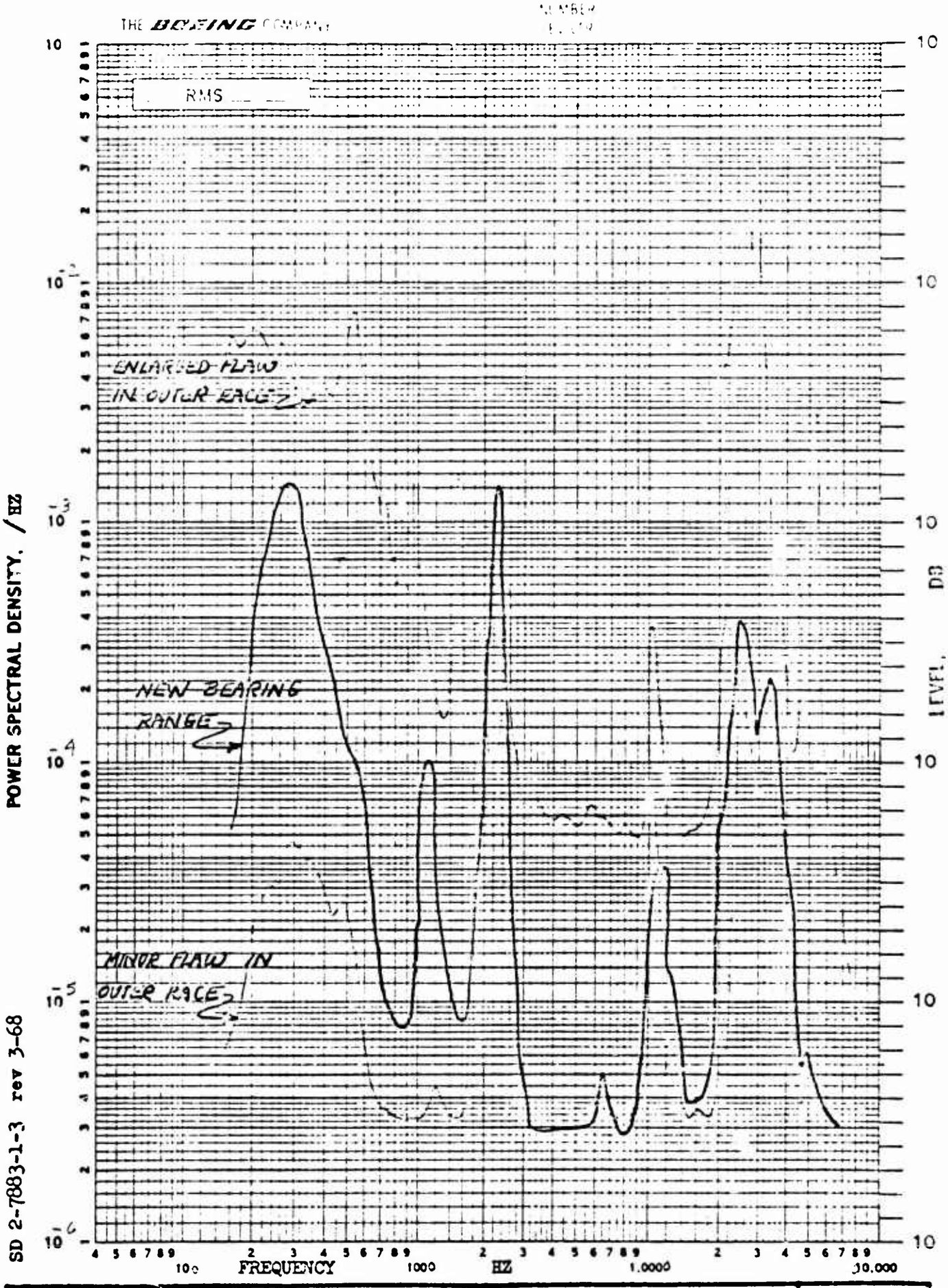

CALC.		D	BEARING #4 FLAW EFFECTS	Figure 15
CHECK		A		D2-113029-3
APP'D		T	OUTER RACE .5000 RPM	
APP'D		E		PAGE: 22

(15)

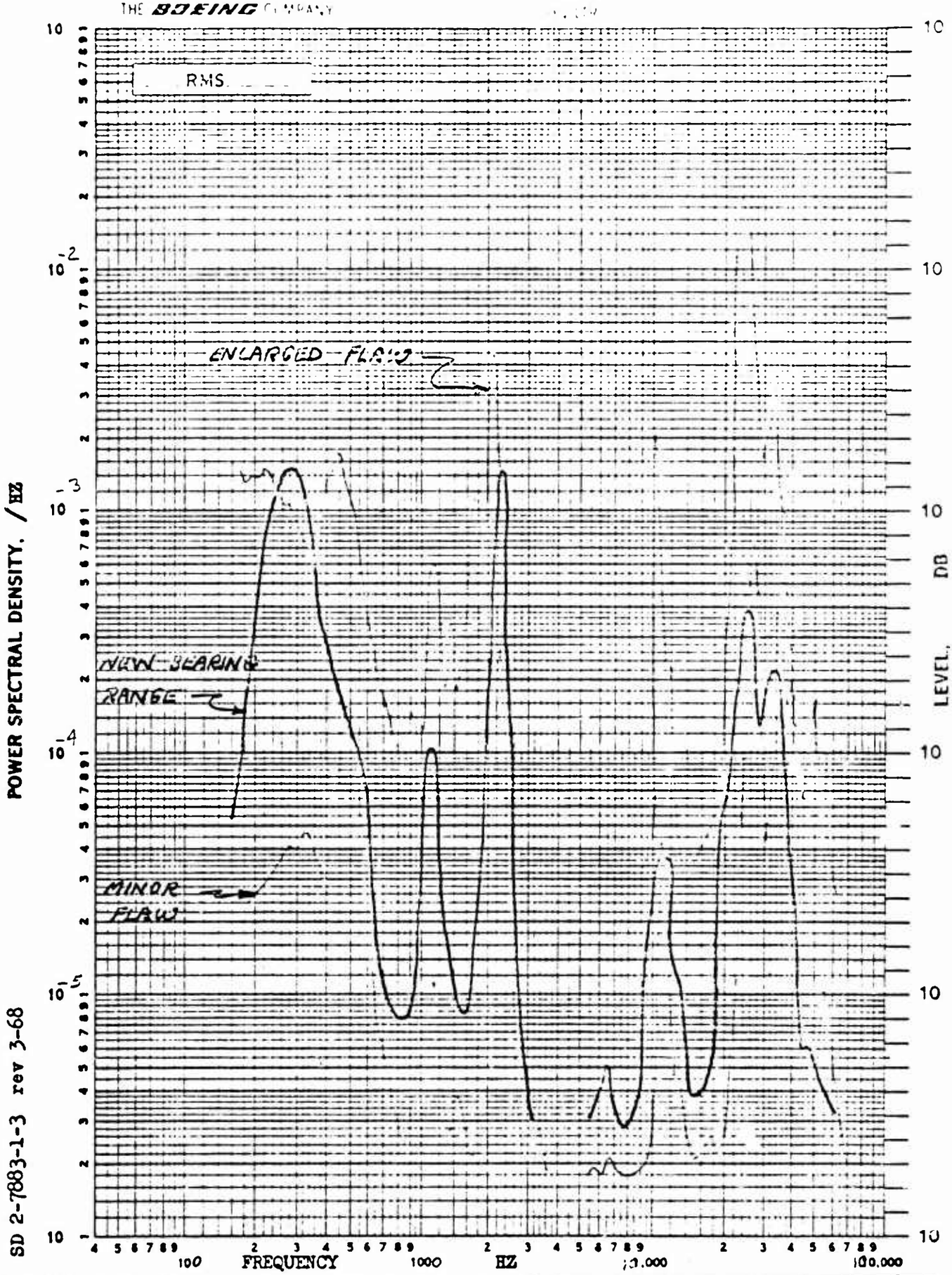

CALC.		D	BEARING #6 INNER RACE FLAW EFFECTS 5000 RPM	Figure 16
CHECK		A		D2-113029-3
APP'D		T		
APP'D		E		PAGE: 23

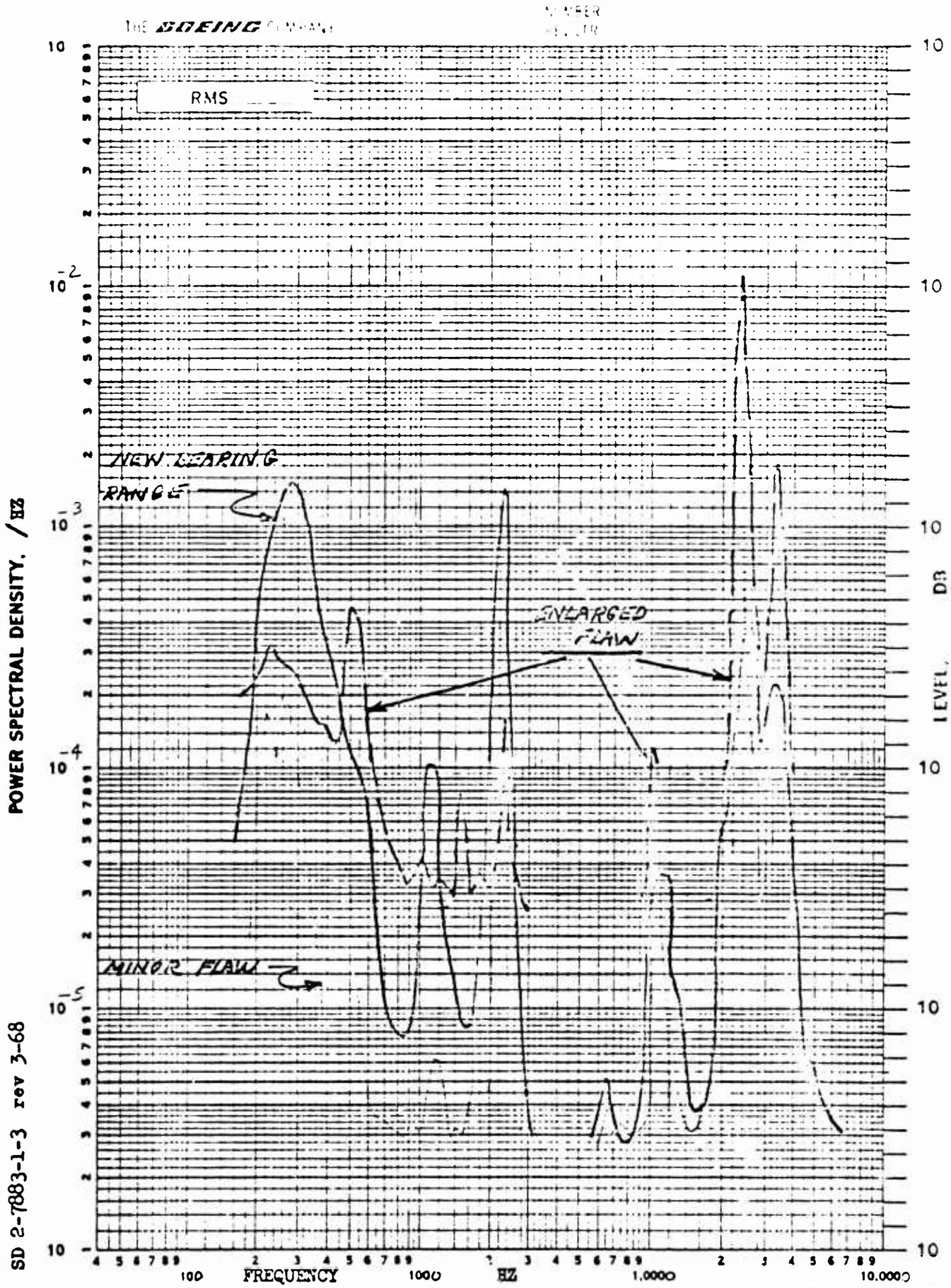

CALC.		D	BEARING #7 BALL FLAW EFFECTS 5000 RPM	Figure 17
CHECK		A		D2-113029-3
APP'D		T		
APP'D		E		PAGE: 24

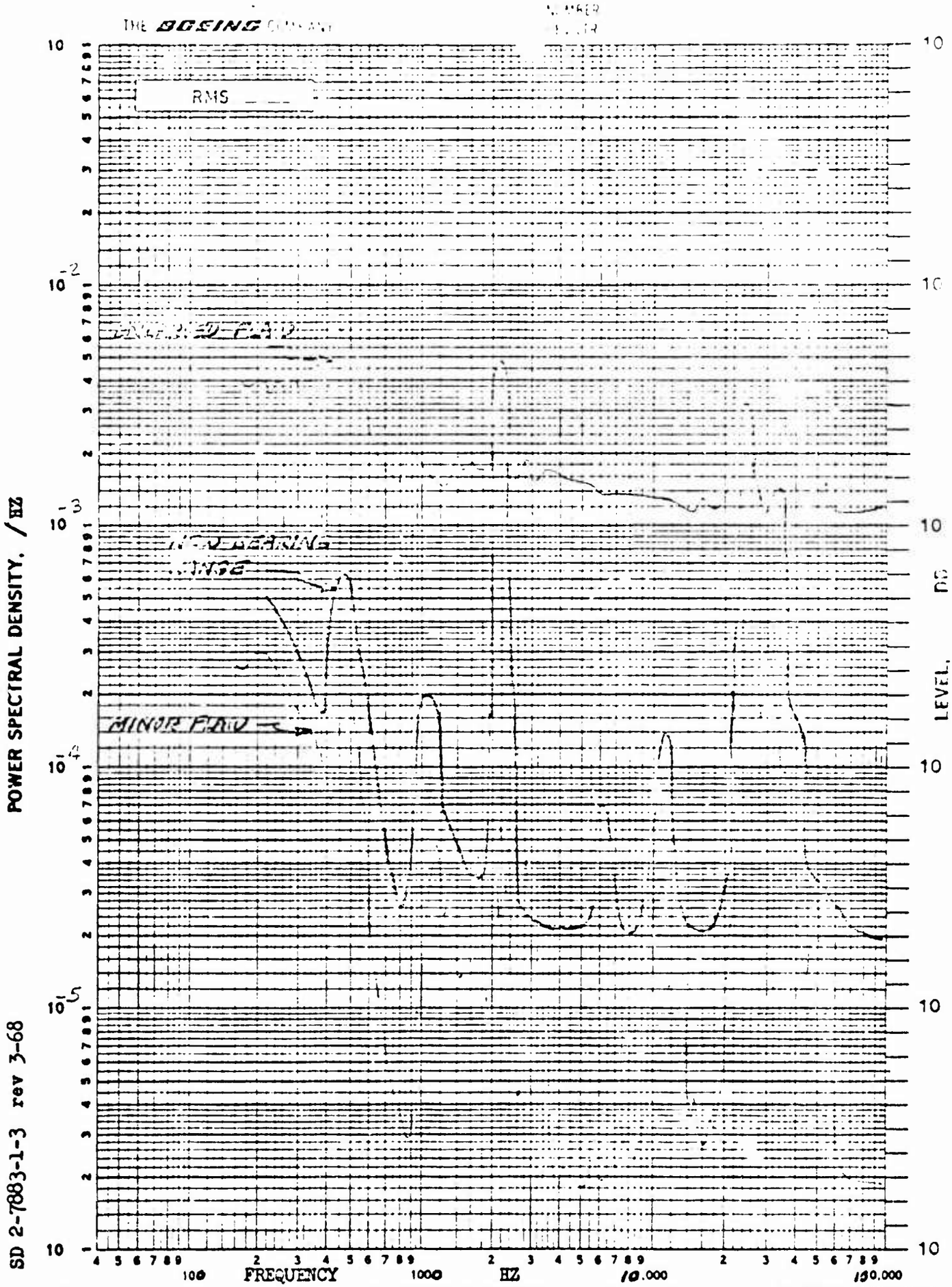

SD 2-7883-1-3 rev 3-68

CALC.		D	BEARING #4 OUTER RACE FLAW EFFECT 10,000 RPM
CHECK		A	
APP'D		T	
APP'D		E	

Figure 18
D2-113020-3
PAGE: 35

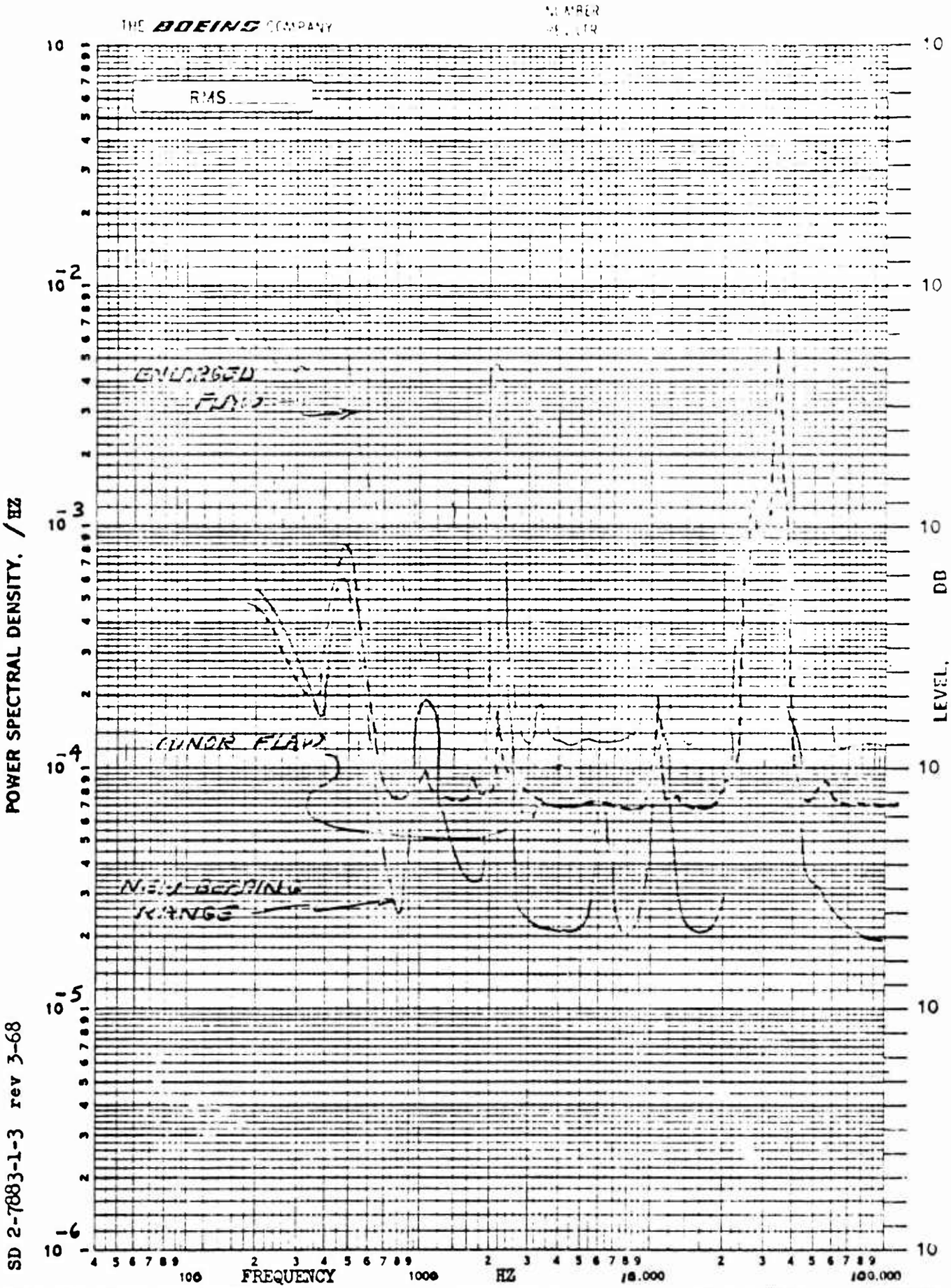

CALC.		D	BEARING #6 INNER RACE FLAW EFFECTS 19000 RPM	Figure 12
CHECK		A		D2-113029-3
APP'D		T		
APP'D		E		PAGE: 25

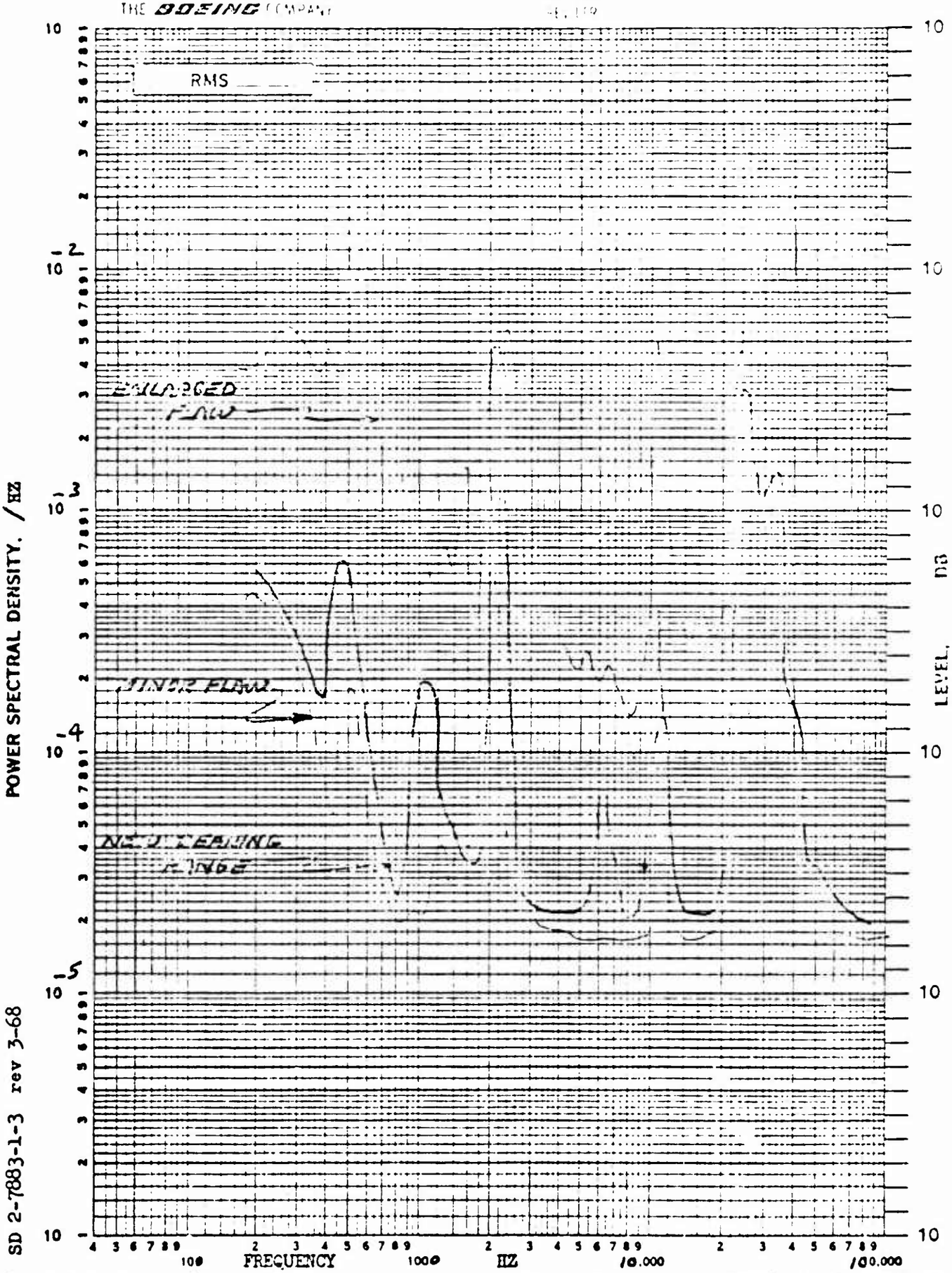

CALC.		D	BEARING #7 PITTED BALL EFFECTS	Figure 20
CHECK		A		D2-113029-3
APP'D		m	19,000 RPM	
APP'D		E		PAGE: 27

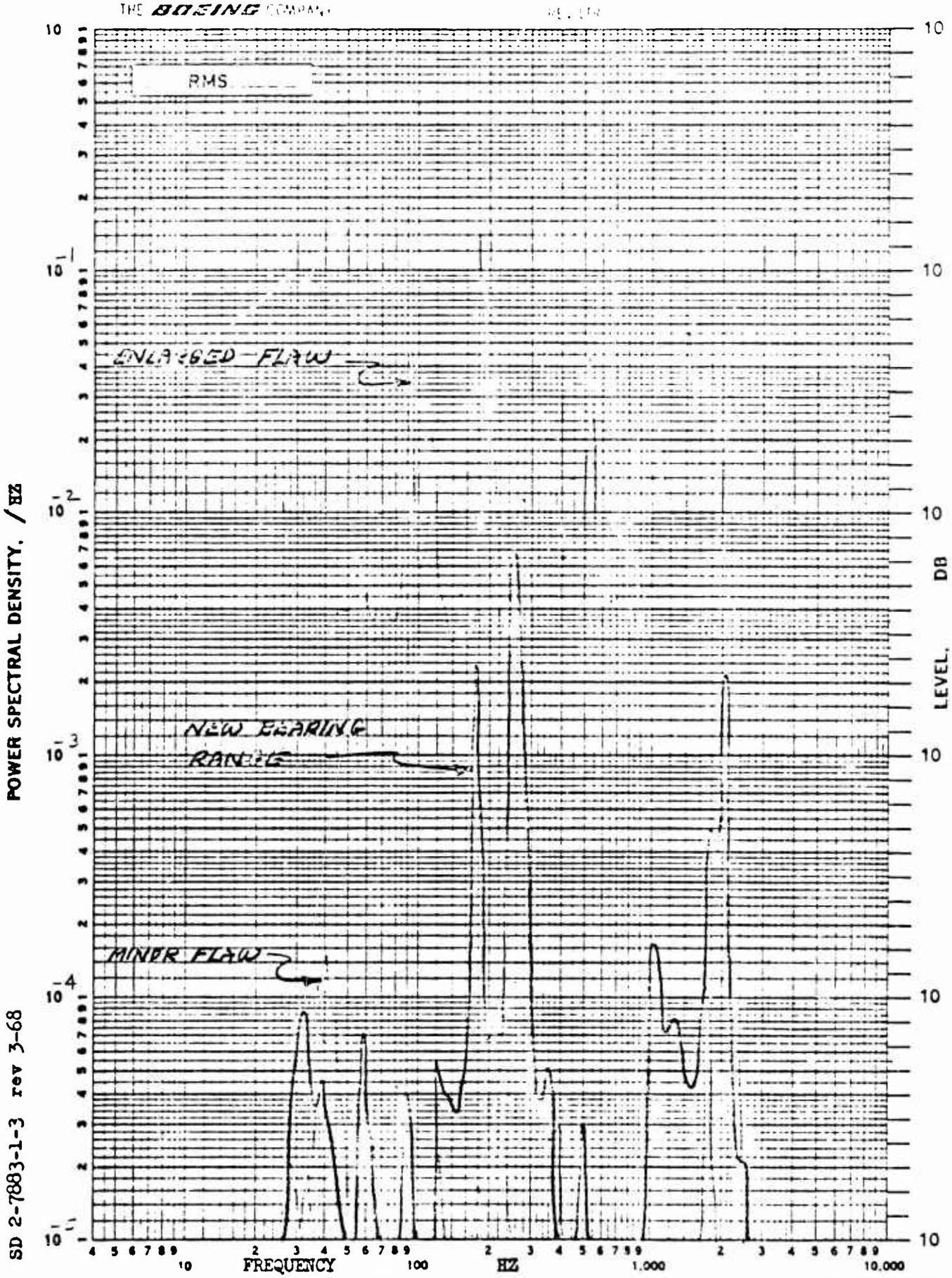

CALC.		D	BEARING #4 OUTER RACE FLAW EFFECTS ·5000 RPM	Figure 21
CHECK		A		D2-113029-3
APP'D		T		
APP'D		E		PAGE: 28

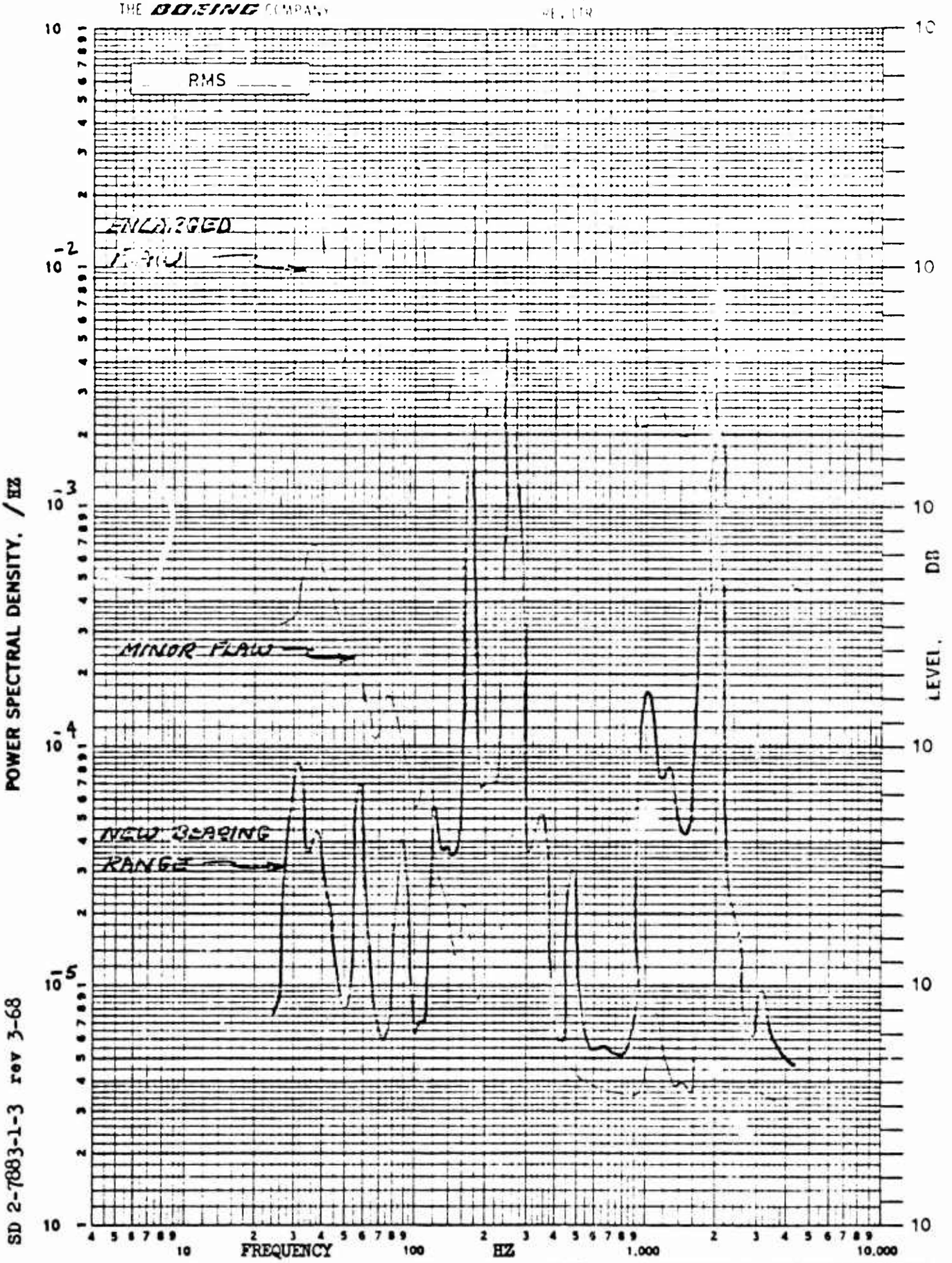

CALC.		D	BEARING #6 INNER RACE FLAW EFFECTS 5000 RPM	Figure 22
CHECK		A		D2-113029-3
APP'D		T		
APP'D		E		PAGE: 29

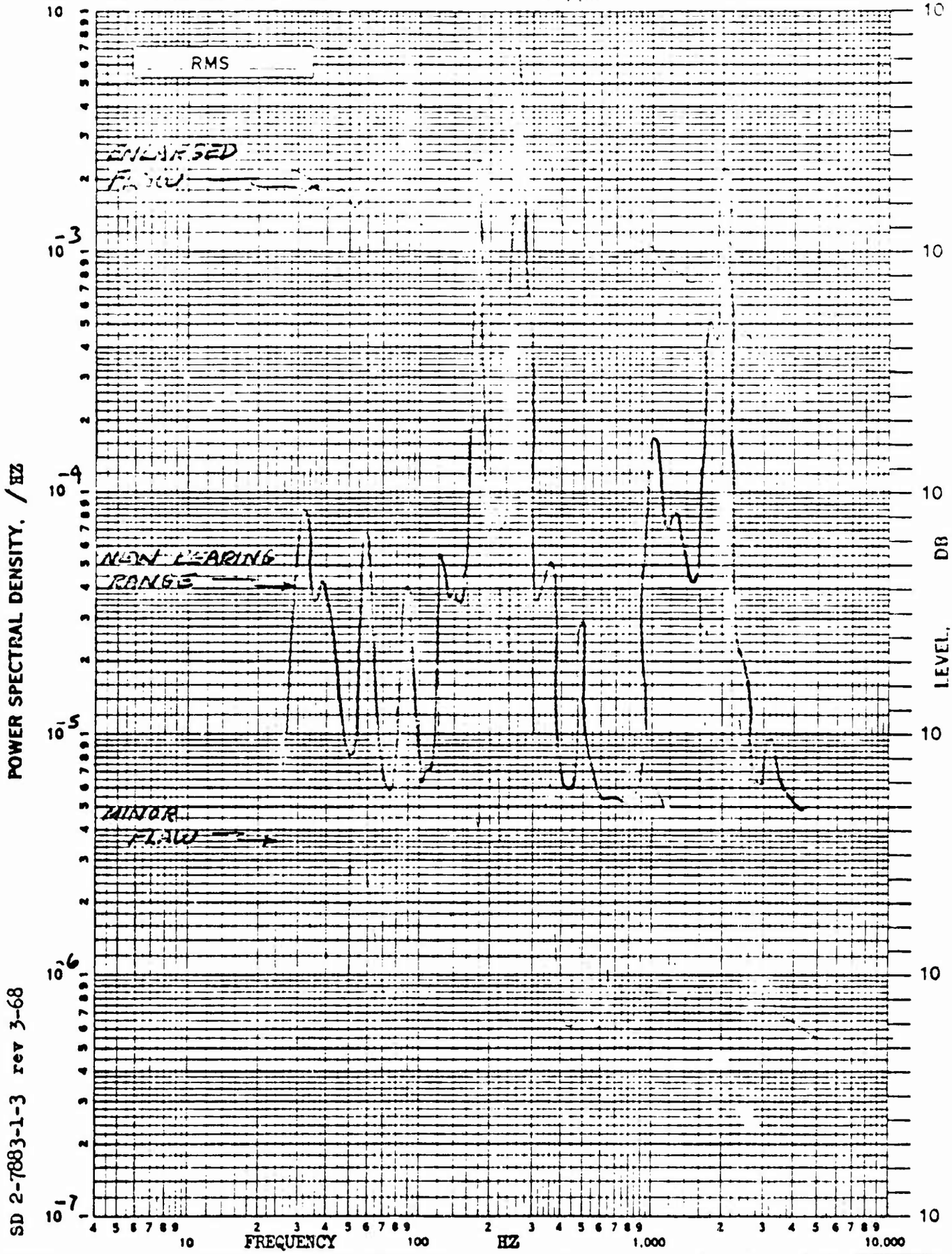

CALC.		D	BEARING #7 BALL FLAW EFFECTS 5000 RPM	Figure 23
CHECK		A		D2-113009-3
APP'D		T		
APP'D		E		PAGE: 30

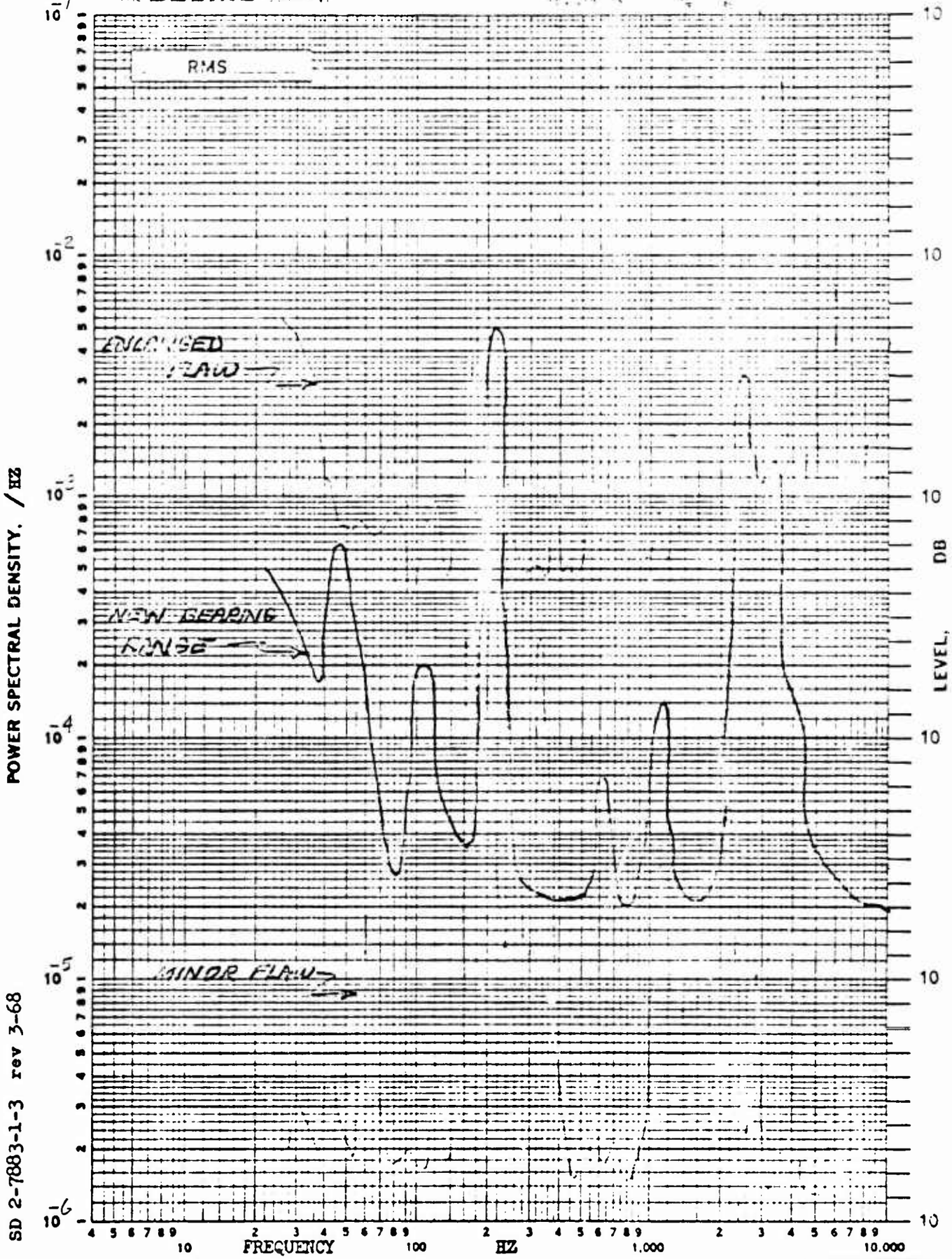

CALC.		D	BEARING #4 OUTER RACE FLAW EFFECTS	Figure 24
CHECK		A		D2-113029-3
APP'D		T		
APP'D		E	10,000 RPM	PAGE: 31

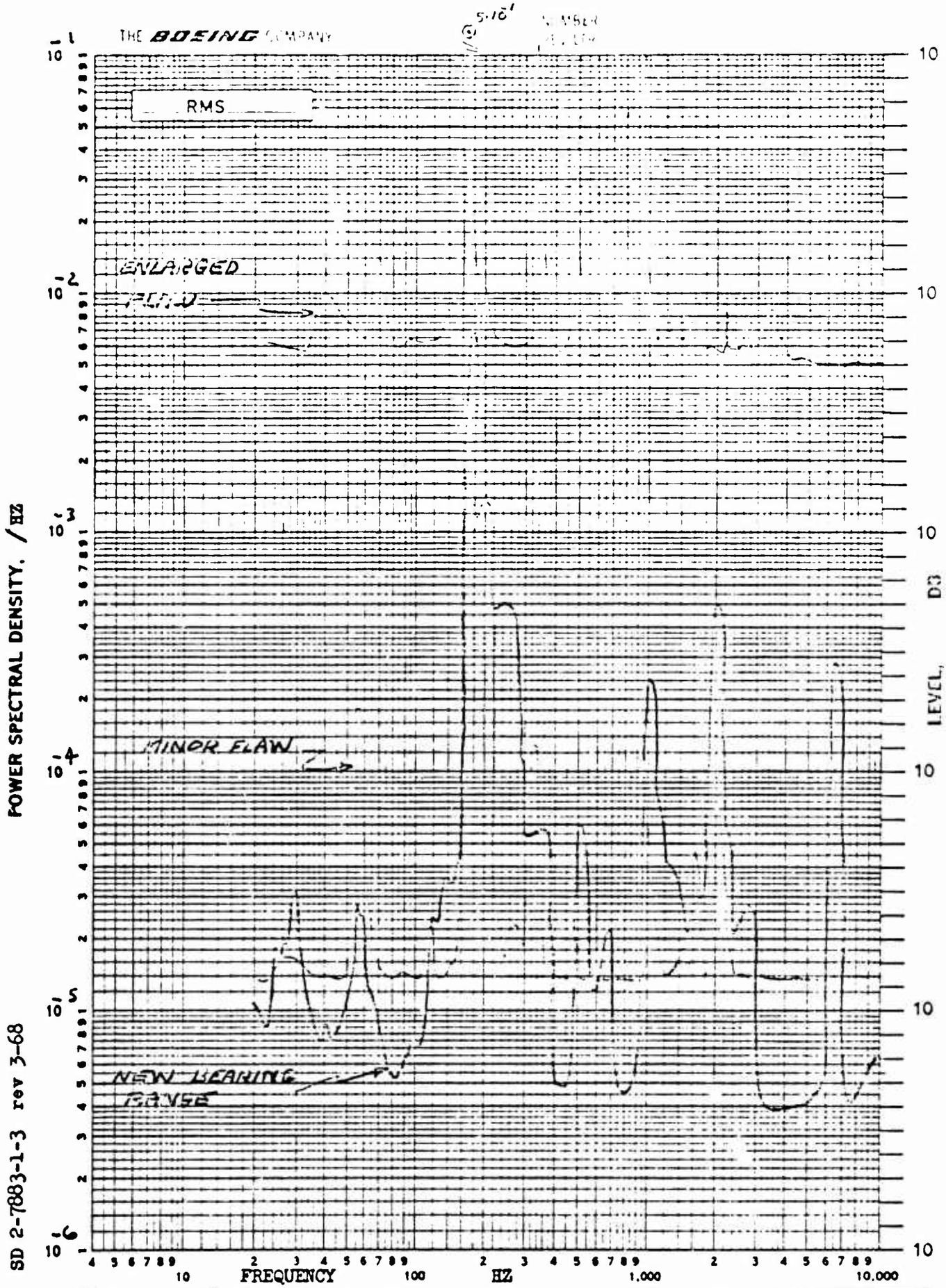

SD 2-7883-1-3 rev 3-68

CALC.		D	BEARING #6 INNER RACE FLAW EFFECTS 10,000 RPM
CHECK		A	
APP'D		T	
APP'D		E	

Figure 25

D2-113029-3

PAGE: 32

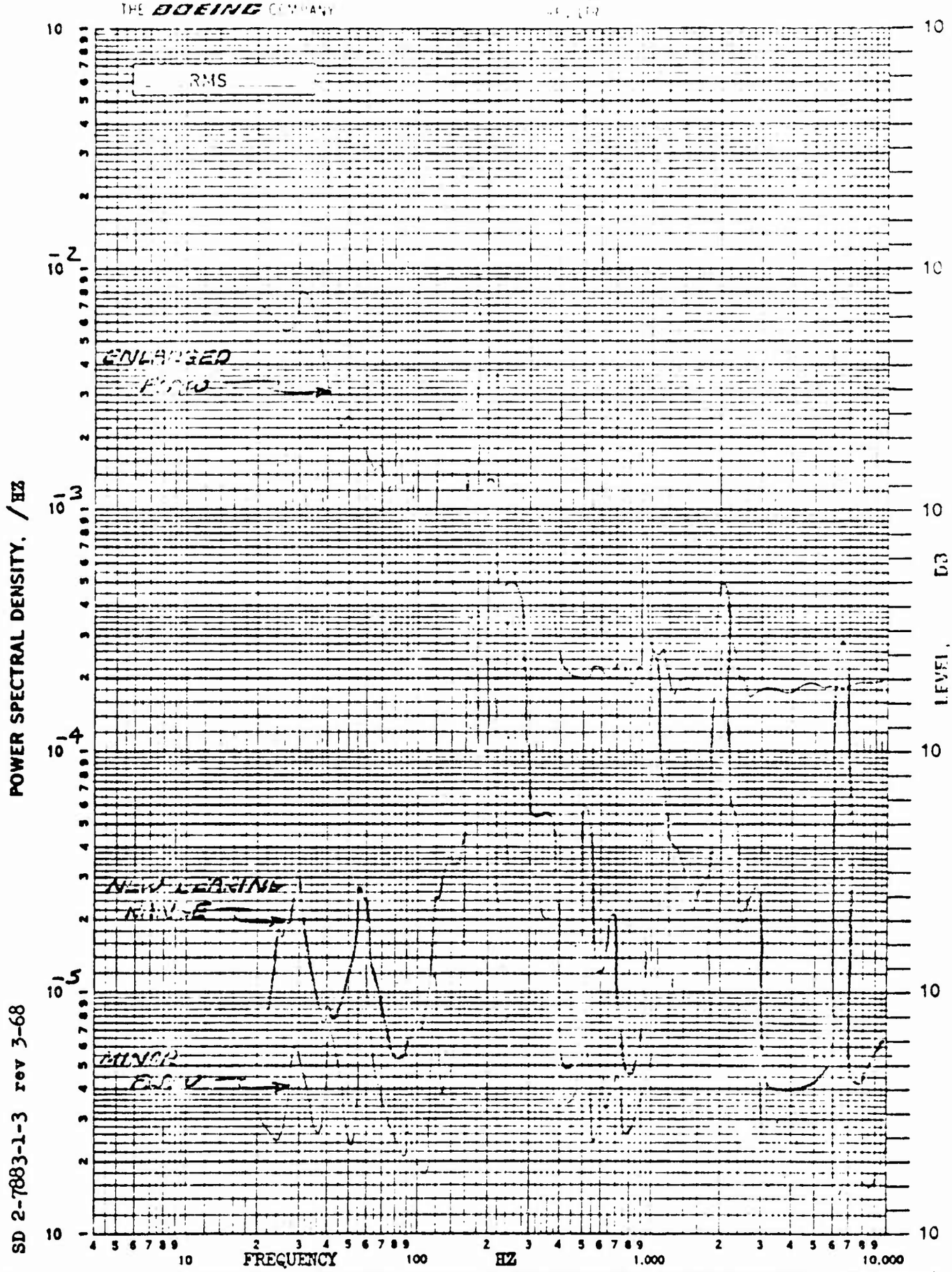

CALC.		D	BEARING #7 PITTED BALL EFFECTS	Figure 26
CHECK		A		D2-113029-3
APP'D		T	10,000 RPM	
APP'D		E		PAGE: 33

1.0 INTRODUCTION

The detection of incipient failure, in general, is related to a thorough understanding of the basic causes of failure. Detection at an early stage of recognized evidence that a failure is incipient will allow action to be taken which can, in some cases, prevent the failure from occurring, and, in others allow scheduled replacement of the affected part or component on a convenience basis. The full development of an incipient failure detection sub-system and/or concept, thus, has the potential of preventing many types of failures or of allowing more maintenance to be scheduled. The elimination of unscheduled maintenance and the elimination of failure itself, to the extent that the detection of incipient failure allows this to be done, will increase the reliability of any operational system to which these techniques are applied. In this report, which represents only one of a series, the problem of detecting incipient failures in bearings is detailed.

1.1 Objectives

It is generally accepted that the acoustic energy emitted by a severe bearing failure is frequently quite audible. However, severe failures, for the most part, start as minute defects, or incipient failures, and it was the primary objective of these experiments to determine if such incipient failures could be discerned by acoustic monitoring.

A secondary objective was to examine three basic sources of acoustic energy to determine which would provide the most reliable indication of trouble. These three sources were (a) rotational frequency energy, (b) mechanical resonance energy, and (c) acoustic emission energy. The first two sources emit energy in fairly well defined frequency ranges, but acoustic emission energy is a very broad band phenomenon.

1.2 Scope

The bearings utilized for these experiments were S-204H ball bearings, installed in the standard Pope lubricant test apparatus described in Federal Standards 791. These tests were run at 5000 RPM and 10,000 RPM with the bearings new, with old grease, dry, and with small flaws in the inner race, the outer race, and one ball. The types of acoustic energy emitted from these several conditions were analyzed and compared for differences.

1.3 Method

The method utilized to evaluate and compare the acoustic energy emitted from the various test conditions consisted of examining the energy-frequency relationships for each bearing condition. This type of relationship is readily apparent when the data is graphed in the power-spectral-density (PSD) form. The acoustic energy was detected by piezoelectric transducers and recorded on magnetic tape for subsequent data processing into the PSD form. The instrumentation system, currently available, limited the frequency range to approximately 100 kilocycles per second.

USE FOR TYPEWRITTEN MATERIAL ONLY

U3 4802 1434 REV. 8-65

2.0 SUMMARY

These tests indicate that there is positive correlation between bearing condition and the change in emitted acoustic energy. There is, as one would expect, a sensitivity threshold for this method. That is, certain small flaws can be present which may not be detected by this method without further refinement, such as the utilization of some discrete frequency band which is highly indicative of flaw occurrence.

The frequency spectrum of emitted energy was analyzed to determine if the rotational frequencies and mechanical resonance frequencies would provide positive indicators of flaw presence. The rotational frequencies (i.e. the pulse-repetition-frequencies of physical defects) were found to be of negligible value when viewing a wide frequency spectrum of emitted energy, as was done here. Rotational frequencies might be usable if different data processing techniques were employed. The explanation for this is detailed later in this report.

For these tests, the most positive indicator of flaw presence appeared to be energy in the frequency band from 20 KC to 40 KC. A low frequency technique used with three of the test bearings, specifically, FM monitoring between 100 cycles and 10,000 CPS, indicated that the overall energy level was the most practicable indicator with the FM system.

3.0 CONCLUSIONS AND RECOMMENDATIONS

Three sources of acoustic energy related to bearing failure have been examined in this test program. These are (1) rotational noise, (2) resonant noises of the total system, and (3) acoustic emission. A direct relation exists between acoustic emission, the resonant noise, and the severity of bearing defects. The rotational noise energy appears to be distributed across the bandwidth of frequencies studied here, namely 100 to 50 KC. The system predominant resonances appeared to provide data in three different frequency bands. In most of the tests of the S-204H bearing, a blank space existed between 3 KC and 10 KC on the spectral density plots. This space would permit detection of burst type acoustic emission, when and if it occurred.

Direct correlation of severity of defects to amplitude was observed within specific bandwidths. Direct correlation was also observed between severity of defects and total noise. If the resonant and rotational frequencies are translated downward to 1/16 (compressed), the higher resonant frequencies are brought within the range of human hearing so that bearing defects can be readily distinguished, one from the other. This was done, using a tape recorder, by recording at 60 inches per second and playing back at 3 3/4 inches per second.

Our research thus far has shown that bearing defects can be detected prior to failure of the bearing. A prototype piece of test equipment has been built which has the capability of monitoring the true RMS energy content within a selected frequency band. Once a pre-set limit has been set into this test equipment, it will indicate by "go, no-go" lights whether the test article exceeds the red-line condition. We believe that we will be able to detect bearing defects in the presence of the noise of jet engines by this method, using the resonant rather than the rotational frequencies. We believe that the employment of resonant frequencies to detect incipient failure is our most important present contribution to the detection of such incipient failures.

USE FOR TYPEWRITTEN MATERIAL ONLY

U S 4802 1434 REV. 8-65

We also believe that the use of the acoustic emission phenomena will become more important with the development of wider band transducers and charge amplifier systems. We are doing a minimum amount of work in this area. It is recommended that this activity be increased and broadened in scope.

4.0 DISCUSSION

4.1 Techniques Employed

4.1.1 Test Description

The equipment used for bearing testing (see Figure A) was a standard Pope Spindle described in Federal Standards 791, Method 33, which is used for testing lubricants. It consisted of a cartridge spindle with a shaft supported by two #204 sized ball bearings, which in these tests were of the angular contact variety, so that they could be easily disassembled. The spindle was belt-driven by an electric motor at speeds of 5,000 and 10,000 RPM.

Two distinct series of tests were run. The first series of tests consisted of tests of four S-204H bearings (Nos. 1, 2, 3, and 5). For these bearings, the data was recorded in the direct mode (from 1 KC to 100 KC), and the bearings had only one flaw injected into each. Subsequently, a second series was run (bearings 4, 6, and 7) with minor flaws first and then with enlarged flaws. In this second series, it was decided to investigate the intelligence carried in the lower frequencies, so the data was recorded in the FM mode (100 CPS to 10,000 CPS) in addition to the direct mode. In all conditions the bearings were run at 5000 RPM and 10,000 RPM. These bearings were all run in the unloaded condition.

The test conditions are detailed below:

First Series:

NO. 1 -

NEW, LUBED. Bearing was lubricated with MIL-G-23827 (Aeroshell-7) grease.
NO LUBE. The bearing was cleansed of all grease and run completely dry. This condition was run only long enough to acquire data; approximately 30 seconds.
RE-LUBED. The bearing was re-lubricated as above.
PITTED BALL. A fatigue spall was simulated on one ball by etching a small pit in the ball with an electric pencil. The pit was polished to remove any protruding metal.

NO. 2 -

NEW, LUBED. Same as bearing #1.
PITTED OUTER RACE. A pit was made in the outer race with an electric pencil. The pit was then polished so that no metal protruded above the race surface.

USE FOR TYPEWRITTEN MATERIAL ONLY

U3 4802 1434 REV. 8-65

NO. 3 -

NEW, LUBED. Same as bearing #1.
OLD GREASE. The bearing was cleaned and re-packed with old, hardened MIL-G-7711 grease which had been installed in a Minuteman generator for three years.
WORN CAGE. The cage pockets were enlarged with a file. The bearing was re-assembled and lubricated as in the new condition.

NO. 5 -

NEW, LUBED. Same as bearing #1.
PITTED INNER RACE. A pit was made in the inner race in the same manner described for bearing #2 outer race.

Second Series:

NO. 4 -

NEW, LUBED. Same as bearing #1.
PITTED OUTER RACE. The pit in this race was made with an S. S. White Industrial Abrasive Cutting Unit. It was found that this method provided a better simulation of incipient spalling than the electric pencil used in the first series.
ENLARGED PIT. The initial pit was enlarged to approximately three times its initial size.

NO. 6 -

NEW, LUBED. Same as bearing #1.
PITTED INNER RACE. A small pit was cut into the inner race in the same manner described above for bearing #4.
ENLARGED PIT. The initial pit in the inner race was enlarged approximately three times.

NO. 7 -

NEW, LUBED. Same as bearing #1
PITTED BALL. A small pit was placed in one ball with the S. S. White unit.
ENLARGED PIT. The pit in the ball was enlarged approximately three times.

4.1.2 Instrumentation and Data Processing

The transducers utilized to pick up the acoustic energy were piezoelectric crystal transducers which respond to frequencies up to approximately 100 KC. The dynamic response of these transducers is not flat throughout this range. For the purposes used here, the dynamic response curve of the transducers is irrelevant since the data has value only on a comparative basis. That is, incipient failure intelligence is derived from the differences between two PSD plots, any single PSD plot carries practically no information by itself. Since the dynamic response of these transducers differ from one another, it is important to compare only data recorded from the same transducer. As will be

USE FOR TYPEWRITTEN MATERIAL ONLY

U3 4802 1434 REV. 8-65

noted for the second series of tests, the data in the frequency range of overlap, between the FM (100 to 10,000 CPS) and the Direct (1,000 to 100,000 CPS), plots does not necessarily appear similar. This is to be expected since different transducers were used to record these two types of data. In addition, the state of the art of transducer development is such that an absolute calibration above 6,000 CPS is unattainable. Therefore, the shape of the PSD curve cannot be interpreted as an absolute measure of the bearing energy emission. Certain frequency spikes on the PSD plot may rise to a high amplitude due either to a transducer resonance at that frequency or a high energy emission from the bearing. However, it must be made clear that this "unknown" does not detract from the validity of the data, since the plots are used in a comparative sense only. A transducer resonance merely serves to magnify the presence of emitted energy at that frequency and makes comparison that much more significant.

The transducer signals were amplified by charge amplifiers and recorded on the Ampex FR-1300 tape recorder at 60 inches per second. These recordings were subsequently operated on by the frequency analyzer to provide the PSD plots. The FR-1300 tape recorder response at this speed is flat up to nearly 300 KC. The response of the charge amplifiers, Dynamics 6937, were flat up to approximately 70 KC. This upper frequency limit explains the apparent "roll-off" on the PSD plots around 50 KC and above.

4.1.3 Data Analysis

Each bearing appeared to have a unique initial PSD signature, as the variation between bearings in the new, lubricated condition shows in Figures 1 through 6. This spread in data can be attributed to several factors, the most predominant two being actual small structural differences between new bearings, and different run-in times before data acquisition. The noise (or acoustic energy) emitted from a bearing is normally high when the bearing is initially used, but, as the bearing surfaces tend to lap each other, the bearing becomes quieter. Of course, as this wearing process transcends the condition of optimum parts fit, the noise increases again. Wear-in time is a function of the lubrication, speed, and load on the bearing in service.

The PSD plots for the first series of tests (Bearings 1, 2, 3, and 5) are presented in Figures 7 through 14. These Figures show, among other things, that the two test conditions of lack of adequate lubrication, specifically the "no lube" and "old grease" conditions, result in a general increase of noise level which exceeds the maximum new bearing envelope by a factor of 100 to 300 times. Such an incipient failure as no lubrication would, indeed, be readily detected. These Figures also show the effects of the minor flaws inserted into these bearings. In each case, these flaws result in noise increases which exceed the new bearing range limit in certain frequency bands. The worn cage condition (Figure 9) shows the least indication of change of any other condition. However, even this condition manifests itself at about 12 KC and 40 KC to 50 KC. It is interesting to note, and Figure 9 shows this nicely, that the overall energy level is not always a good fault indicator; one should examine the emission behavior within discrete frequency bands. In this series of tests, the frequency bands of 1,500 to 3,000 CPS, 10,000 to 15,000 CPS, and 20,000 to 50,000 CPS appear to be the bands of major significance. In the second series, these same frequency bands carry the predominance of fault indication information in the direct data.

USE FOR TYPEWRITTEN MATERIAL ONLY
U3 4802 1434 REV. 8-65

As pointed out earlier, the second test series included more than a single small flaw injection into the test article. Figures 15 through 20 are the direct data recorded on these bearings. These plots show that, in nearly every case, the first flaw, which was very small, failed to give a strong indication when compared to the maximum noise level of the three bearings in the new condition. This effect is attributable to the decrease in general noise level due to the run-in process, coupled with the fact that these initial flaws were very small. After enlargement of the flaws approximately three times, the data shows a very distinct indication of trouble in every case. The low frequency, FM, plots for this series (Figures 21 to 26) show the same thing, except here there are no clear cut frequency bands which manifest the onset of failure. The primary purpose for recording this low frequency data was to examine the possible occurrence of rotational frequencies and to determine if these would provide specific indicators of bearing failure.

There appear to be three basic sources of noise in bearings: rotational motion, structural resonance, and acoustic emission phenomenon. The rotational frequencies for these tests were all below 2,000 cycles per second. The resonant frequencies spanned the region from about 10,000 cycles to 90,000 cycles per second. The acoustic emission phenomena, when present, create a broad band of frequencies covering the entire spectrum. The so-called "burst" type of acoustic emission will occur during the work-hardening processes associated with fatigue. This would occur in heavily loaded bearings and/or bearings operated at high speed. Since the so-called "acoustic emission phenomena" are classically associated with the formation of defects, such as cracks, flaking, etc., it should be quite valuable in the detection of incipient failures in bearings. See references (1) and (2).

It appears that any one of the three basic sources of noise--or any combination--can be utilized for the detection of incipient failure. However, the sounds of rotation would have to be detected and presented by some means other than the power spectral density (PSD) method utilized here.

A study of the power spectral density plots for these tests revealed that the rotational frequency energy was negligible when compared to the energy content of other frequencies. This appeared to be true for even the largest flaw injected into these test bearings. Although this seems contrary to intuition, it can be understood by considering the make-up of the "rotational frequencies" and the significance of the information presented in the power spectral density graphs.

The "rotational frequencies" are periodic occurrences caused by some repetitive mechanical impact within the rotating machinery (e.g. the rolling elements of a bearing striking a flaw in the race). Each impact is an impulse function which contains a multiplicity of frequencies which are multiples of the pulse repetition frequency (see Appendix 5.1), and it excites various system resonances at each occurrence. In effect, then, these periodic impulses "gate" energy over a wide frequency range into the instrumentation system. On the power spectral density plot, this energy appears to be distributed over this wide frequency range, rather than concentrated at a discrete rotational frequency.

The occurrence of rotational frequencies might possibly be detected by a modulator-detector scheme, but this was not attempted for this series of tests.

USE FOR TYPEWRITTEN MATERIAL ONLY

U3 4802 1434 REV. 8-65

For a relatively simple mechanism, this technique might be quite effective, provided that these frequencies could be predetermined. However, in more complex equipments, the sounds of rotation of other components may very well drown out the sounds of rotation of the bearings. This is the case with jet engines. If one desired to detect incipient failure in the form of fatigue, it is doubtful that the sounds of rotation would give as early a warning as could be obtained from the acoustic emission phenomena. Thus, in analyzing power spectral density curves, one selects a band of frequencies which can be correlated to a bearing defect and which are not overridden or camouflaged by noises from other sources. Thus, the mechanical resonant frequencies may be a valuable tool, since they are of much higher frequency, falling in the range of 10 kilocycles to 90 kilocycles. If the higher resonant frequencies are interfered with by other equipment noises and/or resonances, then one could use the acoustic emission phenomena, which characteristically gives off a burst of energy covering a very broad frequency spectrum. Thus, it would be possible to detect the formation of a crack, the growth and propagation of a crack, at frequencies far above 100 kilocycles. This would require, however, that higher frequency and/or wide band acoustic transducers be employed.

To understand more thoroughly the possible conditions under which each of the three phenomenon mentioned above could be employed in incipient failure detection, the following subsections will define and examine the source of each phenomena insofar as possible:

4.2 Rotational Frequencies

The sounds of rotation of simple rotating equipments are characteristically low in frequency, the frequency being related to the configuration of the rotating element and the RPM with which it rotates. Thus, the sound of rotation of a shaft is equal to the RPM divided by 60; the sound of rotation of a fan blade is equal to the number of blades on the fan multiplied by RPM and divided by 60; the sound of rotation of a centrifugal blower is equal to the RPM of the blower multiplied by the number of vanes and divided by 60. The sounds of rotation of a bearing are a bit more complex. Because of the interaction between the bearing balls, the inner race and the outer race, and the differences in diameter between the inner race and the outer race, the calculation of rotational frequency is more difficult. For example, from Palmgrin, "Ball and Roller Bearing Engineering," Section 24, the frequency of rolling elements passing over a spot on a stationary outer race is given by the formula:

$$f_{outer} = \frac{n}{2} f_r \left(1 - \frac{D_w}{d_m} \cos \alpha\right) \qquad (\#1)$$

where

D_w = ball diameter

d_m = pitch circle diameter

α = contact angle

n = number of balls

USE FOR TYPEWRITTEN MATERIAL ONLY

f_r = speed of rotation in revolutions per second

$= \frac{RPM}{60}$

The frequency of rolling elements passing over a spot on the moving inner race is given by the expression -

$$f_{inner} = \frac{n}{2} f_r \left(1 + \frac{D_w}{d_m} \cos \alpha\right) \qquad (\#2)$$

The rotational speed of one ball about its own axis is given by the expression -

$$n_b = f_r (0.5) \frac{d_m}{D_w} \left(1 - \frac{D_w}{d_m} \cos \alpha\right) \left(1 + \frac{D_w}{d_m} \cos \alpha\right) \qquad (\#3)$$

The frequency of a defect in one ball bearing striking the cage twice each revolution is equal to twice equation #3.

The rotational frequencies computed from equations #1, #2, and #3 for these bearings are:

	5,000 RPM	10,000 RPM
Ball flaw striking cage only	342	684
Ball flaw striking cage and races	684	1368
Ball striking outer race flaw	356	712
Ball striking inner race flaw	562	1124

Examination of the appropriate power spectral density plots showed that when a frequency spike is present at one of these rotational frequencies, it is very minor compared with other frequencies. This is explained in Appendix 5.1.

Also, it should be noted that, if a defect in a ball were lined up correctly, it would strike both the inner and outer races at the same frequencies as the ball striking the cage twice. However, since the ball travels in a spiral as it rolls, the variations in these frequencies appear to be modulated by the speed with which the ball spirals. The effect can be readily noted when one listens to the translated higher frequencies of the bearing; more so than if one listens directly to the sounds of rotation.

Translation of these high, sometimes inaudible, frequencies to the range audible to humans is accomplished by playing back the taped data at a reduced speed. In the case of these tests, a speed reduction of 16:1 was found to be excellent. In effect, this process merely expands the time scale of the recorded event a sufficient amount to permit the human ear to follow the frequency excursions. Since the time scale is the only change in this process, the interrelationships between the frequencies making up the data are unaffected.

USE FOR TYPEWRITTEN MATERIAL ONLY
U3 4802 1434 REV. 8-65

It is evident from the above that the frequencies of rotation are relatively low and well within the range of hearing of the human ear. However, other sounds produced by the speed of rotation may not be within the range of the human ear. For example, in the case of a fan, the frequencies produced by the blade of the fan striking air molecules at high speed and the resultant collisions of air molecules produce a band of frequencies above and below 40 kilocycles.

The frequencies of rotation could be a very important diagnostic tool in relatively simple mechanisms, wherein their occurrence increases the overall noise level appreciably. They are highly effective in diagnosing the existence of defects which could result in failure and are particularly effective in diagnosing failure itself. There are, however, limitations. These limitations are experienced in more complex equipment, such as a jet engine, wherein the rotation of the major elements, such as the N-1 and N-2 rotor, can produce sounds which are much greater in magnitude than those produced by the bearing and other small accessories, such as generators and gear boxes, driven by the jet engine. If one were able to mount a transducer directly on the bearing or gear housing, this interference would not be so pronounced. However, if one is forced to mount the transducer on the outer case of the engine or on an engine cowling, the sounds of the bearing might very well be overridden. In addition, within a complex system such as an airplane, the sounds of the other engines and other accessories provide interference and further complicate identification of the basic rotational frequencies of small components and the effects upon amplitudes at these frequencies by defects existing within the components of interest. Accordingly, it is sometimes necessary and effective to utilize the resonant frequencies of the components under observation.

4.3 Resonant Frequencies

Resonant frequencies are a function of the mass configuration and type of material involved. They are usually initiated by the shock excitation associated with minor structural irregularities and/or defects.

The amplitude of acoustic energy at resonant frequencies is much higher than the amplitude of the sound of rotation. In addition, resonant frequencies are usually much higher in frequency than those of rotating elements. The frequencies of resonance of components under observation do not vary with RPM. Their amplitudes, however, will vary directly with the RPM. Variations in amplitude due to the severity of a defect in a bad bearing may be as high as 1,000,000 times that of a new bearing.

The advantages of using the high resonant frequencies over the rotational frequencies are two-fold: (1) they do not vary with RPM and (2) there is less confusion with the rotational frequencies of other components. This is particularly true with ball bearings. In utilizing this technique of incipient failure detection in bearings, it is not specifically necessary to identify all of the resonant frequencies of the system under test. Simply monitoring the frequency content of the data at several speeds will disclose those frequencies which are unaffected by speed, whereupon one can reasonably conclude that these are the resonant frequencies in question.

USE FOR TYPEWRITTEN MATERIAL ONLY

U3 4802 1434 REV. 8-65

The theoretical determination of total system dynamic response characteristics is completely impracticable in most instances, as it has been for the relatively simple machines used for these tests. However, to acquire an order-of-magnitude approximation to some of the resonances expected during these tests, the resonant frequencies of the major components of the S-204-H bearing were computed. The computations are detailed in Appendix 5.2. The frequencies for these bearing elements are presented in the table below:

Ball: f_1 = 383 KC

Mode, n:	2	3	4	5
Outer Race	3.29 KC	9.32 KC	17.9 KC	28.9 KC
Inner Race	16.25 KC	46.0 KC	88.0 KC	142.3 KC

The degree to which these frequencies will be changed by assembly within a complete structure is unknown, but there is evidence that certain structures do not change these frequencies greatly but merely increase the damping.

4.4 Acoustic Emission

B. H. Schofield in the Dictionary of Physics defines acoustic emission phenomena as follows:

> "Acoustic Emission is a generic term denoting the occurrence of deformation induced sound pulses or elastic waves in metals. This term includes those sounds that are usually audible, as well as those that are not (that is, ultrasonic frequencies, Ed.) The audible sounds are more commonly known as the phenomenon 'tin cry,' which is produced by the twinning deformation so common in the tetragonal and hexagonal crystallographic structures. Two other processes which may also produce audible (and ultrasonic, Ed.) sounds are: (1) sudden re-orientation of large grains in a polycrystalline material, and (2) the martensite transformation associated with the heat treatment of steel. The inaudible emission (ultrasonic frequency, Ed.) is of greater import, since it is ubiquitous in metals, being related to the more efficacious deformation process, slip.*
>
> "Evidence of acoustic emission becomes apparent almost immediately upon stressing many metals, particularly those that do not exhibit a 'linear' response of the stress-strain curve. In other metals, it appears at stress levels 1/3 to 1/2 the nominal engineering yield point. Characteristically, all metals exhibit two distinct types of emission, referred to as burst type and high frequency type. The relative activity of the two types varies with different metals and alloys, with pure zinc and pure aluminum representing the extremes; zinc being predominantly a burst type and the aluminum almost entirely the high frequency type.*

* Clarification and revised punctuation of these and the following quoted paragraphs provided by the editor.

USE FOR TYPEWRITTEN MATERIAL ONLY

U3 4802 1434 REV. 8-65

"As observed on an oscilloscope screen, the burst type appears as an exponentially decaying ring down pulse, with a periodicity of occurrence long relative to the pulse time constant. The high frequency type is somewhat more subtle, and appears as an amplitude rise of the general background noise level, with occurrence periodicity of the pulses comparable to their time constant. In contrast to the burst type, which does not change amplitude significantly as deformation proceeds, the high frequency rises to appreciable amplitude levels, usually becoming maximal just prior to gross yielding and again prior to final failure. Of the two types, the high frequency (ultrasonic, Ed.) is most interesting from the deformation mechanics view.

"Significant characteristics of the acoustic emission are: it is irreversible (Kaiser Effect); it is a volume, as opposed to a surface phenomenon; the amplitude level (high frequency type) is proportional to strain rate, the emission signal repetition rate ranges from a few hundred counts per second to 75,000 per second at normal loading rates, (and, Ed.) evidence indicates a direct correlation between the number of fine slip lines and the number of acoustic pulses. These acoustic pulses evidence the discontinuous nature of deformation on a micro-scale suggestive of the macro Portevin-LeChatelier Effect and stepped stress-strain curve.

"The irreversibility characteristic is most unique and, aside from its physical implications, offers the possibility of application as a tool with non-destructive potentialities. Once the material is subjected to a given state of stress and deformation, during which considerable emission is generated, subsequent restressing up to the previous stress level will not induce emission. Exceeding the previous stress level produces an abrupt reappearance of the emission at usual tensile loading rates. This property is the most positive evidence of the intimate relationship between emission and permanent deformation. The appearance of the emission in aluminum, for example, at 1/3 the nominal yield strength demonstrates the existence of localized plastic deformation. Aging, heat treating, or otherwise restoring the material to the un-stressed state will, of course, restore the emission; the degree of restoration depending on the completeness of the treatment.

"The fundamental mechanism giving rise to the inaudible emission has not been conclusively idenitified to date. Present results indicate a source intimately associated with the dynamic response of dislocation blocking and unblocking."

The burst type and high frequency type emission referred to above, in current practice, are known as burst type and continuous type. Work done by D. L. Parry of the Phillips Petroleum Company in the detection of defects in large nuclear reactor pressure vessels indicates that burst type signals emanate from the growth of defects and/or flaws within the pressure vessel. He states:

"During our feasibility studies, two types of acoustic emissions have been characterized; the 'Burst' signal, indicative of material flaw growth, and the low amplitude, so-called continuous emission, due primarily to stress-induced dislocation movement. The 'Burst' signals allowed location of the flaw through triangulation techniques. Times of arrival of

USE FOR TYPEWRITTEN MATERIAL ONLY

U3 4802 1434 REV. 8-65

the initial, high amplitude 'Burst' signal from three transducers provide information for triangulation purposes. The detection threshold for the 'Burst' type signal was 0.1 to 30% of normal vessel operated stress and 0.02% to 5% of the nominal material yield."

Thus, Parry concludes that, with proper detection, signal conditioning, and diagnostics, acoustic signals could be detected, recorded, and analyzed to yield information regarding the presence of flaws in large, complex, reactor vessels under low stress conditions. Parry anticipates that the continuous-emission, energy-released signature of the pre-annealed hydrostatic test will yield information on the degree of change in vessel embrittlement when compared with the post-annealed acoustic signature.

In ball bearings, both of these types of acoustic emission have been observed. The characteristic "burst" type emission occurred when flaws were placed in the inner race, the outer race, and on a ball. The so-called continuous signal has been observed in a dry bearing operated at 5000 to 10,000 RPM and in a bearing operated through a 30 degree arc at low speed, with the application of 450 degrees of heat in a vacuum, under 20 pounds of stress. In the latter bearing test setup, wherein one bearing was failed using only dry lubricant, a very high rate of acoustic emission signals occurred during and prior to actual seizure of the bearing. A great deal of wear occurred in this particular bearing due to oxidation of bearing surfaces and subsequent scaling of the oxidized layer. A large number of "burst" signals, as many as 30,000 per minute, were observed during this wear process. In the bearings tested in the Pope Spindle, operated at 5000 and 10,000 RPM, the "burst" type signals were attributed to growth of the artificially placed flaw and to resonant ringing of the bearing components.

Acoustic emission monitoring was attempted as a sideline on a bearing fatigue test being run. The bearing was a front main bearing from a J-69 jet engine. It was run at 3600 RPM under 3000 lbs. radial load until the first indication of fatigue failure was noted. The piezoelectric transducer output was passed through a high-pass (20 KC) filter and into a Berkeley EPUT counter, which was set to count all bursts over 1.0 volt amplitude. A plot of the counts per unit time is shown in Figure 27 below.

It will be noted in Figure 27 that a marked rise in counts per minute occurred approximately 45 minutes before actual spalling of the bearing. If this count history were adjusted to conform to the normal service life conditions, it is felt that impending failure would have occurred sufficiently early to permit preventive maintenance action.

USE FOR TYPEWRITTEN MATERIAL ONLY

U3 4802 1434 REV. 8-65

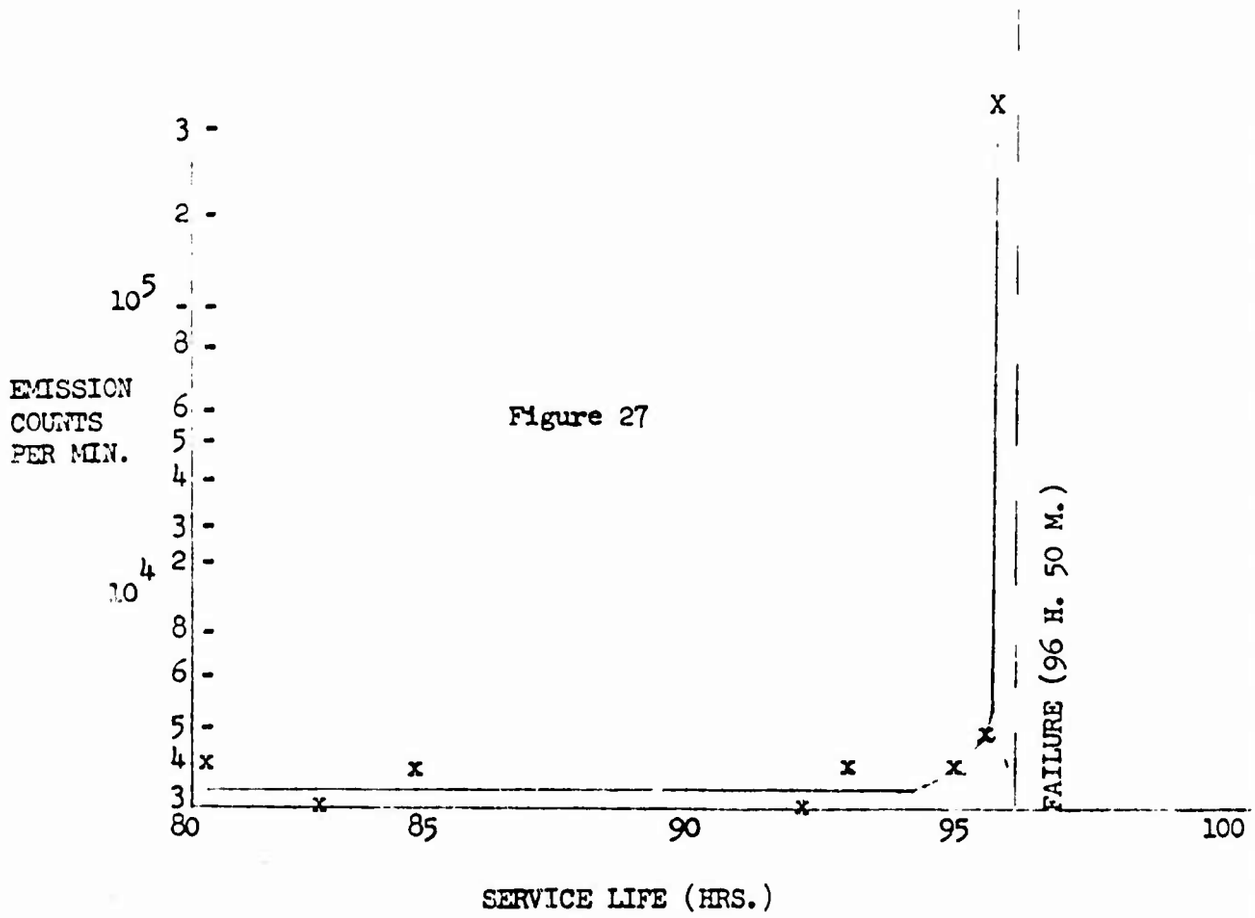

Figure 27

USE FOR TYPEWRITTEN MATERIAL ONLY

U3 4802 1434 REV. 8-65

5.0 DEFINITIONS

A. Reliability (R)

The probability that a system or portion of a system will perform its specified function(s) under specified conditions for the specified period of time or number of cycles or trials, when installed, tested/used, maintained, and logistically supported as specified.

B. Failure

The inability of a system or portion of a system to perform its specified function(s) under specified conditions for the specified period of time or number of cycles or trials, when installed, tested/used, maintained, and logistically supported as specified. Number of failures is denoted by "f."

C. Defect

A non-conformance to specification/drawing which has not resulted in a failure.

D. Wear

Gradual, cumulative change to a physical or chemical characteristic of a device resulting from continued operation or use. (Not as a result of failure).

E. Maintenance *

All the activities necessary to keep subsystems in, or restore them to, a satisfactory operating condition. Scheduled maintenance is preplanned for accomplishment at given points or intervals. All other maintenance is classed as unscheduled.

F. Incipient Failure **

An impending failure or an existing characteristic or defect which will lead to failure.

---

* Not a reliability definition, but included herein for convenience. Ed.

** This is a tentative definition, i.e., not formally accepted at this time. Ed.

USE FOR TYPEWRITTEN MATERIAL ONLY

U3 4802 1434 REV. 8-65

6.0 REFERENCES

1. Parry, D. L., "Non-destructive Flaw Detection, Nuclear Power Installations," Page 111, Incipient Failure Diagnosis for Assuring Safety and Availability of Nuclear Power Plants, United States Atomic Energy Commission, Division of Technical Information, Published January 1968.

2. Sternlicht, Veno, "Analysis, Detection and Control of Failures in Mechanical Equipment," Page 284, Incipient Failure Diagnosis for Assuring Safety and Availability of Nuclear Power Plants, United States Atomic Energy Commission, Division of Technical Information, Published January 1968.

3. Love, A. E. H., Treatise on The Mathematical Theory of Elasticity, New York, N. Y.: Dover Publications, Inc., 1944. (Pages 204-206, 451-453).

4. Schofield, B. H., Encyclopaedic Dictionary of Physics, Supplementary Volume 1, (Pg. 1, 2, & 3), Oxford, London, New York, Paris· Pergamon Press, 1967.

5. Palmgrin, Arvid, Ball and Roller Bearing Engineering, Section 24, Philadelphia, Penn: S. H. Burbank & Co., 1959.

USE FOR TYPEWRITTEN MATERIAL ONLY

U3 4802 1434 REV. 8-65

7.0 BIBLIOGRAPHY

Crimmins, P. P., Green, A. T., Development of a Nondestructive Testing Technique to Determine Flaw Criticality, Advanced Research Projects Agency, ARPA Order No. 1244, Program Code Number 8D10.

Dunegan, H. and Harris, D., Acoustic Emission-A New Nondestructive Testing Tool, Lawrence Radiation Laboratory, University of California, Livermore, 16 January 1968.

Hutton, Phillip H., Acoustic Emission in Metals as an NDT Tool, Pacific Northwest Laboratories, Battelle Memorial Institute, Richland, Washington, 16-19 October 1968.

Kusenberger, Felix N., Leonard, Byron E., Barton, John R., and Donaldson, W. Lyle, Nondestructive Evaluation of Metal Fatigue, Southwest Research Institute, 8500 Culebra Road, San Antonio, Texas 78206, March 1965.

Parry, D. L., Nondestructive Flaw Detection by Use of Acoustic Emission, Phillips Petroleum Company, AEC Research & Development, Reactor Technology, TID 4500, May 1967.

Randall, R. L., Application of Noise Analysis Techniques to Detection of Incipient Malfunctions, Atomics International, Canoga Park, California, 30, 31 October and 1 November 1967.

Schofield, B. H., Acoustic Emission Under Cyclic Stress, Final Report, TR 796/P31, (Lessells & Assoc.), July 1964.

Schofield, B. H.,"Acoustic Emission from Metals, Its Detection, Characteristics and Source," Proceedings of the Symposium on Physics and Nondestructive Testing, Southwest Research Inst., San Antonio, Texas, 1963.

Weiss, V., et al; Crack Initiation and Crack Propagation in Structural Metal Alloys, Final Report, SURI Met-E-1209-0666F (Syracuse Univ. Res. Inst.), June 1966.

The Early Detection of Fatigue Damage, North American Rockwell/Los Angeles Division, First Semiannual Report, 1968 July 1 - 1969 February 28.

USE FOR TYPEWRITTEN MATERIAL ONLY

U 3 4802 1434 REV. 8-65

USE FOR TYPEWRITTEN MATERIAL ONLY

SECTION 8.0 APPENDICES

8.1 Rotational Frequencies

The frequencies of rolling elements passing over a spot on the inner and outer races, as given by equations (1) and (2) in the text are:

	5000 RPM	10,000 RPM
f_{outer}	356 CPS	712 CPS
f_{inner}	562 CPS	1124 CPS

When the "spot" on one of the races is a flaw, these frequencies are the pulse-repetition frequencies of a series of mechanical impacts, and is therefore a pulse train.

For the purpose of detecting these rotational frequencies on a power spectral density plot, we must examine the pulse train to ascertain the frequency content of such a function. This is accomplished by a Fourier wave form analysis.

The pulse train function is described in Figure A-1 below -

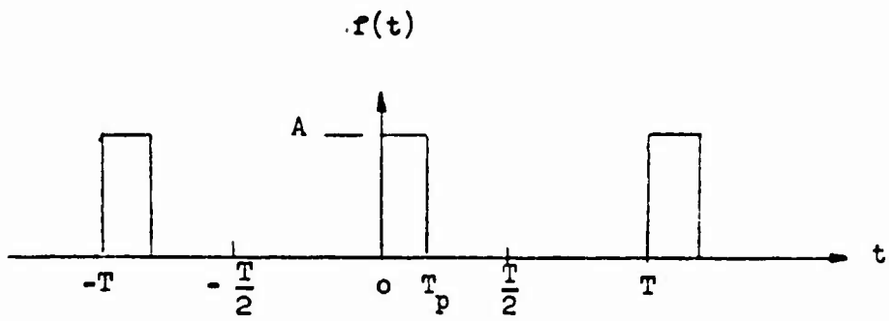

Figure A-1

In Figure A-1, T is the period of the function, T_p is the pulse width, and A is the pulse amplitude.

The expression for this function in one period is:

$$f(t) = \begin{cases} o, & -\frac{T}{2} < t < o \\ A, & o < t < T_p \\ o, & T_p < t < \frac{T}{2} \end{cases} \qquad \text{(A-1)}$$

The exponential form of a Fourier series expansion of a periodic function of period T is [1]:

$$f(t) = \sum_{n=-\infty}^{+\infty} \alpha_n \, e^{jn\omega t} \qquad \text{(A-2)}$$

1.) D. K. Cheng, Analysis of Linear Systems, Reading, Mass.: Addison-Wesley Publishing Co., May 1961

USE FOR TYPEWRITTEN MATERIAL ONLY
US 4802 1434 REV. 8-65

$$\alpha_n = \frac{1}{T} \int_{-T/2}^{T/2} f(t)\, e^{-jn\omega t}\, dt \qquad \text{(A-3)}$$

Where:

$j = \sqrt{-1}$

$\omega = \frac{2\pi}{T}$ and

α_n = the average value of the exponential form of f(t) in one period.

Substituting the expression (A-1) for f(t) into (A-3) gives

$$\alpha_n = \frac{A}{n\pi}\, e^{jn\pi \frac{T_p}{T}} \sin\left(n\pi \frac{T_p}{T}\right) \qquad \text{(A-4)}$$

The frequency spectrum of the pulse train is obtained by plotting

$2\left|\alpha_n\right|$ versus $n\omega = \left(\frac{2\pi n}{T}\right)$

$$2\left|\alpha_n\right| = \frac{2A}{n\pi}\left|\sin n\pi \frac{T_p}{T}\right| \qquad \text{(A-5)}$$

For n = o, equation (A-4) is evaluated using l'Hospital's rule and

$$\alpha_o = A\,\frac{T_p}{T} \qquad \text{(A-6)}$$

This is the equivalent DC component of the series.

To evaluate the ratio $\frac{T_p}{T}$:

The pulse width, T_p, is the time duration of the physical impact; in this case, the time during which a ball is impacting a flaw in one of the races. The period of impacts is, of course, T. To evaluate T_p, we assume the ball rolls down into the flaw and the impact commences when the ball strikes the far edge of the impact. If the flaw width is small relative to the ball diameter, then the ball center is over the center of the flaw at this point - see Figure A-2. Assuming a perfectly plastic impact (i.e. no bounce), the duration of the impact is equal to the time required for the ball to roll up and over the far edge of the flaw.

Again, relying on the assumption that the flaw width (W) is small compared to the ball diameter, the horizontal ball velocity is essentially constant, and the impact duration equals the time required for the ball to travel $\frac{W}{2}$.

Therefore, $T_p = \frac{W}{2\,v}$

where v is the ball velocity relative to the race. Assuming that the slippage between the ball and race is negligible, the velocity becomes

$$v = 2\pi\, r_b\, f_b \qquad \text{(A-7)}$$

USE FOR TYPEWRITTEN MATERIAL ONLY
U3 4802 1434 REV. 8-65

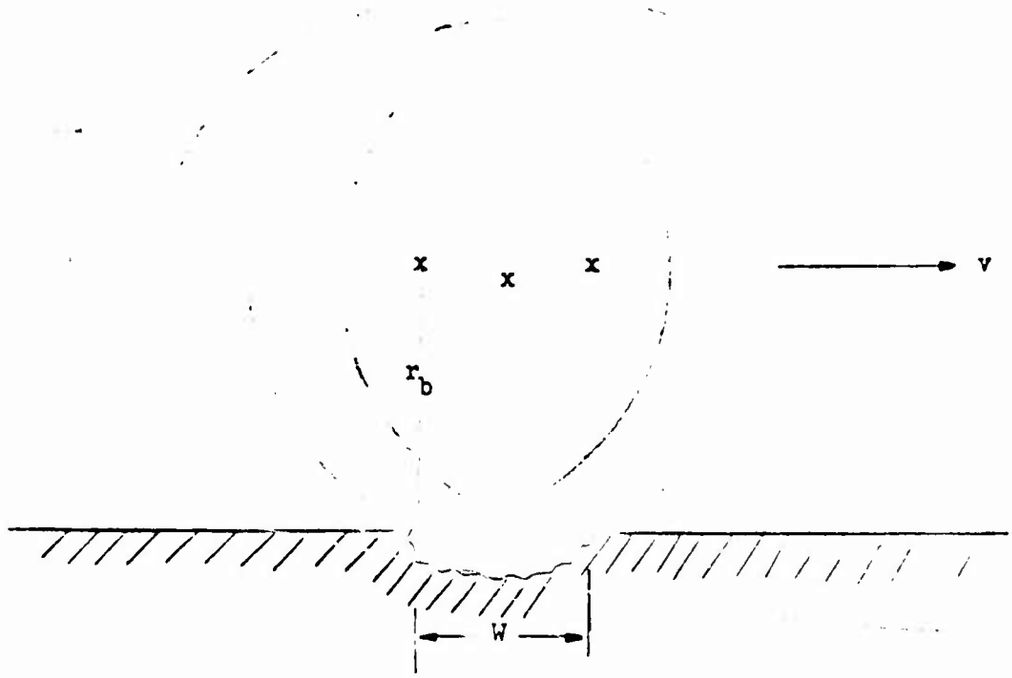

Figure A-2

where r_b is the ball radius and f_b is the ball rotational frequency given by equation (3) in the text.

$$\text{Therefore,} \quad T_p = \frac{W}{4\pi\, r_b\, f_b} \qquad \text{(A-8)}$$

The period (T) depends upon which race the flaw is in. For the inner race, the period is the reciprocal of equation (2) and, for the outer race, it is the reciprocal of equation (1). The ratio T_p/T is independent of bearing RPM; these two ratios for inner and outer race flaws being:

$$\text{Inner Race:} \quad T_{p/T} = 1.675\ W \qquad \text{(A-9)}$$

$$\text{Outer Race:} \quad T_{p/T} = 1.06\ W \qquad \text{(A-10)}$$

The width (W) of the largest flaw injected into bearings 4, 6, and 7 was approximately 0.02 inches. Using this as the typical width, and substituting this into equations A-9 and A-10, the ratios become:

$$\text{Inner Race:} \quad T_{p/T} = 0.0335$$

$$\text{Outer Race:} \quad T_{p/T} = 0.0212$$

Substituting these values in the expression (A-5), and plotting these values versus n, yields the pulse train frequency spectrum shown in Figure A-3 below.

USE FOR TYPEWRITTEN MATERIAL ONLY
U3 4802 1434 REV. 8-65

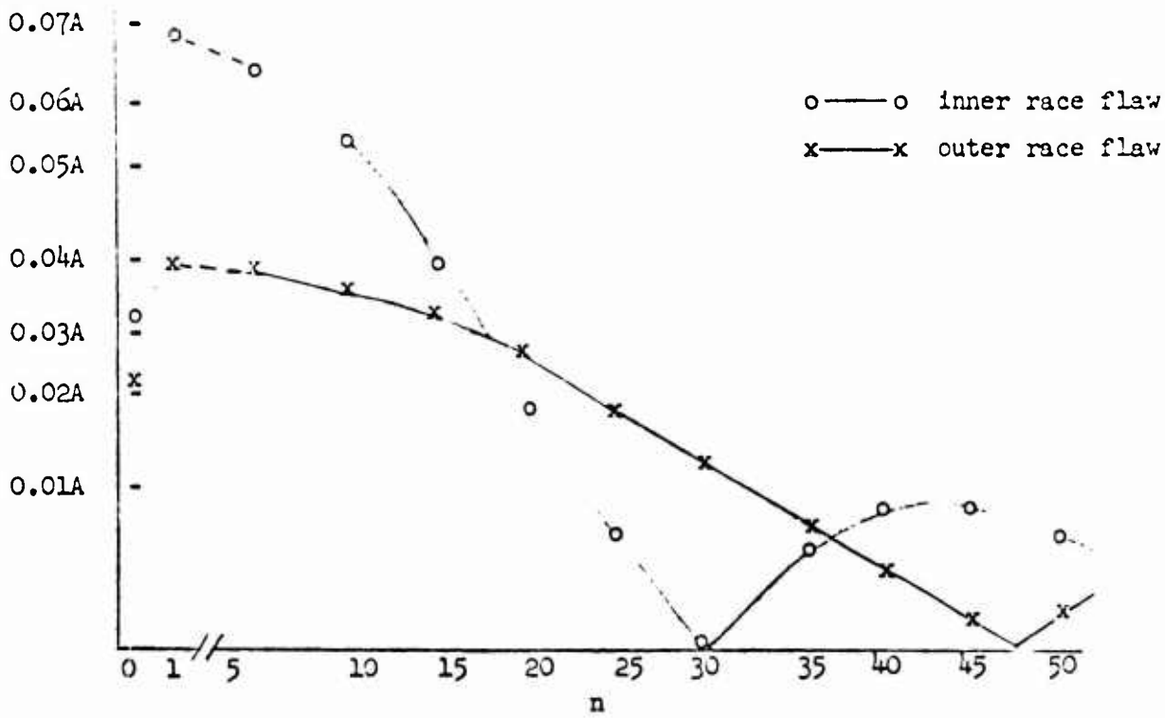

Figure A-3

Figure A-3 shows that the fundamental frequency is the largest amplitude and even this is only a small fraction of the pulse train amplitude. In these series of tests, the amplitude of the pulses would be small in view of the small flaw width and the fact that the bearings were run unloaded.

USE FOR TYPEWRITTEN MATERIAL ONLY

8.2 Resonant Frequencies

The resonant frequencies of the major components of the S-204H bearing are "free-free" oscillations and would not necessarily be exhibited as calculated when the bearing is assembled into a structure and subjected to loading. The variation from the calculated frequencies may be considerable, depending upon the lubrication, loading, and overall fit of all components within the bearing and the fit into the structural assembly. The calculation of these frequencies is based on M-50 Tool Steel material with a density of 0.283 lb/in^3 and a Young's modulus of elasticity of 30×10^6 PSI. It was assumed that the cross-sectional area of the races were rectangular.

The equations used are as follows:

Ball: $$f\ (cps) = \frac{0.424}{r}\sqrt{\frac{E}{2\rho}} \qquad (\#4)$$

Ring: $$f\ (cps) = \frac{n\,(n^2 - 1)\sqrt{\frac{E\,I}{m}}}{2\pi\ a^2\ \sqrt{n^2 + 1}} \qquad (\#5)$$

Where:

r (ball)	=	radius (ft)
a (ring)	=	radius to neutral axis (ft)
E	=	Young's modulus (Lb/ft^2)
I	=	Moment of inertia of cross-sectional area about the neutral axis (ft^4)
ρ (ball)	=	density ($slugs/ft^3$)
m (ring)	=	density (slugs per linear foot)
n	=	number of waves around circumference of ring

<u>MATERIAL: M-50 TOOL STEEL</u>:

$$E = 30.10^6 \text{ psi}$$

$$\rho = 0.283\ Lb/in^3$$

$$\rho = 0.283\ \frac{Lb}{in^3} \times 1728\ \frac{in^3}{ft^3} \times \frac{1}{32.2}\ \frac{slug}{Lb}$$

$$\rho = 15.2\ slugs/ft^3$$

$$E = 30.10^6\ \frac{Lb}{in^2} \times 144\ \frac{in^2}{ft^2}$$

$$E = 4.32 \cdot 10^9\ Lb/ft^2$$

USE FOR TYPEWRITTEN MATERIAL ONLY

U3 4802 1434 REV. 8-65

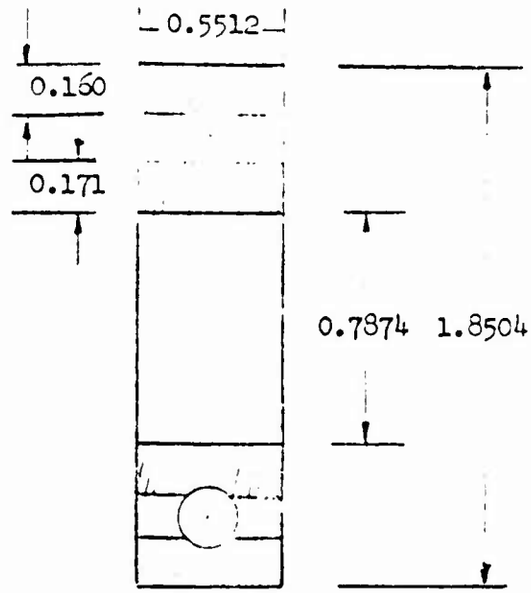

Ball Dia. = 0.3125"

Figure B-1

BALL COMPUTATIONS:

$$\sqrt{\frac{E}{2\rho}} = 11.9 \cdot 10^3$$

$$r = \frac{0.3125}{2 \times 12} = 0.013 \text{ ft.}$$

$$\text{Let } A = \frac{1}{r}\sqrt{E/2\rho}$$

$$A = 0.92 \cdot 10^6$$

DEFORMATIONAL FREQUENCIES:

$$\text{Ball: } f = \frac{0.424}{r}\sqrt{\frac{E}{2\rho}} = 0.388 \cdot 10^6 \text{ cps}$$

$$\text{Ball: } f = 388 \text{ KC}$$

RADIAL MOTION MODES:

$f_1 = 0.92A = 0.84$ MC

$f_2 = 1.49A = 1.36$ MC

$f_3 = 1.96A = 1.79$ MC

$f_4 = 2.47A = 2.26$ MC

$f_5 = 2.97A = 2.72$ MC

$f_6 = 3.98A = 3.64$ MC

USE FOR TYPEWRITTEN MATERIAL ONLY

U3 4802 1434 REV. 8-65

The ball deformational resonant frequency, calculated above as 388 KC, is the lowest frequency for what is termed "spheroidal vibrations." There are vibrations of a dilatational type whereby the sphere dilates and contracts radially and shear types in which there are twisting motions within the ball. It was felt that the spheroidal motions, wherein the sphere was distorted to an ellipsoid of revolution, becoming alternately prolate and oblate on a microscopic scale, are most representative of the actual deflection of the ball within the bearing assembly. The radial motion modes, calculated above, are well above the range of the transducer employed. It is our intention in future work to investigate the possible existence of these frequencies with higher frequency transducers and to determine the effect of defects on these frequencies. Under certain conditions of interference, the frequency band represented by these radial motion modes may be important. The inner race and outer race computations are based upon calculations of ring frequencies taken from page 452 in reference (3). The equation employed for resonant frequency in cycles per second is as follows:

$$f_n = \frac{n\,(n^2 - 1)\sqrt{\frac{EI}{m}}}{2\pi\ a^2\sqrt{n^2 + 1}} \qquad (\#5)$$

Where: $EI = Lb/ft^2$

m = slugs per linear foot

a = ring radius in ft

I = area moment of inertia of race about neutral axis

n = number of waves around ring

n = 2, 3, 4, 5.....

For inner race:

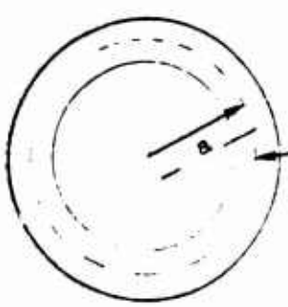

Neutral Axis

$a = 0.5147'' = 0.0428'$

Cross Section

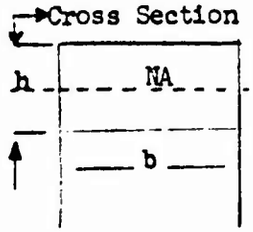

$I_{NA} = \frac{bh^3}{12}$ where $b = 0.046'$, $h = 0.0142'$

$I_{NA} = 1.1 \times 10^{-8}$

USE FOR TYPEWRITTEN MATERIAL ONLY

U3 4802 1434 REV. 8-65

$$E = 30 \cdot 10^6 \ \frac{Lb}{in^2} \times 144 \ \frac{in^2}{ft^2} = 4.32 \cdot 10^9 \ \frac{Lb}{ft^2}$$

$$\rho = 0.283 \ \frac{Lb}{in^3} \times 1728 \ \frac{in^3}{ft^3} = 488 \ Lb/ft^3$$

$$m \left(\frac{Lb}{ft}\right) = p.b.h. = 0.319 \ \frac{Lb}{ft}$$

$$m \left(\frac{slugs}{ft}\right) = \frac{0.319}{32.2} = 0.0099 \ \frac{slugs}{ft}$$

$$\sqrt{\frac{EI}{m}} = \sqrt{\frac{(43.2 \cdot 10^8)\ (1.1 \cdot 10^{-3})}{9.9 \cdot 10^{-2}}} = \sqrt{4.8 \cdot 10^3}$$

$$\sqrt{\frac{EI}{m}} = 69.3$$

$$\frac{1}{a^2} = \sqrt{\frac{EI}{m}} = 3.78 \cdot 10^4$$

n	2	3	4	5
$\frac{n\,(n^2 - 1)}{2\pi\sqrt{n^2 + 1}}$	0.428	1.21	2.32	3.75
f_n	16.2 K	45.7 K	87.7 K	142.0 K

For outer race:

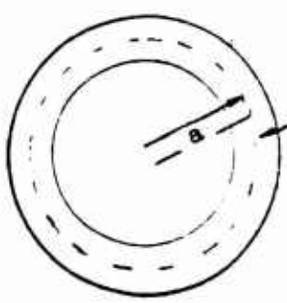

Neutral Axis

$a = 0.99'' = 0.083'$

USE FOR TYPEWRITTEN MATERIAL ONLY

U3 4802 1434 REV. 8-63

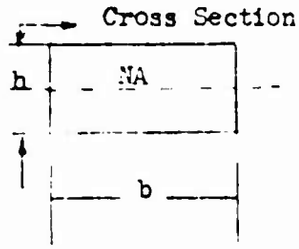

$$I_{NA} = \frac{bh^3}{12}$$

$$I = 0.491 \cdot 10^8 \ ft^4$$

where:

$b = 0.046'$

$h = 0.13'' = 0.0108'$

$$E = 4.32 \cdot 10^9 \ \frac{Lb}{ft^2}$$

$$m = \frac{(488)b \cdot h}{32.2} = 0.00753 \ \frac{slugs}{ft}$$

Thus,

$$\sqrt{\frac{EI}{m}} = 53.1$$

Therefore,

$$\frac{1}{a^2}\sqrt{\frac{EI}{m}} = 0.77 \times 10^4$$

n	2	3	4	5
$\frac{n(n^2-1)}{2\pi\sqrt{n^2+1}}$	0.428	1.21	2.32	3.75
f_n	3.29 K	9.32 K	17.9 K	28.9 K

These calculations indicate that a wide band of frequencies extend from a few kilocycles to 40 kilocycles and above, including harmonics. As these frequencies are driven higher in amplitude, hidden harmonics should appear, extending to and well above 100,000 cycles per second. Because of the interaction between the components of a bearing, a defect in any one component would cause ringing in all components. Accordingly, there exists a direct relationship between amplitude of these frequencies and severity (size and depth) of the defect. Hence, it does not appear necessary to positively identify each resonant frequency, nor does it appear feasible at the present time. Nevertheless, this band of frequencies, directly related as it is to the severity of the defect, can be employed in incipient failure detection. This has been demonstrated by translating this band of frequencies back to the audible region and listening to the sounds of defects in a ball bearing. It has been further demonstrated that the peak spectral density G's correlate directly to the severity of defects in bearings.

USE FOR TYPEWRITTEN MATERIAL ONLY

U3 4802 1494 REV. 8-65

8.3 Raw Data

This appendix contains the power spectral density plots made for each individual test run.

8.3.1 First Series

Figures C-1 through C-22 are the direct recording PSD's made for bearing numbers 1, 2, 3, and 5.

8.3.2 Second Series

Figures C-23 through C-40 are the direct recording PSD's for the second set of bearings, numbers 4, 6, and 7 in the several test conditions.

8.3.3 FM Data

Figures C-41 through C-58 are the PSD's made from the FM data recorded from the tests on bearings 4, 6, and 7.

USE FOR TYPEWRITTEN MATERIAL ONLY

U3 4802 1494 REV. 8-65

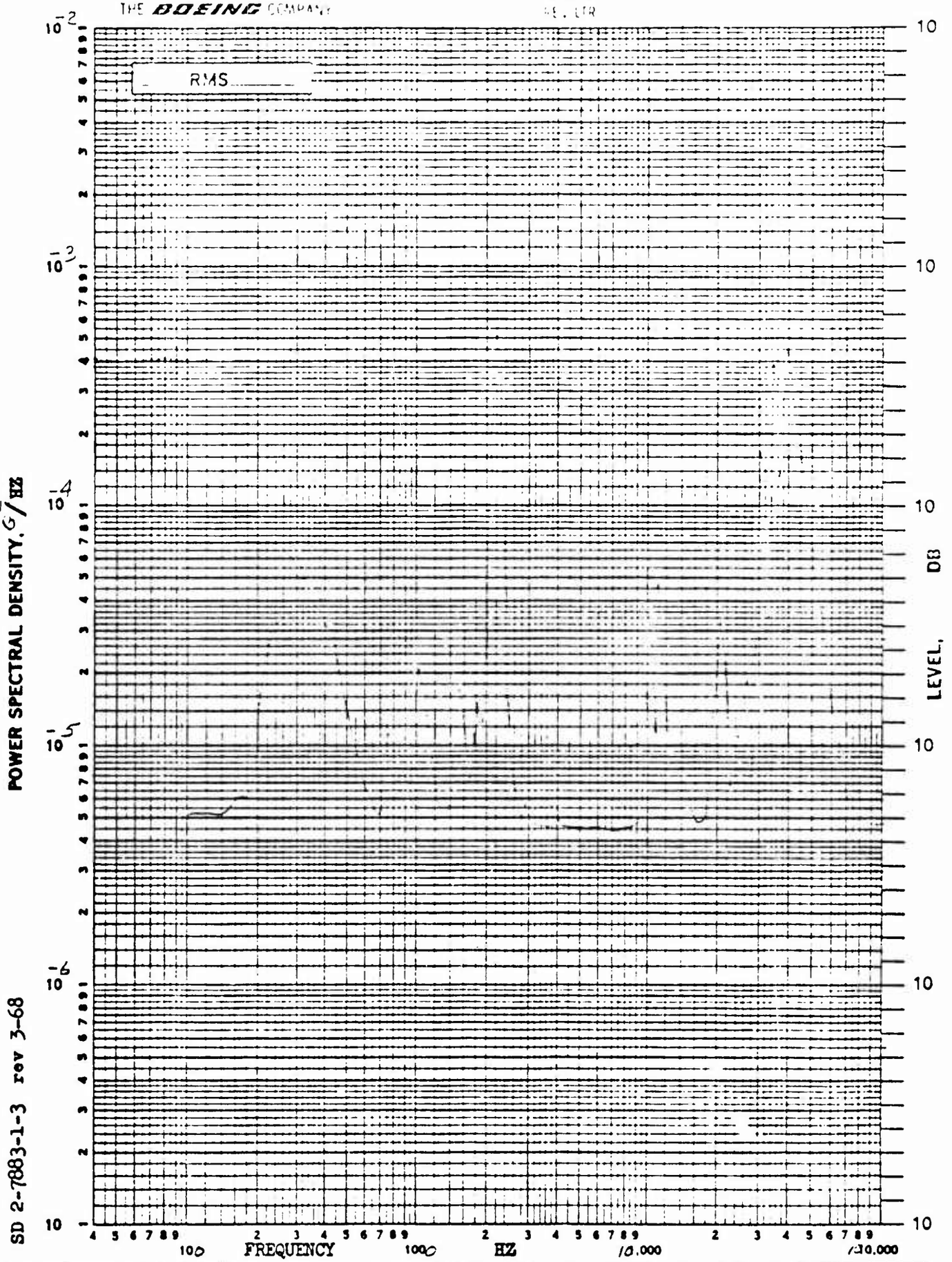

CALC.	[illegible]	D[illegible]	Bearing #1 Max Load 5000 RPM
CHECK	[illegible]	A[illegible]	
APP'D		T	
APP'D		E	

Figure C-1
D2-113029-3

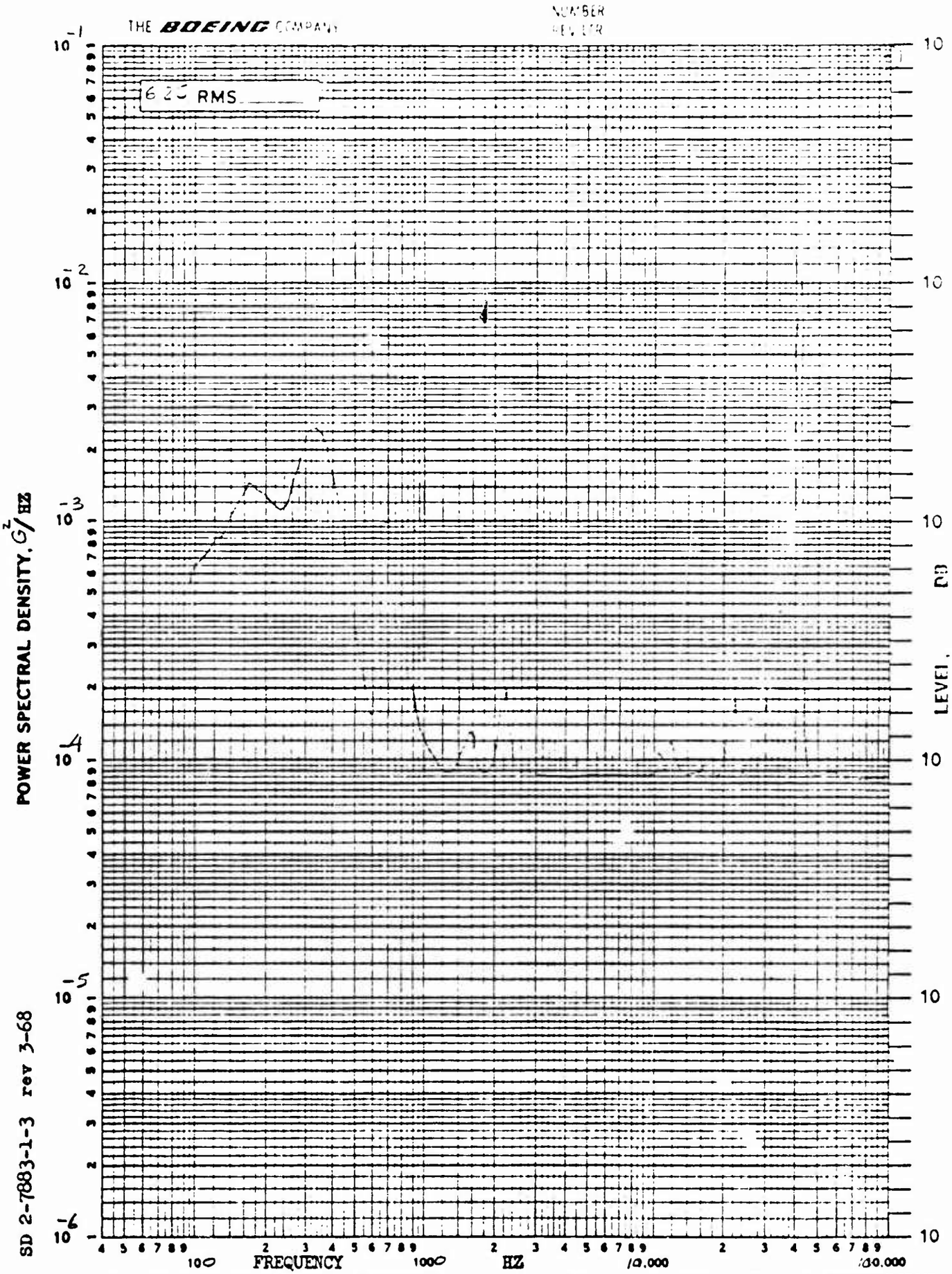

160-3 -20 db .312 VRMS

CALC.		D	
CHECK		A	
APP'D		T	
APP'D		E	

Bearing #1 New Lubed
10,000 RPM

Figure C-2
D2-113029-3

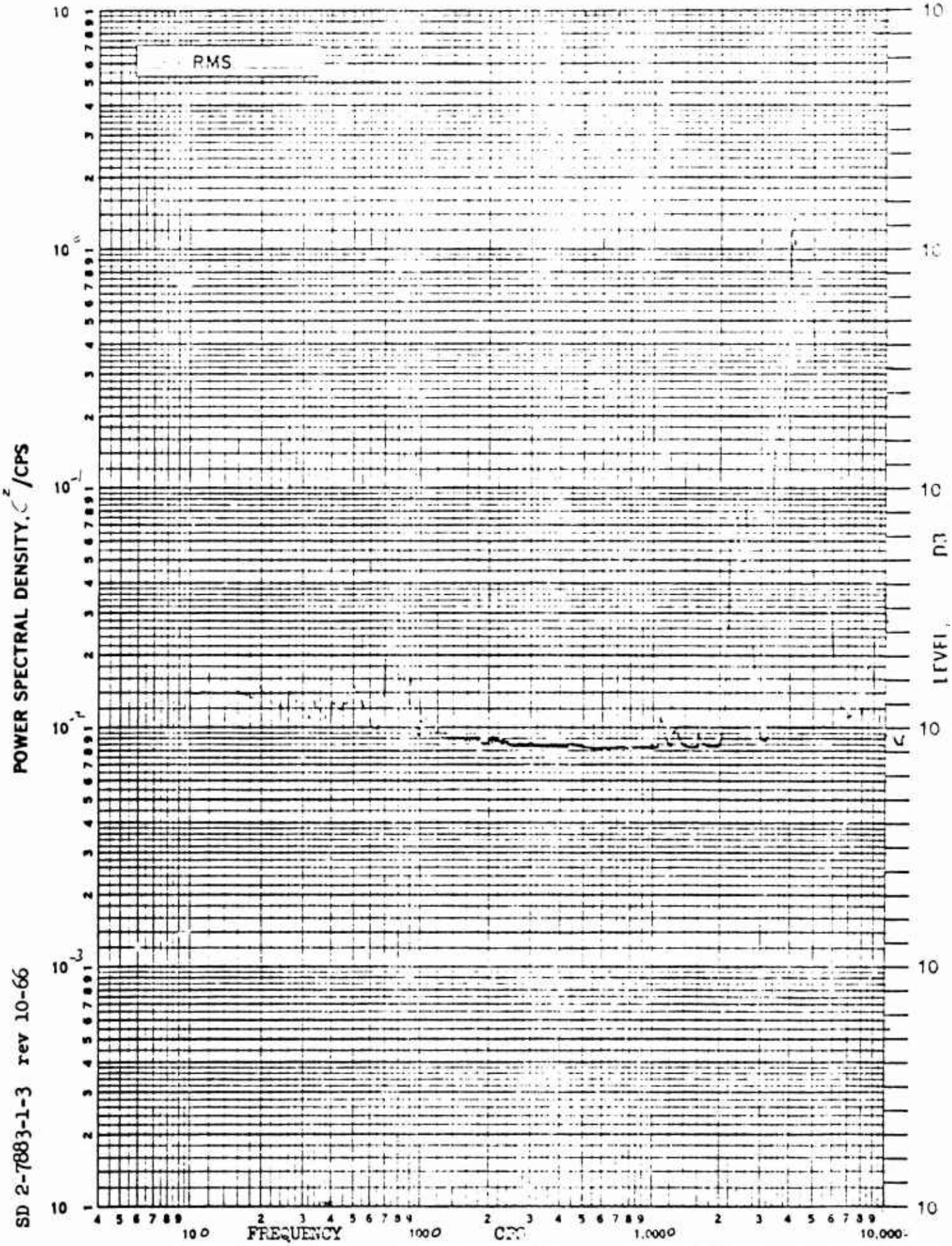

CALC.		D	
CHECK		A	
APP'D		T	
APP'D		E	

5000 RPM

Figure C-3
D2-113029-3

PAGE: 63

SD 2-7883-1-3 rev 10-66

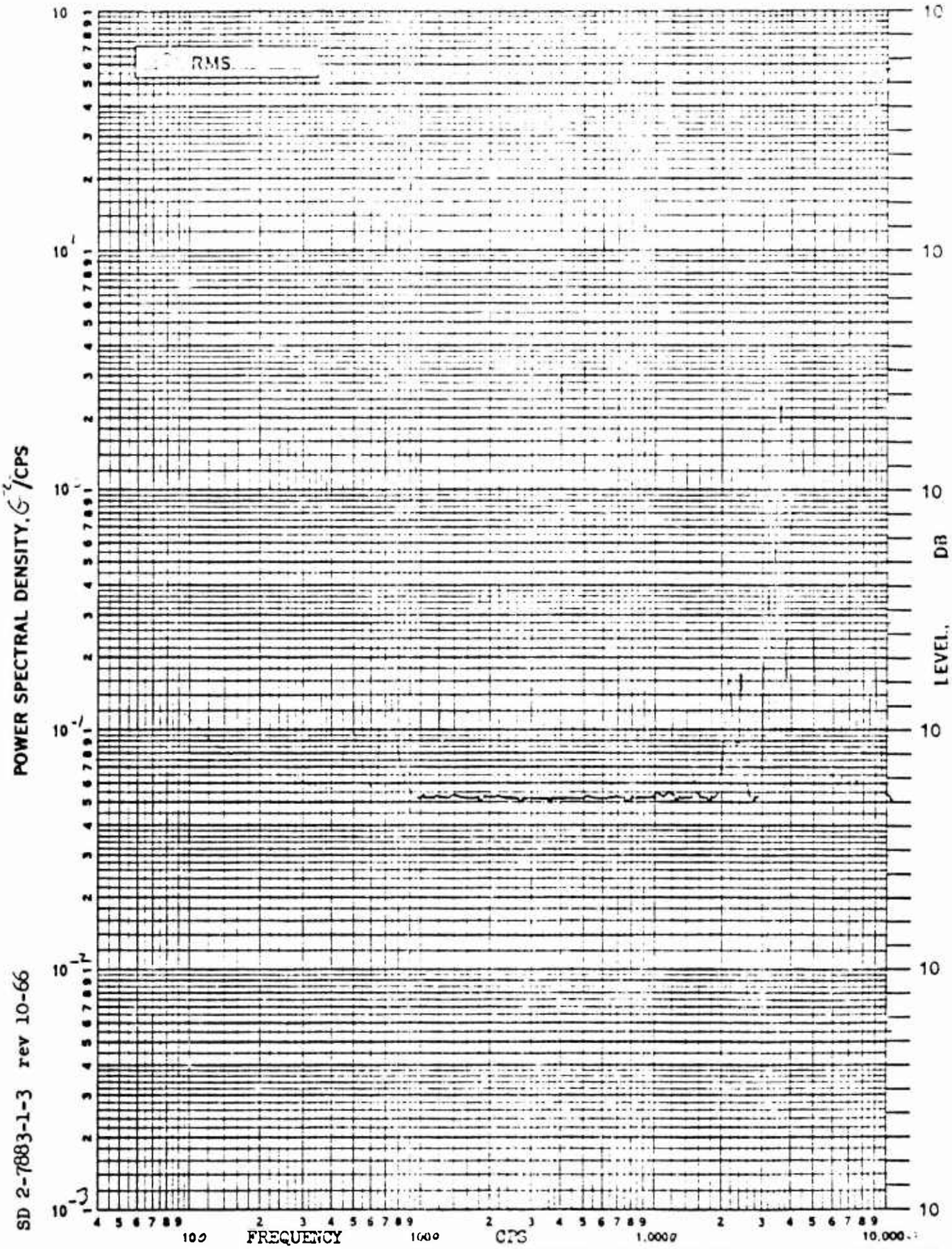

CALC.	[illegible]	D/-17-7	Bearing # 1 No Lube 10,000 RPM.	Figure C-4
CHECK		A[illegible]		D2-113029-3
APP'D		T		
APP'D		E		PAGE: 64

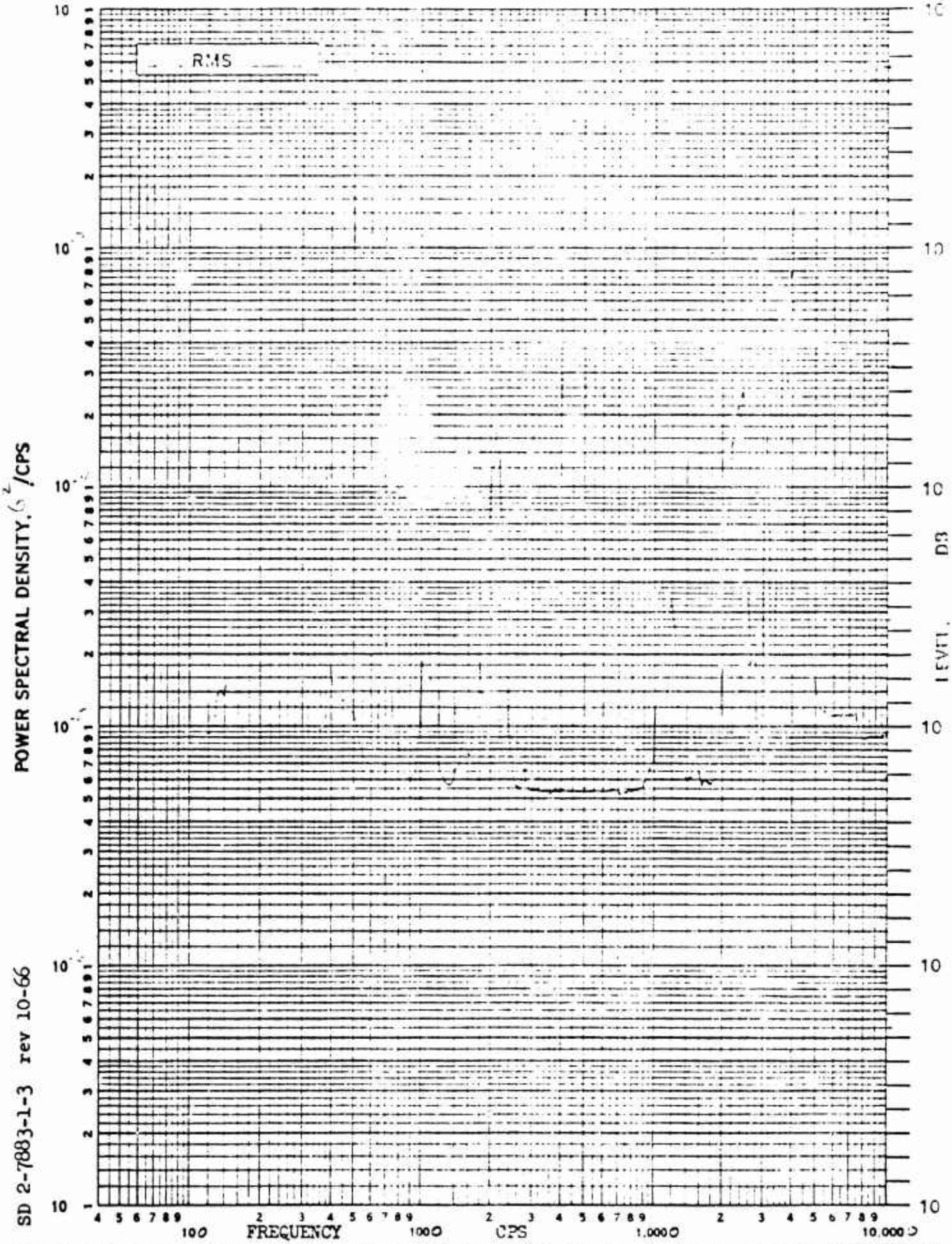

CALC.		D	Bearing #1 Relubed
CHECK		A	5000 RPM (Run in at 10,000
APP'D		T	
APP'D		E	

Figure C-5
D2-113020-3
PAGE: 65

SD 2-7883-1-3 rev 10-66

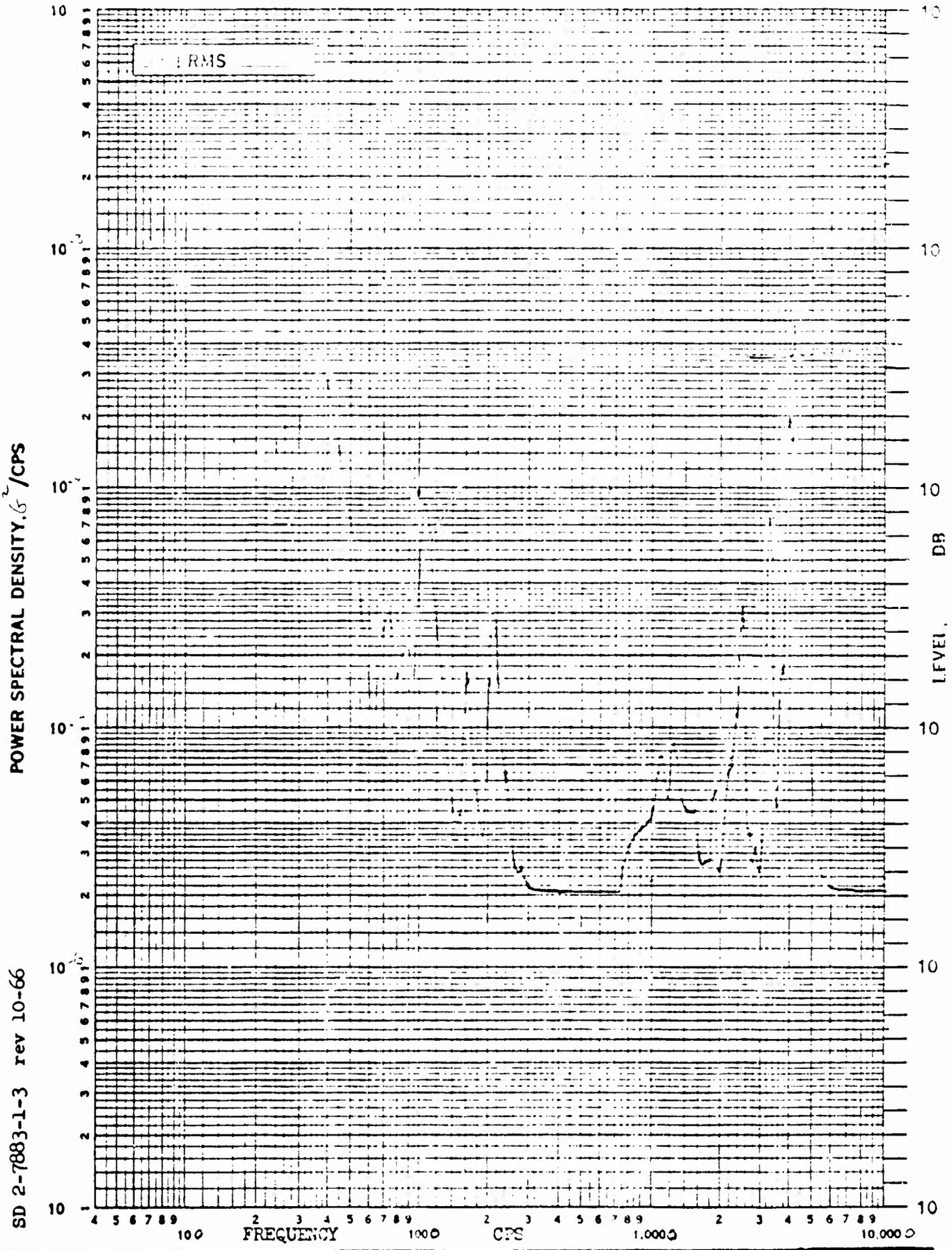

CALC.		D	Bearing # 1 Relaxed 10,000 RPM.
CHECK		A	
APP'D		T	
APP'D		E	

Figure C-6
D2-113029-3

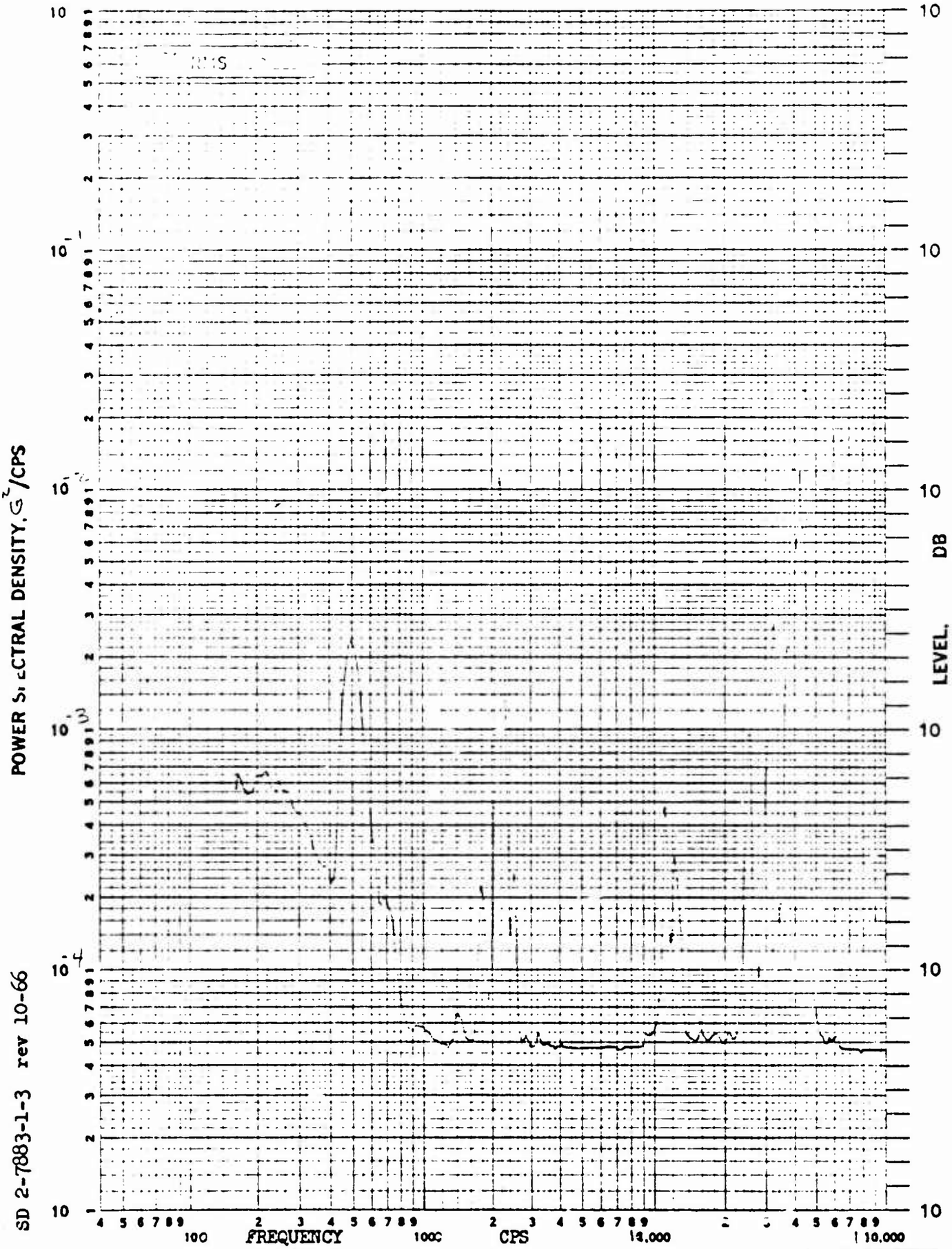

CALC.		D		Figure C-7
CHECK		A		D2-113029-3
APP'D		T		
APP'D		E		PAGE: 67

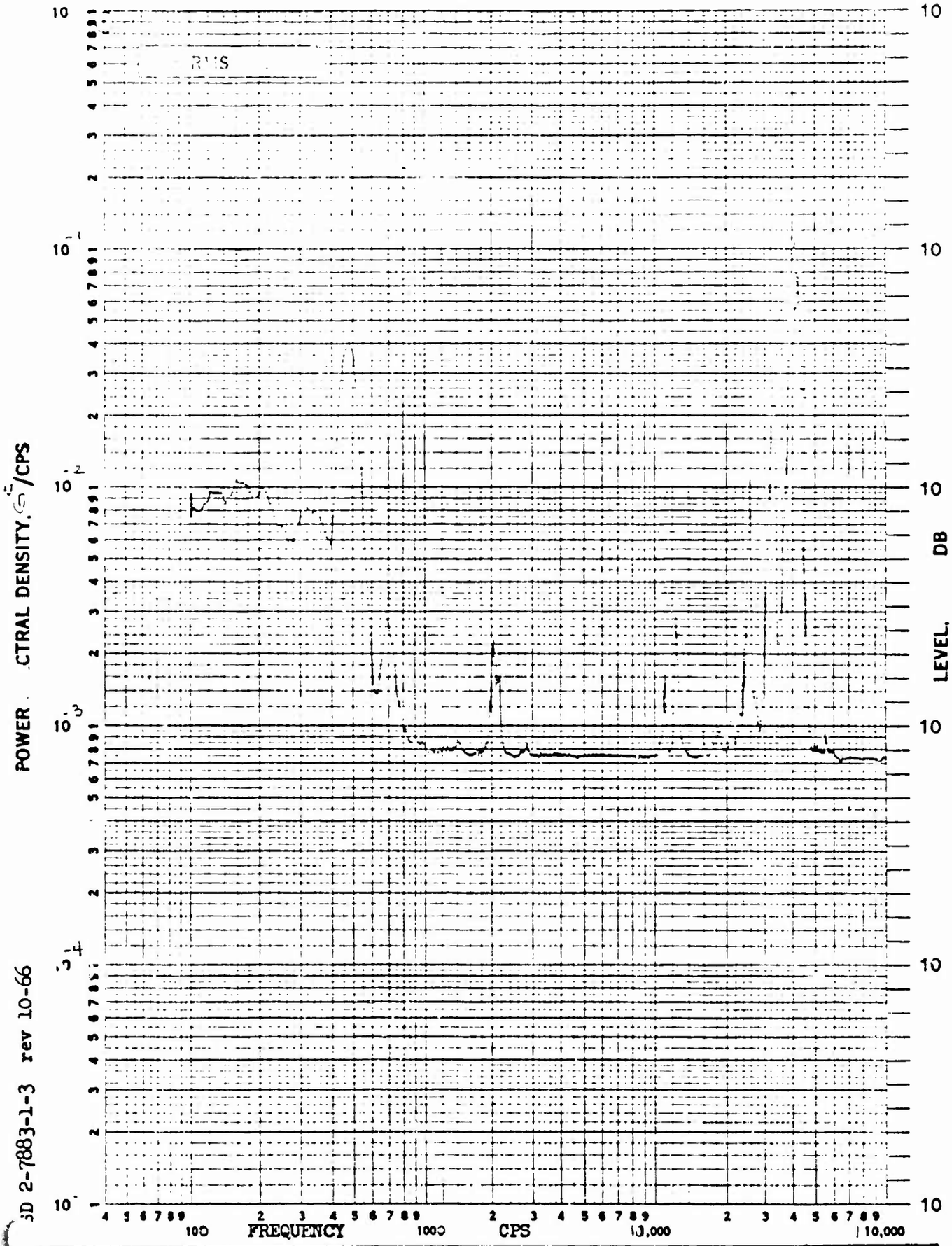

CALC.		D		Figure C-8
CHECK		A		D2-113029-3
APP'D		T		
APP'D		E		PAGE: 68

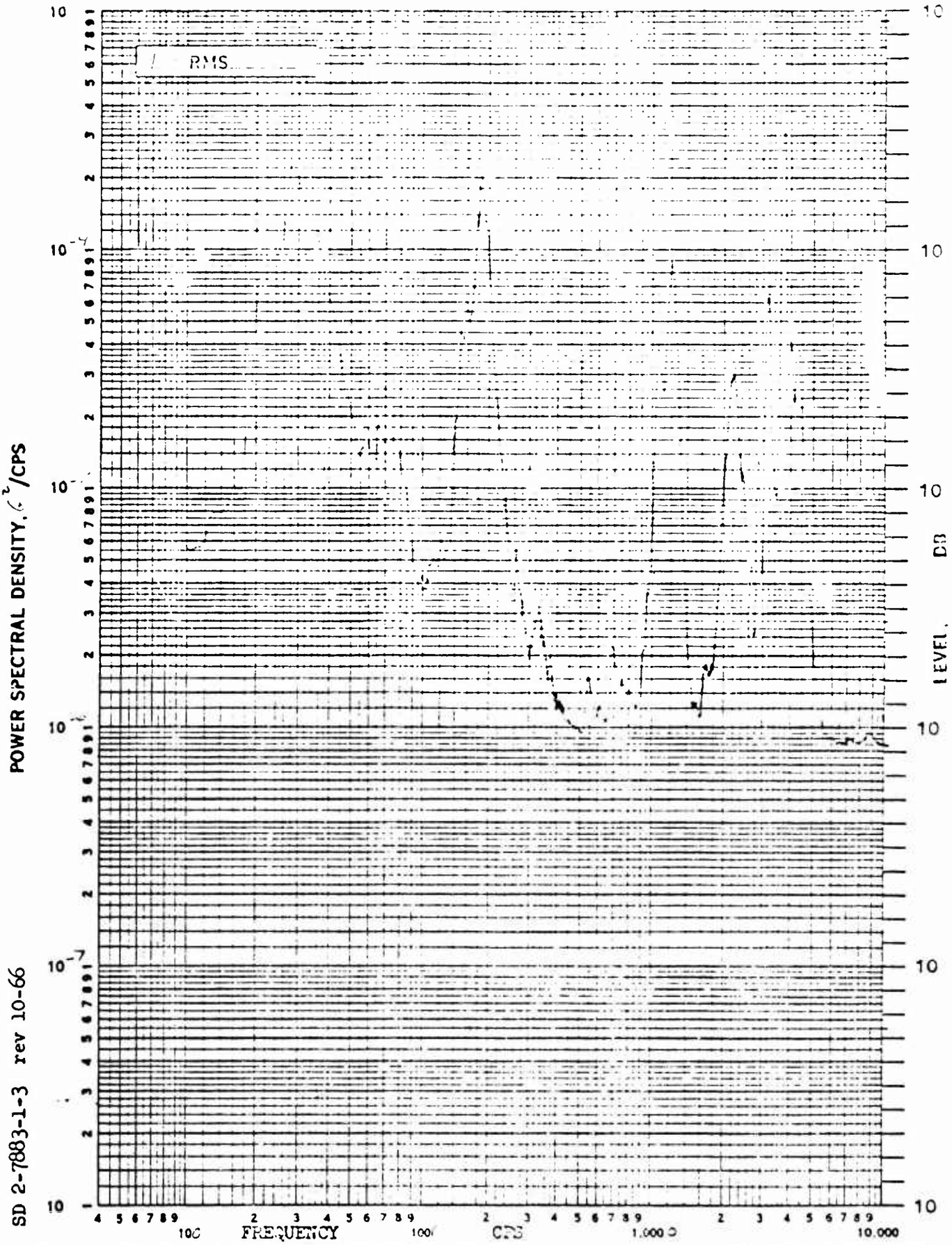

CALC.		D	Bearing #2 New, Lubed 5000 RPM
CHECK		A	
APP'D		T	
APP'D		E	

Figure C-9
D2-113029-3

PAGE: 69

SD 2-7883-1-3 rev 10-66

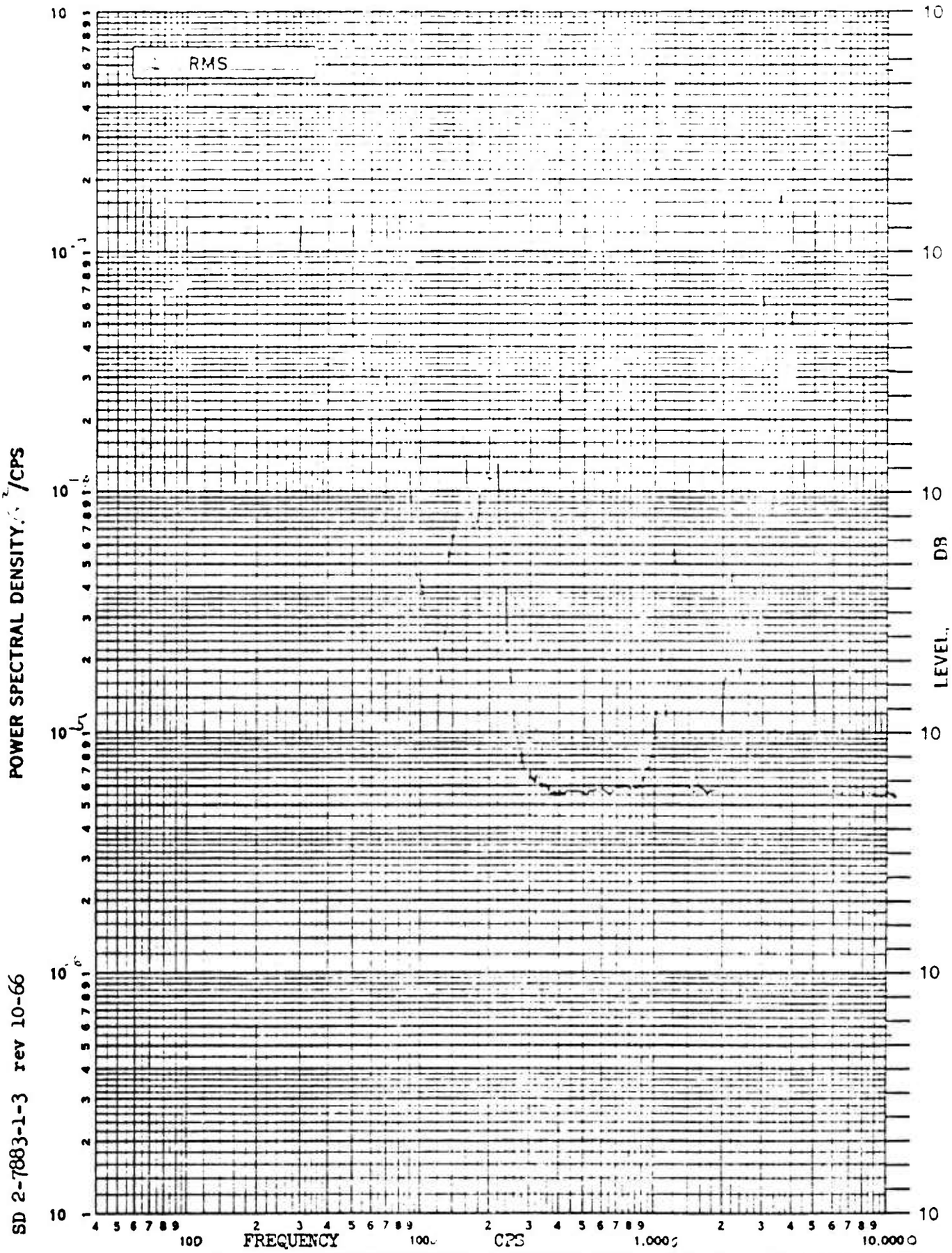

CALC.		D	Bearing # — New Lubed	Figure C-10
CHECK		A	10,000 RPM.	D2-113039-3
APP'D		T		
APP'D		E		PAGE: 70

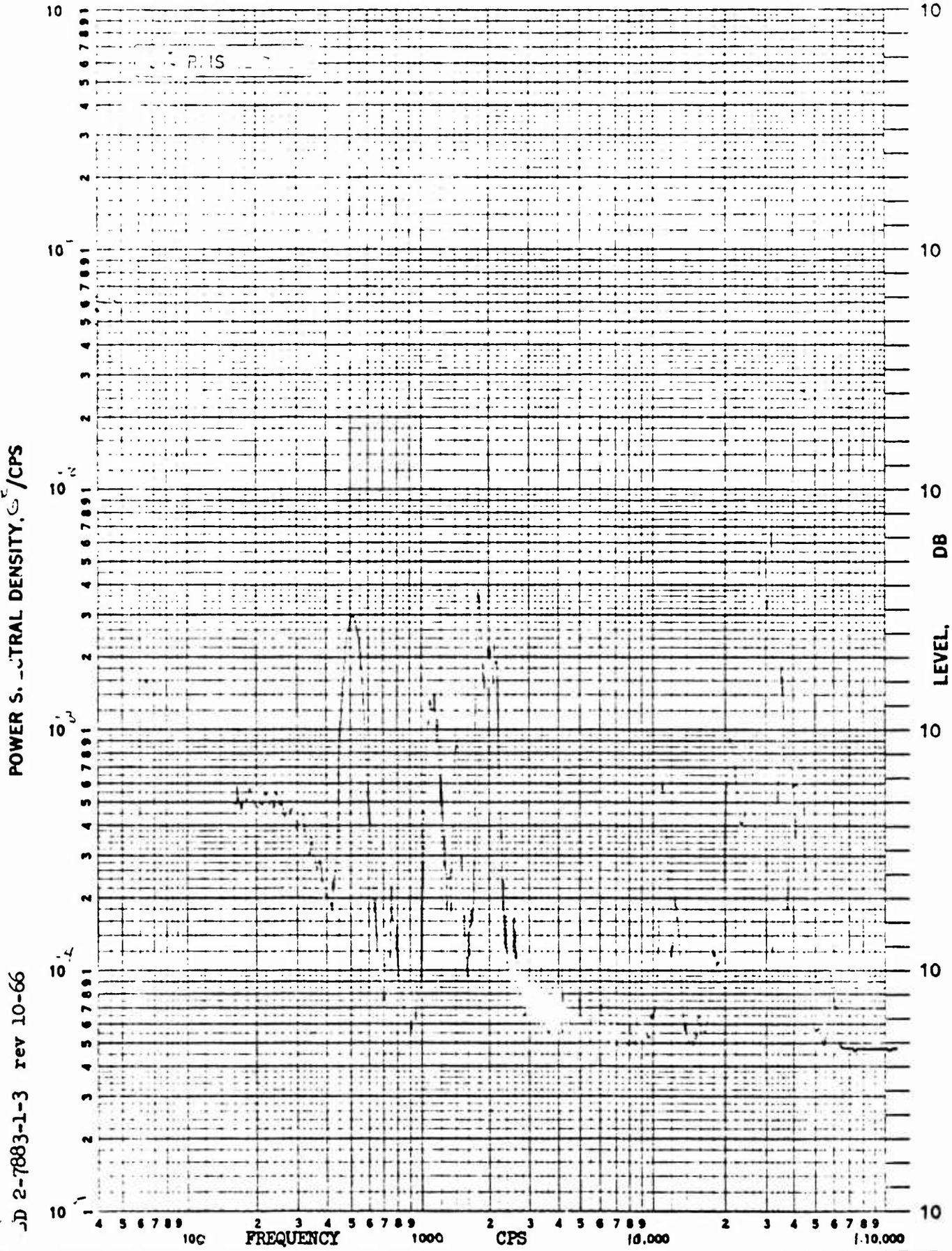

D 2-7883-1-3 rev 10-66

CALC.		D		Figure C-11
CHECK		A		D2-113029-3
APP'D		T		
APP'D		E		PAGE: 71

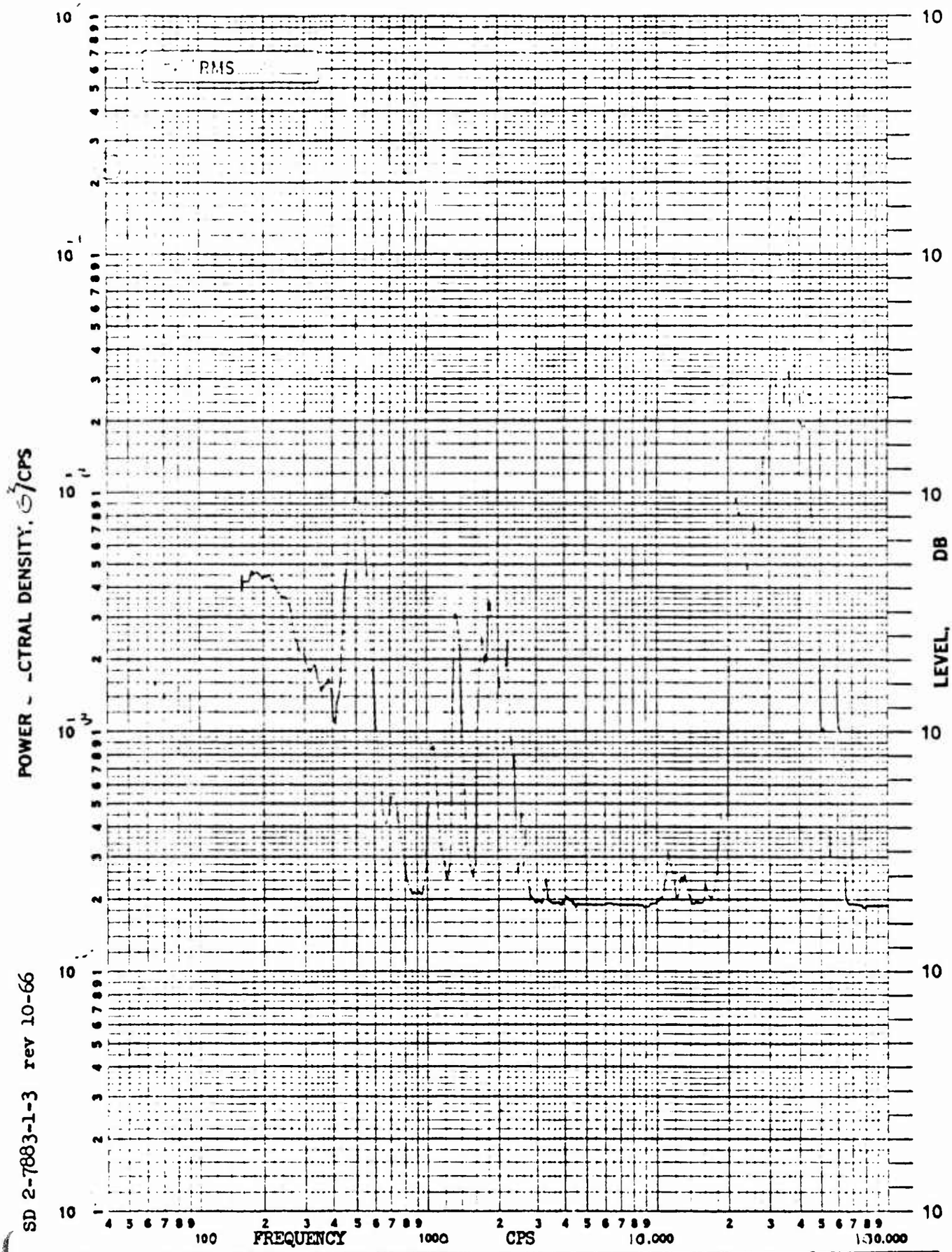

SD 2-7883-1-3 rev 10-66

CALC.		D	Figure C-12
CHECK		A	D2-113029-3
APP'D		T	
APP'D		E	PAGE: 72

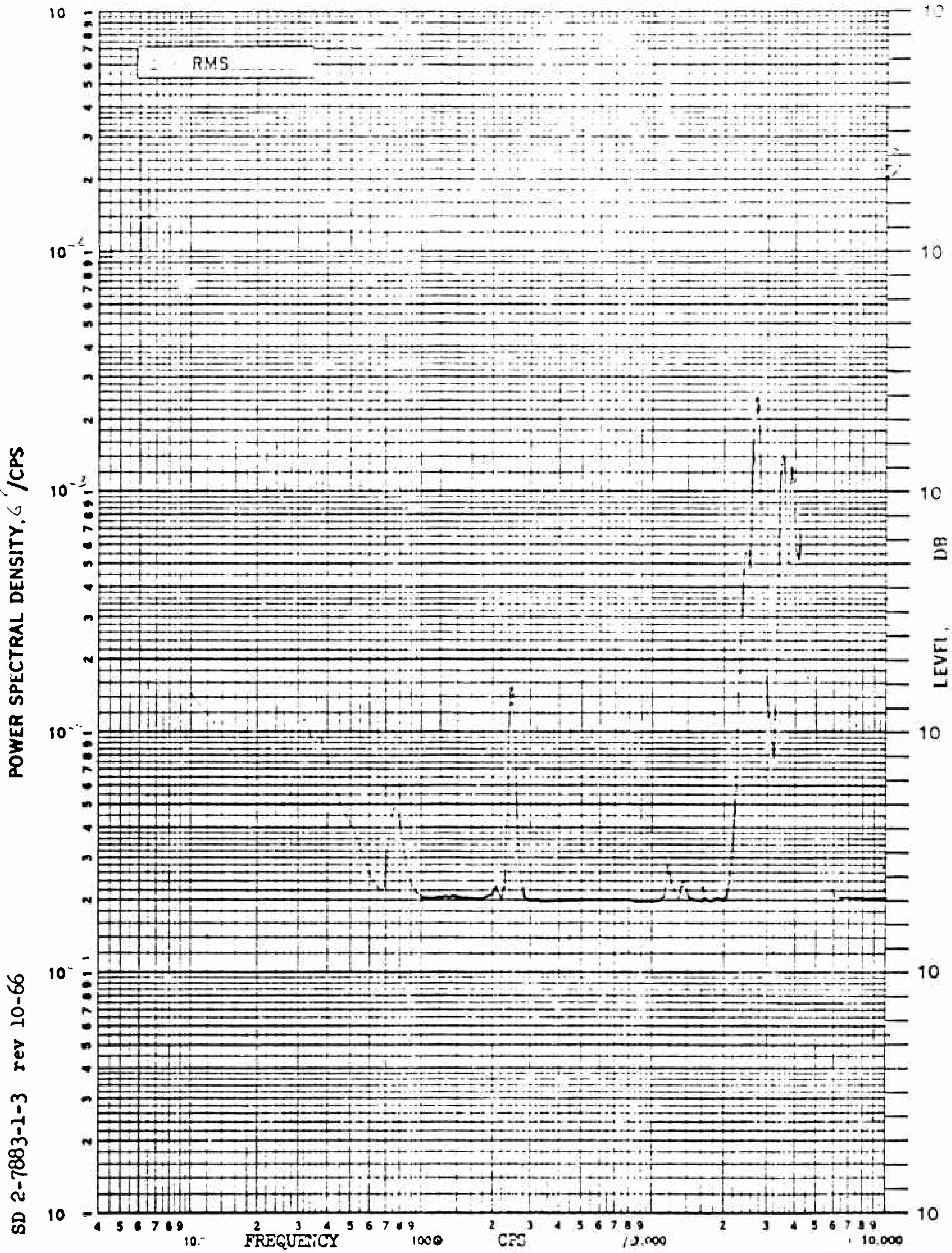

CALC.		D	Bearing #3 (New + Lube) 5000 R.P.M.	Figure C-13
CHECK		A		D2-113029-3
APP'D		T		
APP'D		E		PAGE: 73

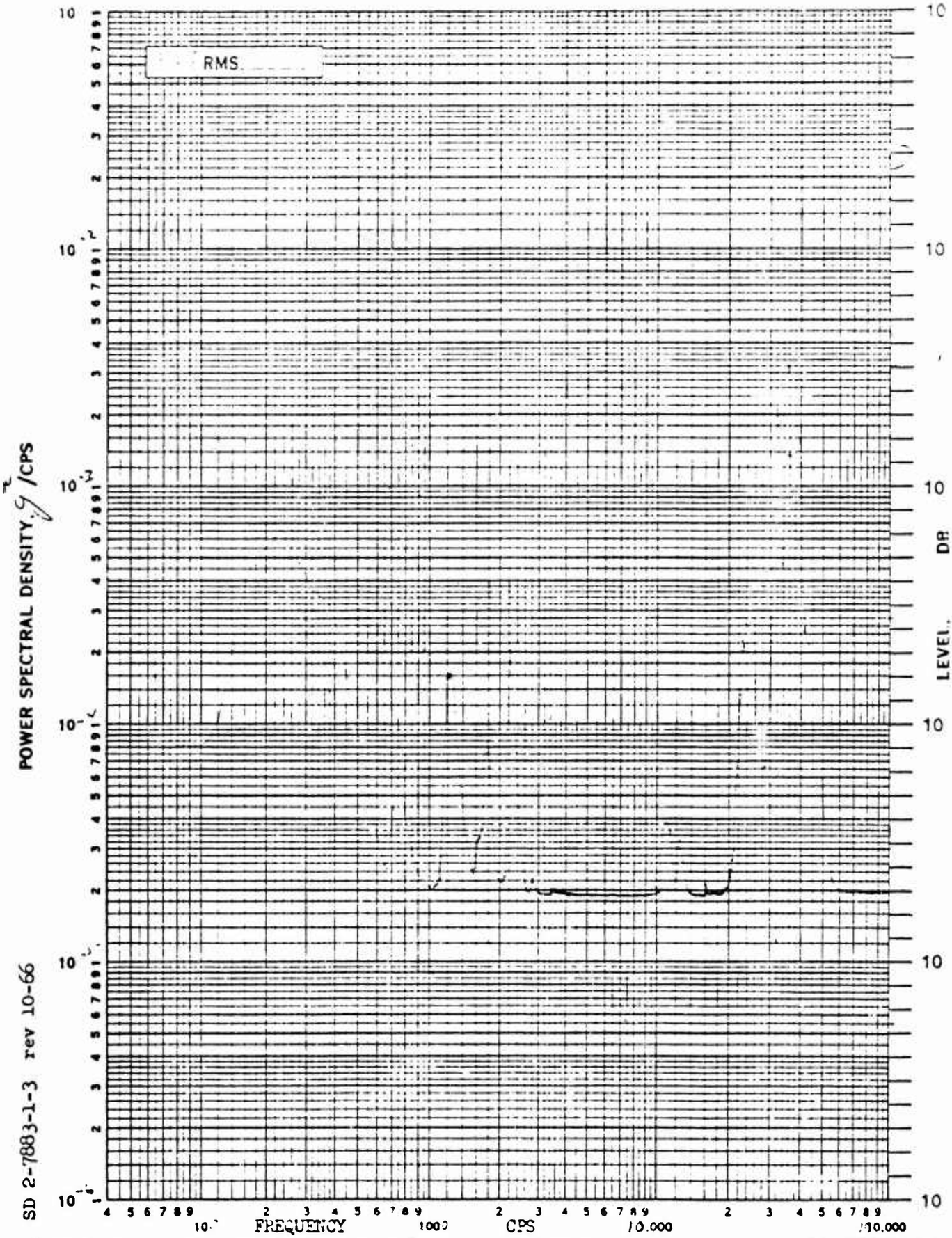

CALC.		D	Bearing # 3 (Non-Lubed) 10,000 RPM.
CHECK		A	
APP'D		T	
APP'D		E	

Figure C-14

D2-113029-3

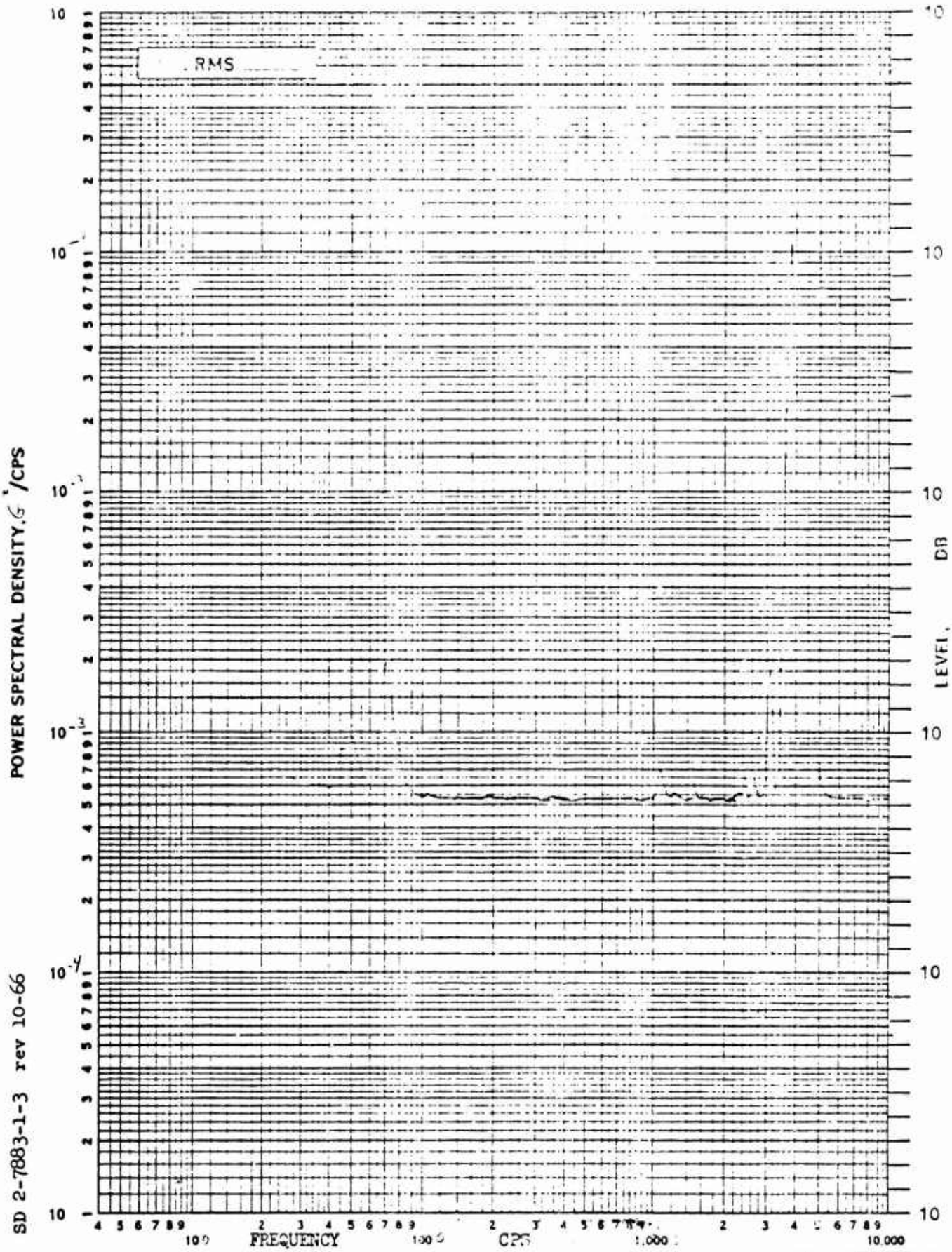

SD 2-7883-1-3 rev 10-66

CALC.		D	Figure #3 (Rubbed with hard, 5000 RPM. dry grease)
CHECK		A	
APP'D		T	
APP'D		E	

Figure C-15
D2-113029-3

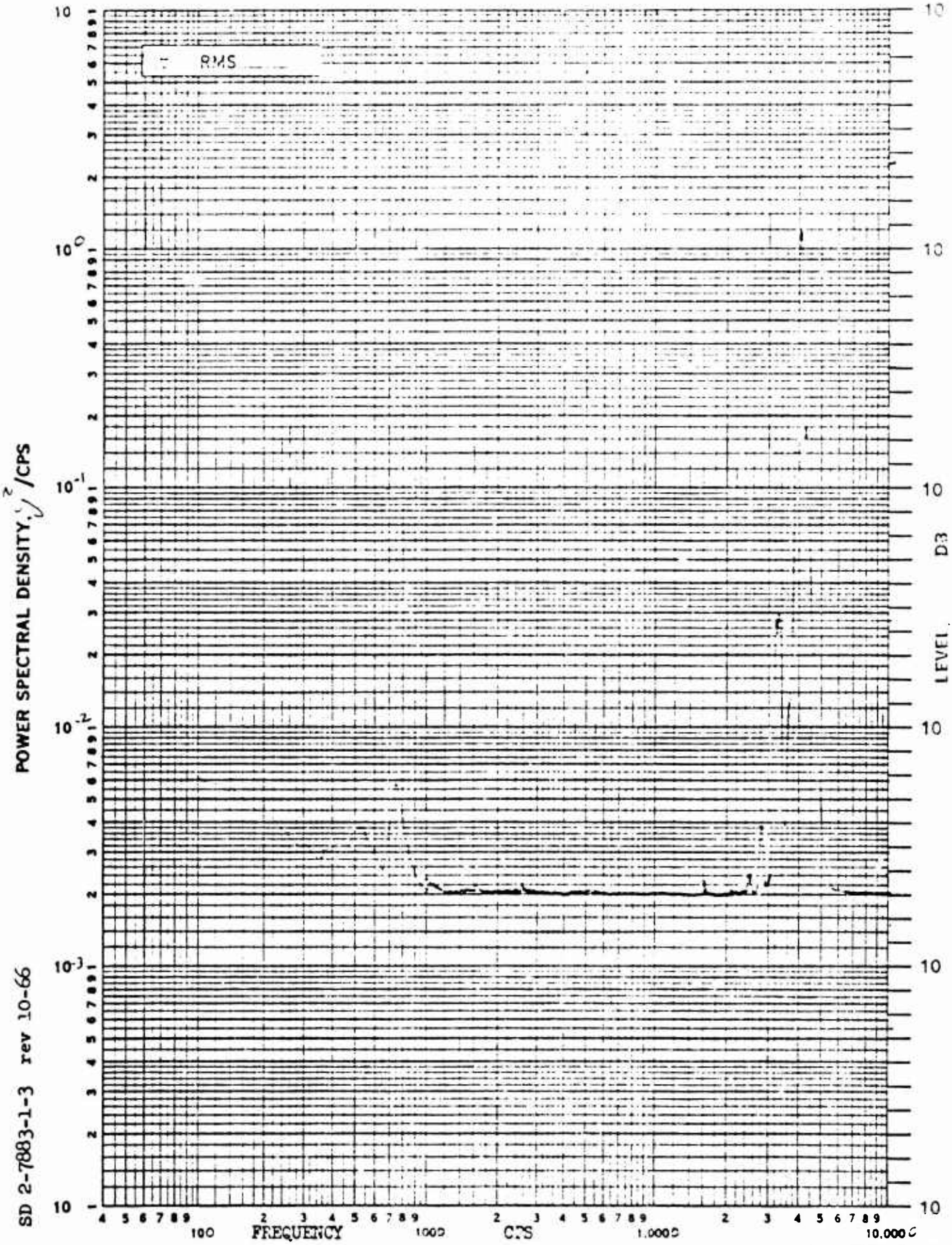

CALC.		D	Bearing #3 (including with hard, dry [illegible])	Figure C-16
CHECK		A		D2-113029-3
APP'D		T	10,000 R.P.M.	
APP'D		E		PAGE: 76

SD 2-7883-1-3 rev 10-66

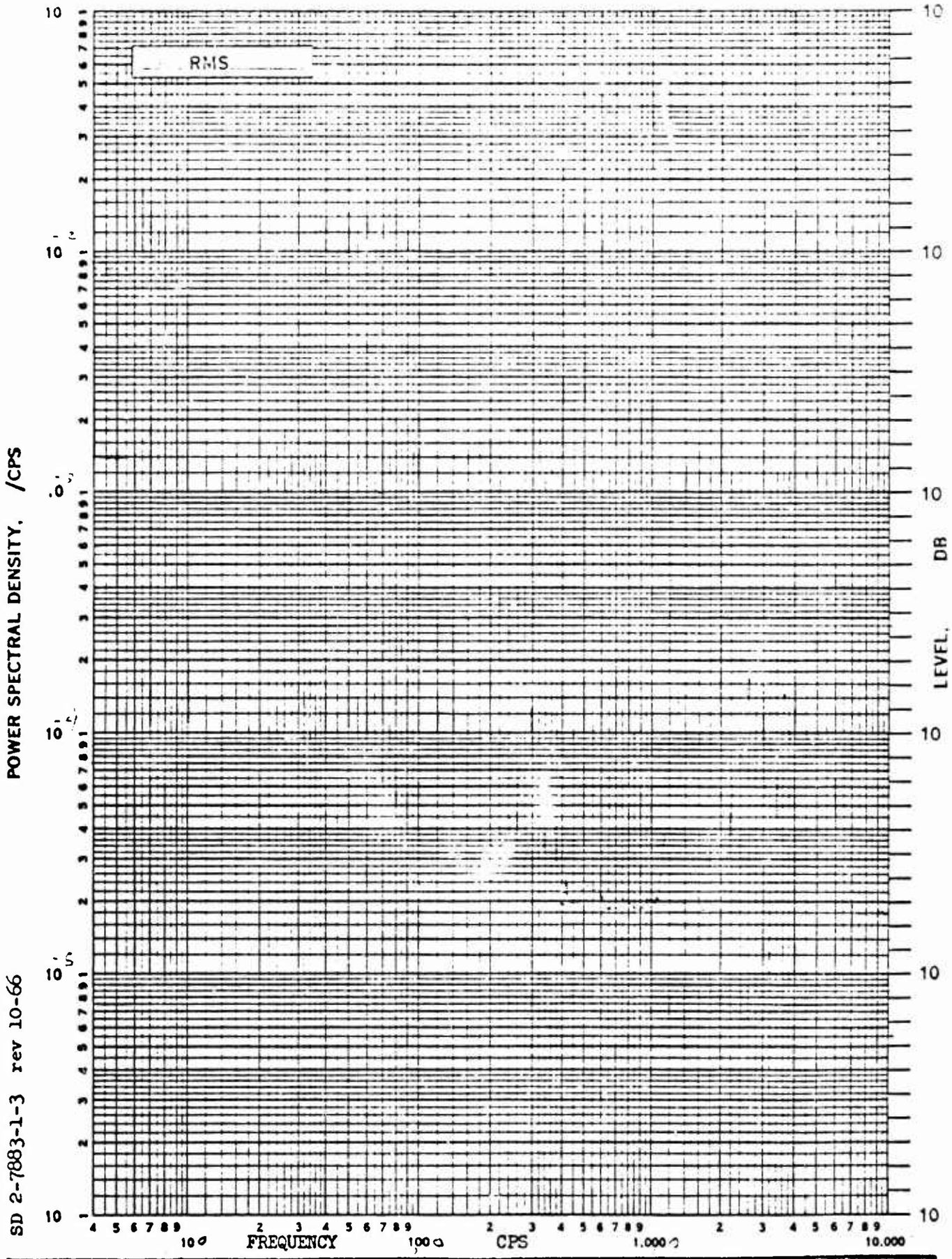

CALC.		D	Bearing #3 Distorted Co[illegible] 5000 RPM.	Figure C-17[illegible]
CHECK		A		D2-113029-3
APP'D		T		
APP'D		E		PAGE: 77

SD 2-7883-1-3 rev 10-66

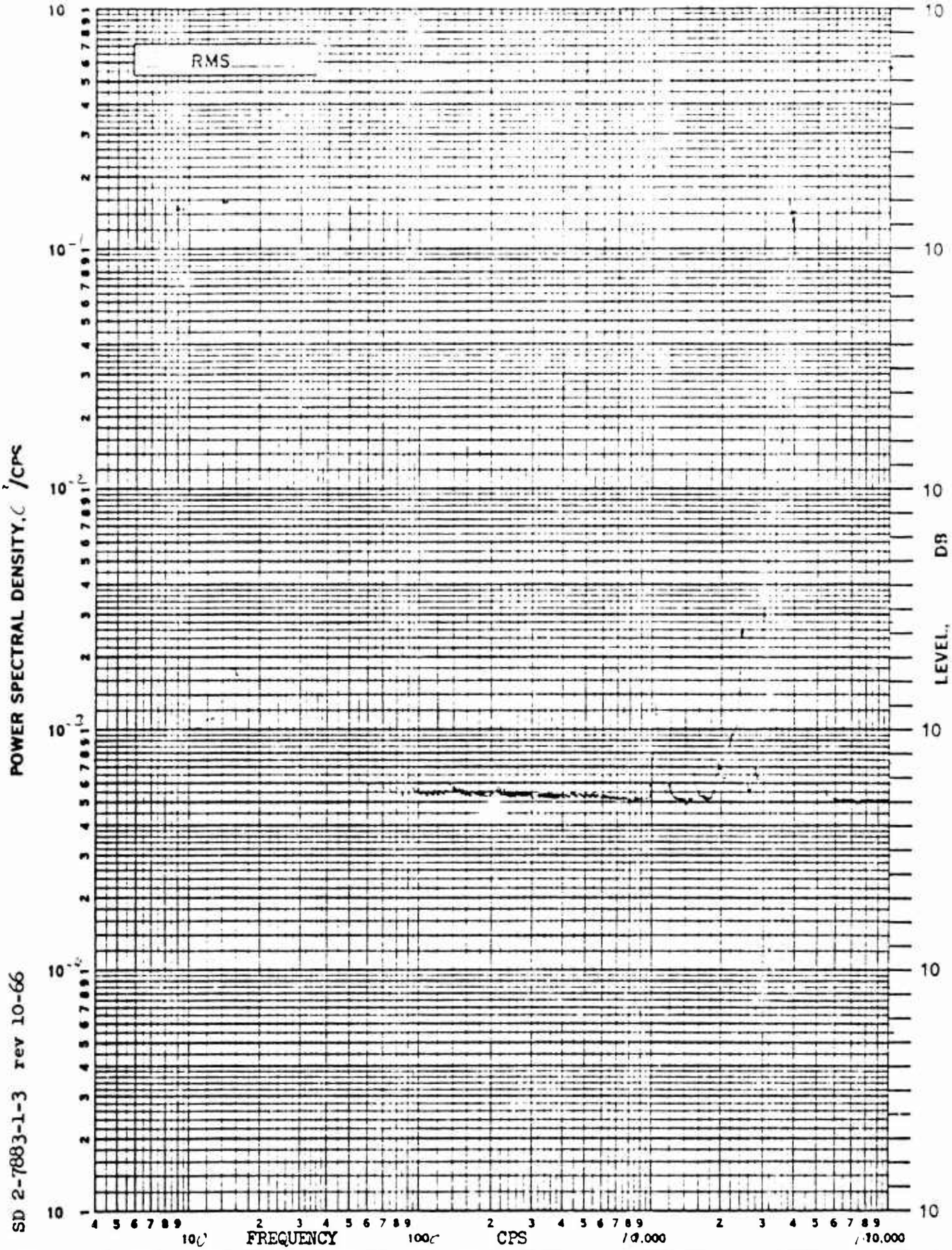

CALC.		D	Bearing #3 Distorted Cage 10,000 RPM.
CHECK		A	
APP'D		T	
APP'D		E	

Figure 18
D2-113029-3

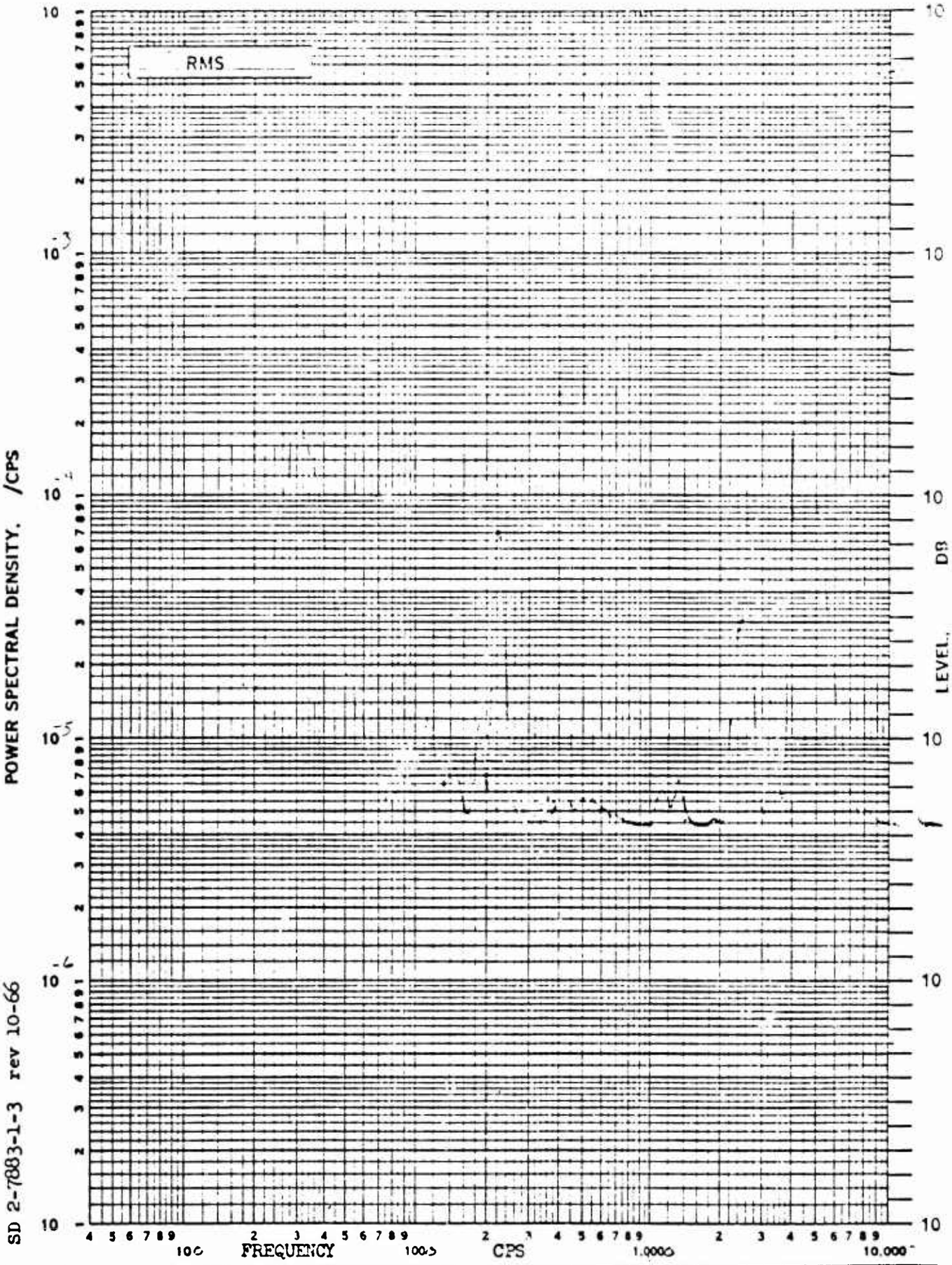

SD 2-7883-1-3 rev 10-66

CALC.		D	Fan #5 New, Lubed 5000 RPM.
CHECK		A	
APP'D		T	
APP'D		E	

Figure C-19
D2-113029-3

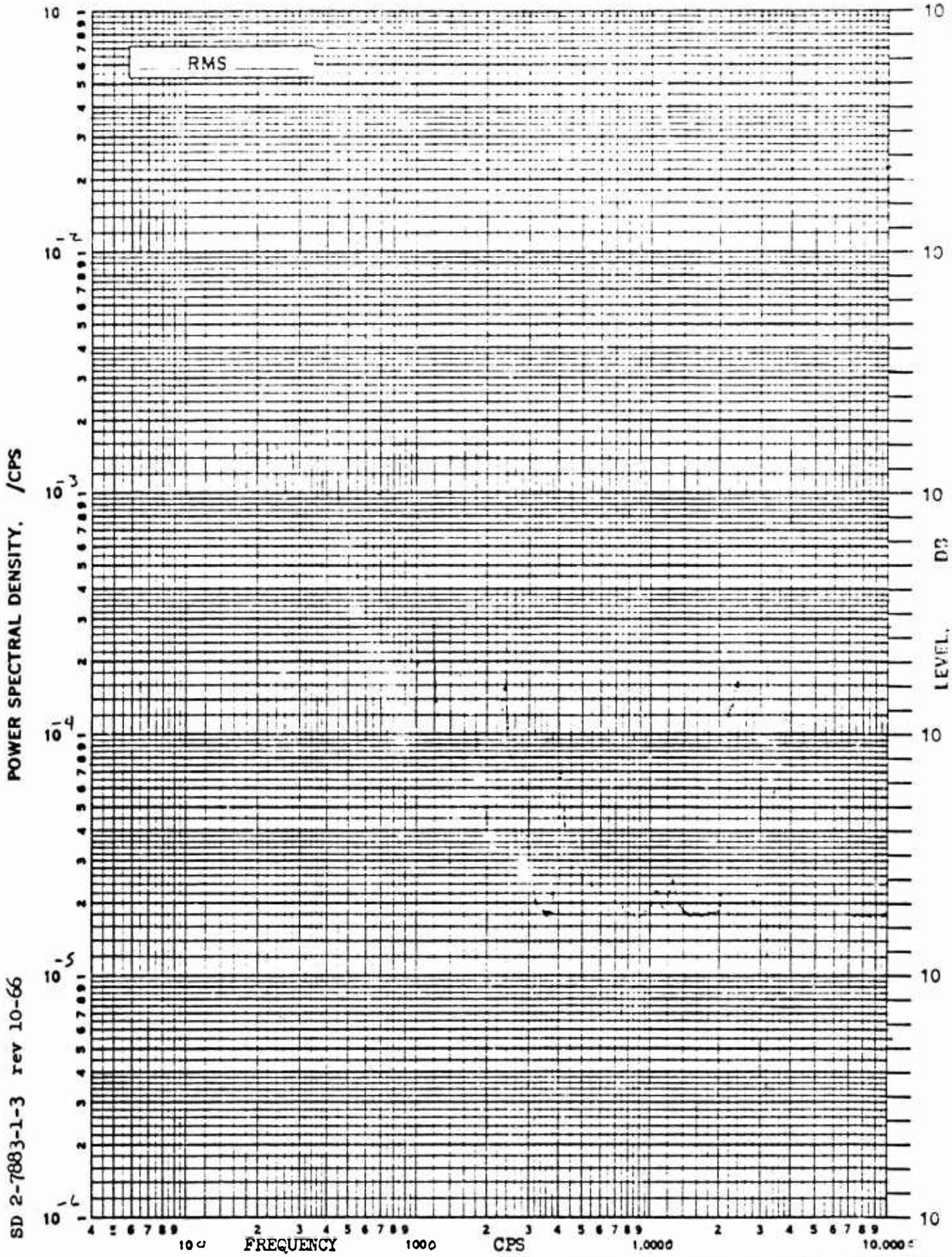

CALC.	DLF	D	Bearing #5 New, Lubed 10,000 R.P.M.
CHECK		A	
APP'D		T	
APP'D		E	

Figure C-
D2-113029-3
PAGE: 80

SD 2-7883-1-3 rev 10-66

761-9 .345 Vrms

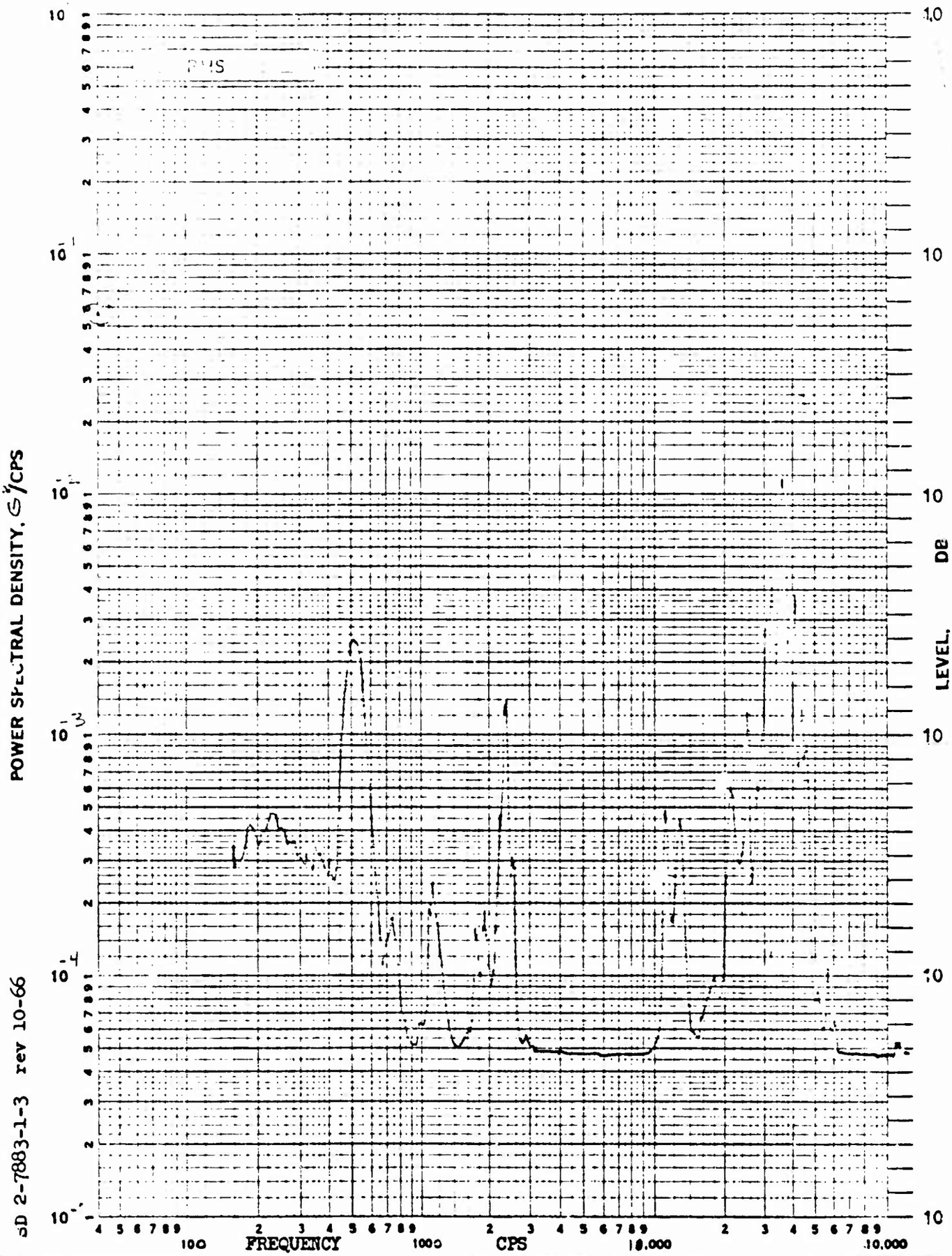

SD 2-7883-1-3 rev 10-66

CALC.		D		Figure C-81
CHECK		A		D2-113029-3
APP'D		T		
APP'D		E		PAGE: 81

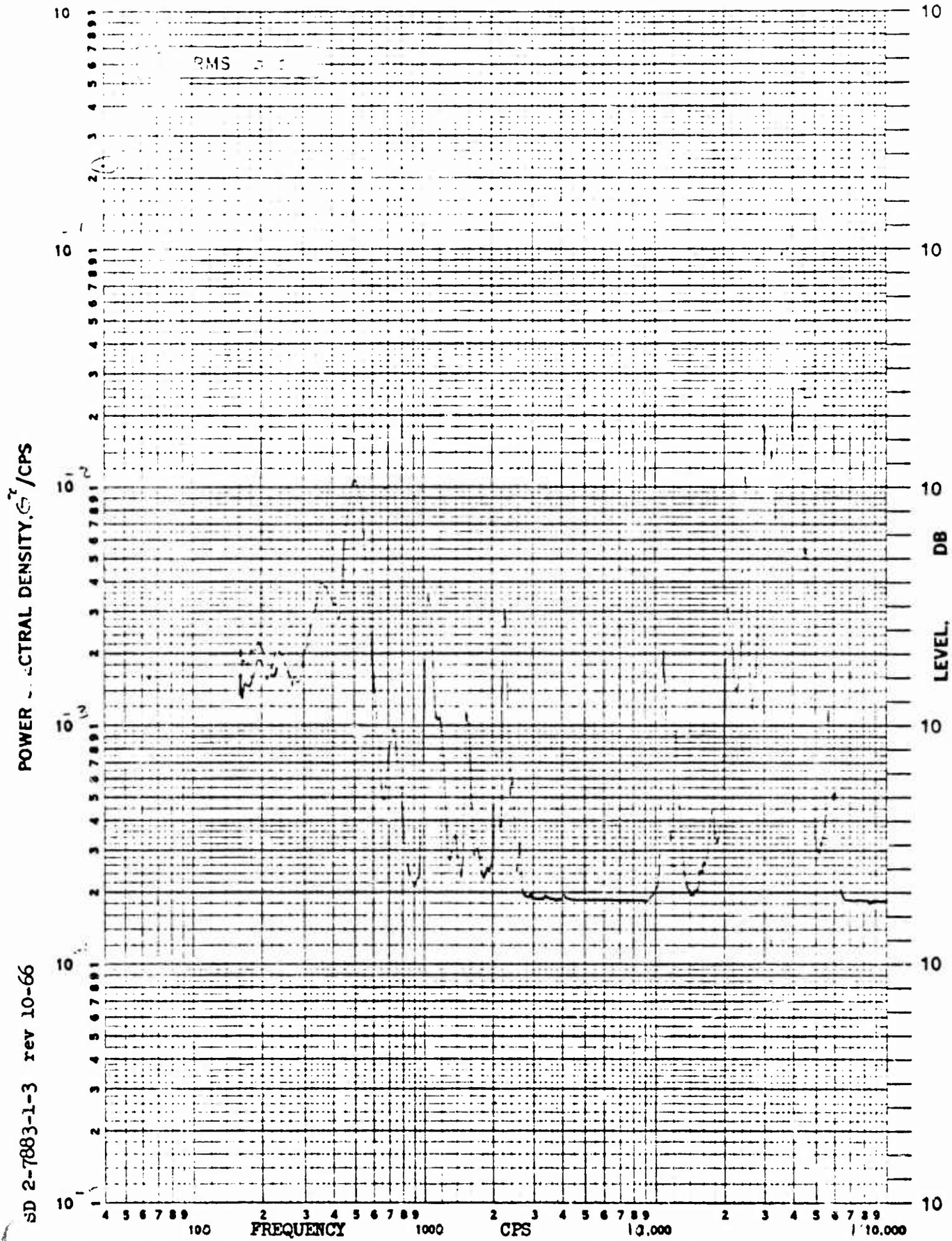

SD 2-7883-1-3 rev 10-66

CALC.		D		Figure C-22
CHECK		A		D2-113029-3
APP'D		T		
APP'D		E		PAGE: 82

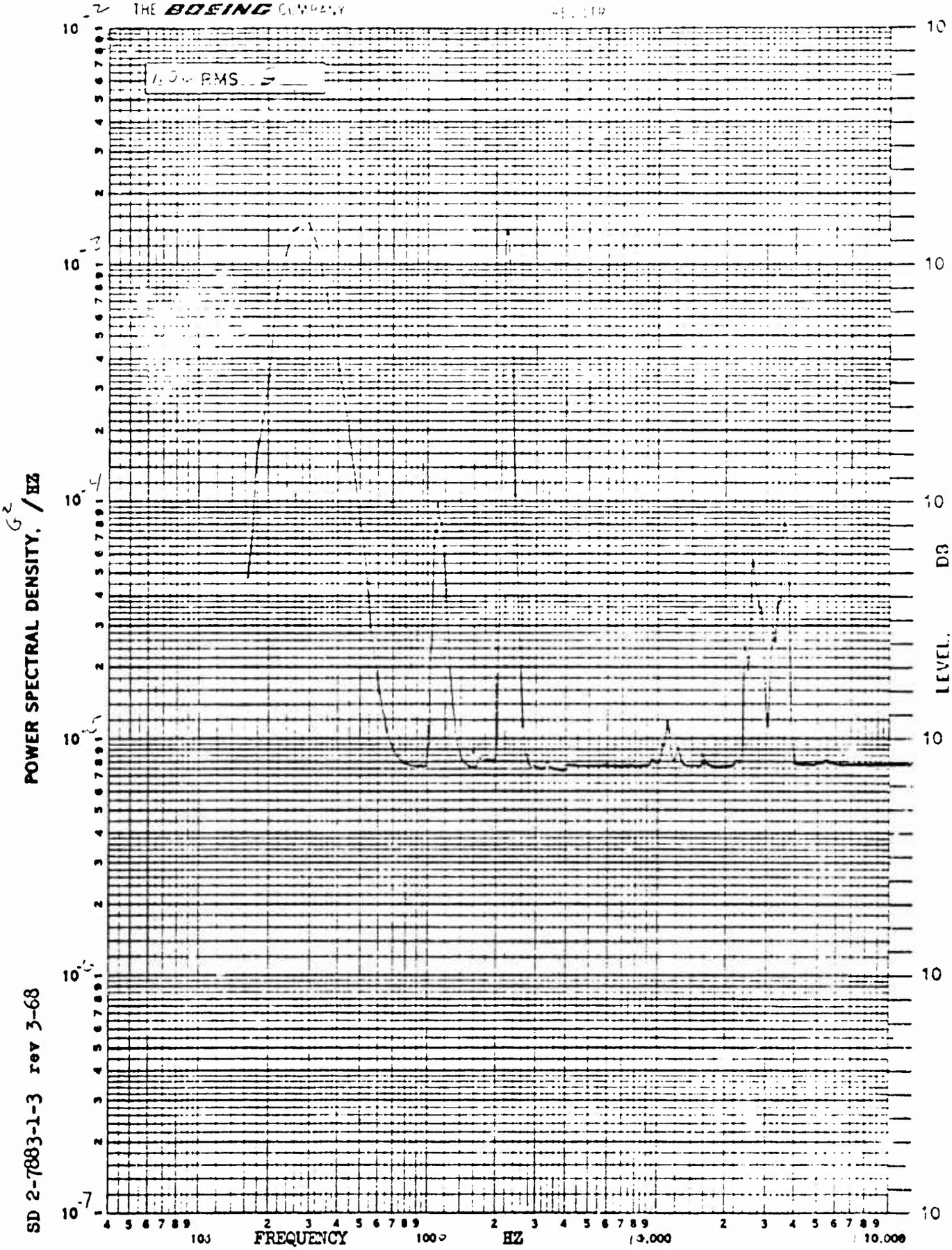

CALC.		D	Bearing # 6 NEW
CHECK		A	
APP'D		T	5000 RPM
APP'D		E	

Figure C-23
D2-113029-3

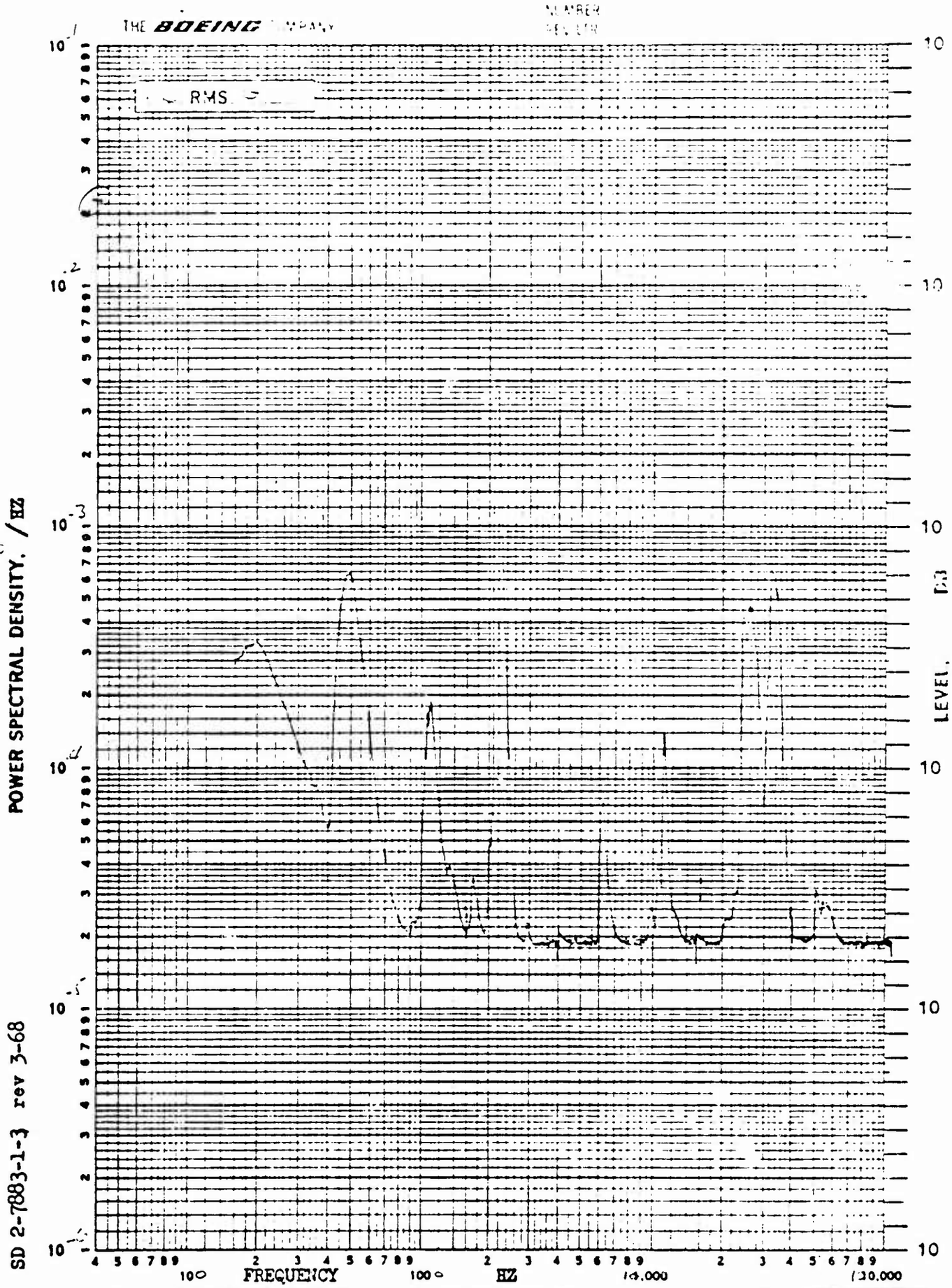

CALC.	6/6/4	D	[illegible] #4 New	Figure C-24
CHECK	[illegible]	A		D2-113029-3
APP'D		T	12,000 RPM	
APP'D		E		PAGE: 84

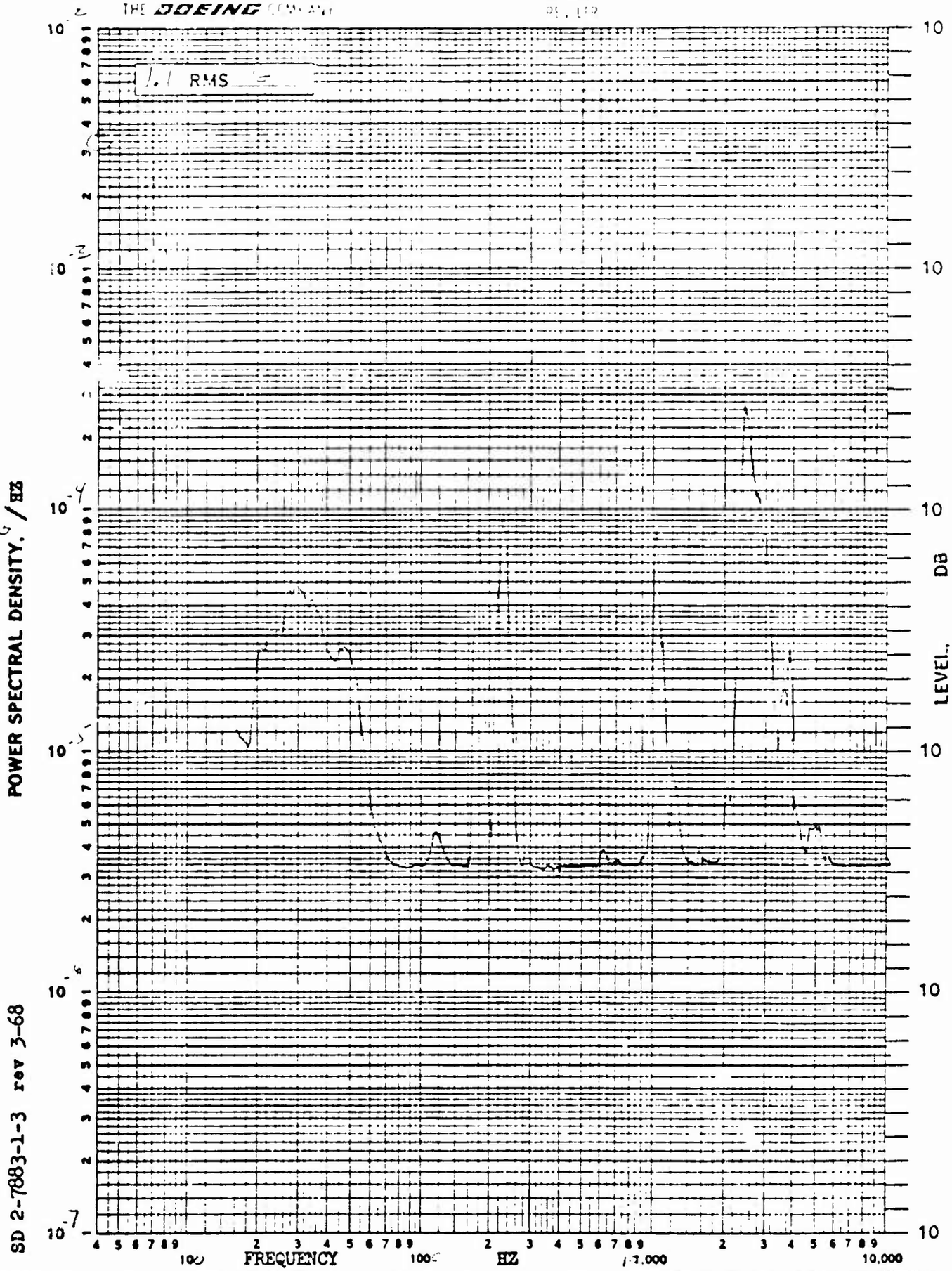

SD 2-7883-1-3 rev 3-68

CALC.		D	Bearing #4 Fault/outer race. 5000 RPM	Figure C-25
CHECK		A		D2-113029-3
APP'D		T		
APP'D		E		PAGE: 85

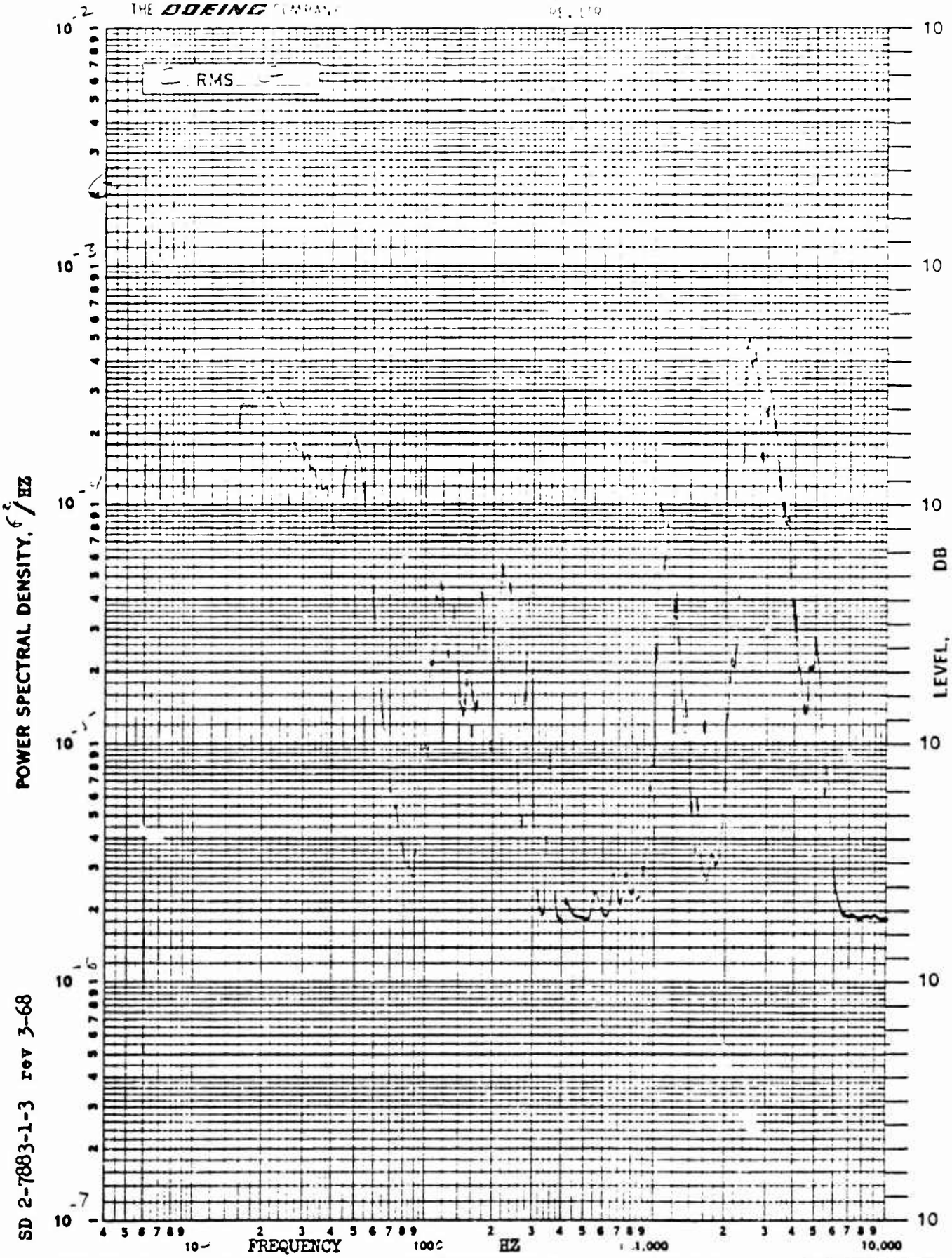

CALC.		D	Bearing #4 Foot/outer race 10,000 RPM	Figure C-26
CHECK		A		D2-113029-3
APP'D		T		
APP'D		E		PAGE: 86

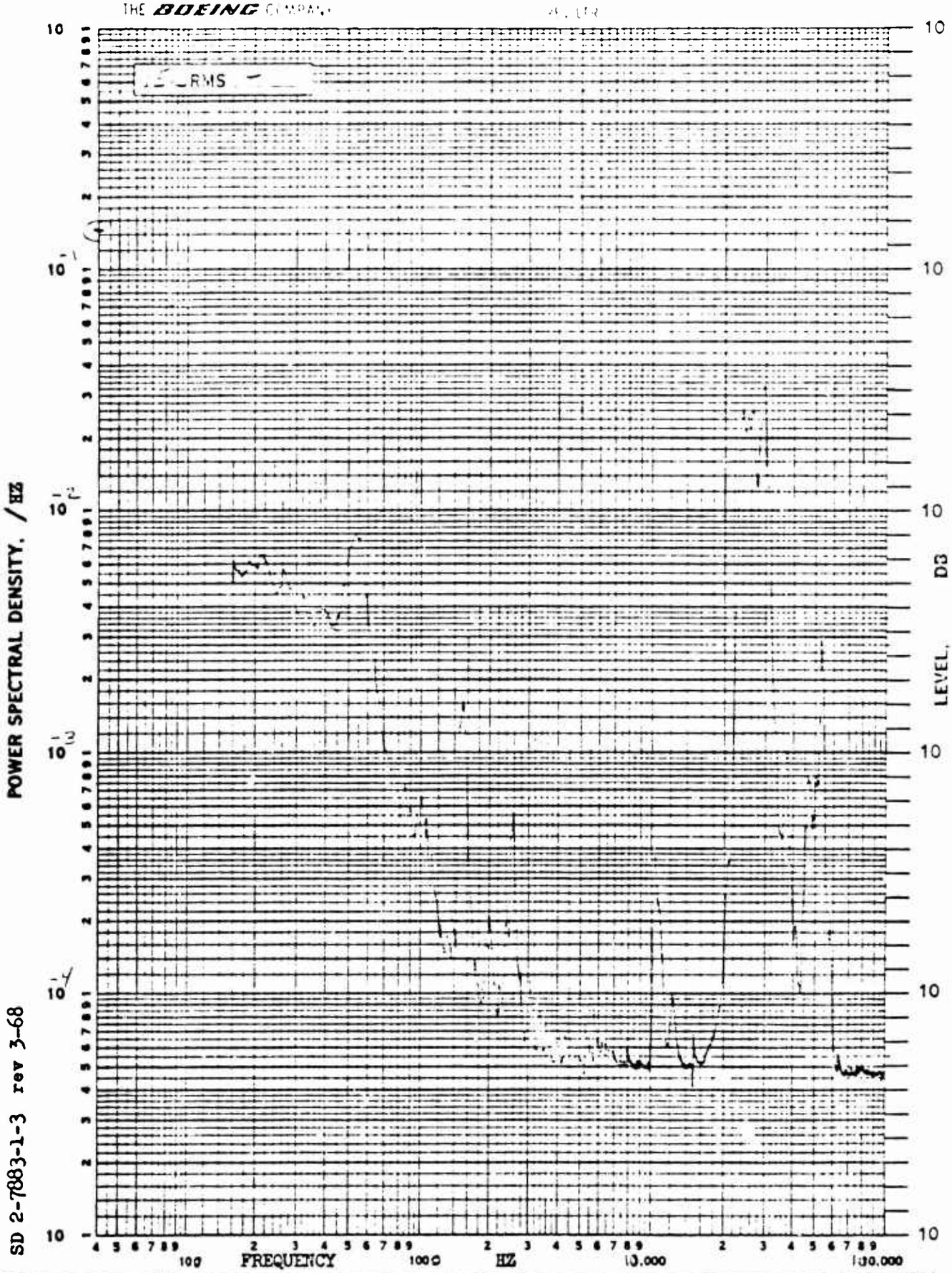

CALC.	DET	D7-17-7	
CHECK	MCK	A7-1-	
APP'D		T	

BEARING #4 5000 RPM
ENLARGED PIT IN OUTER RACE

Figure C-27
D2-113029-3

THE BOEING COMPANY

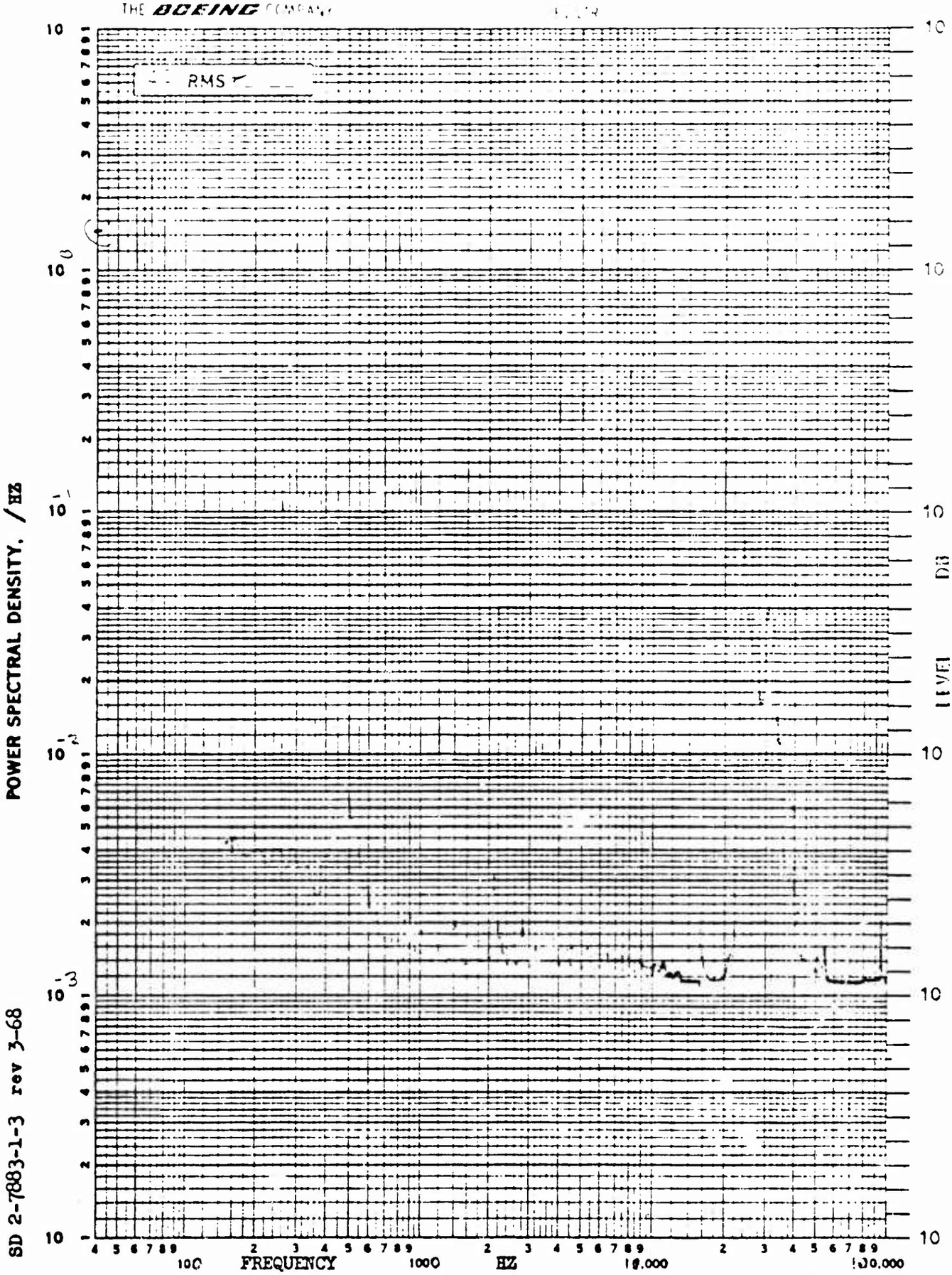

SD 2-7883-1-3 rev 3-68

1328-3 - 30 dB, 2 rad RMS

CALC.	SKT	DATE	BEARING #4 10,000 RPM ENLARGED PIT IN OUTER RACE	Figure C-28
CHECK				D2-113029-3
APP'D		T		
APP'D		E		PAGE: 88

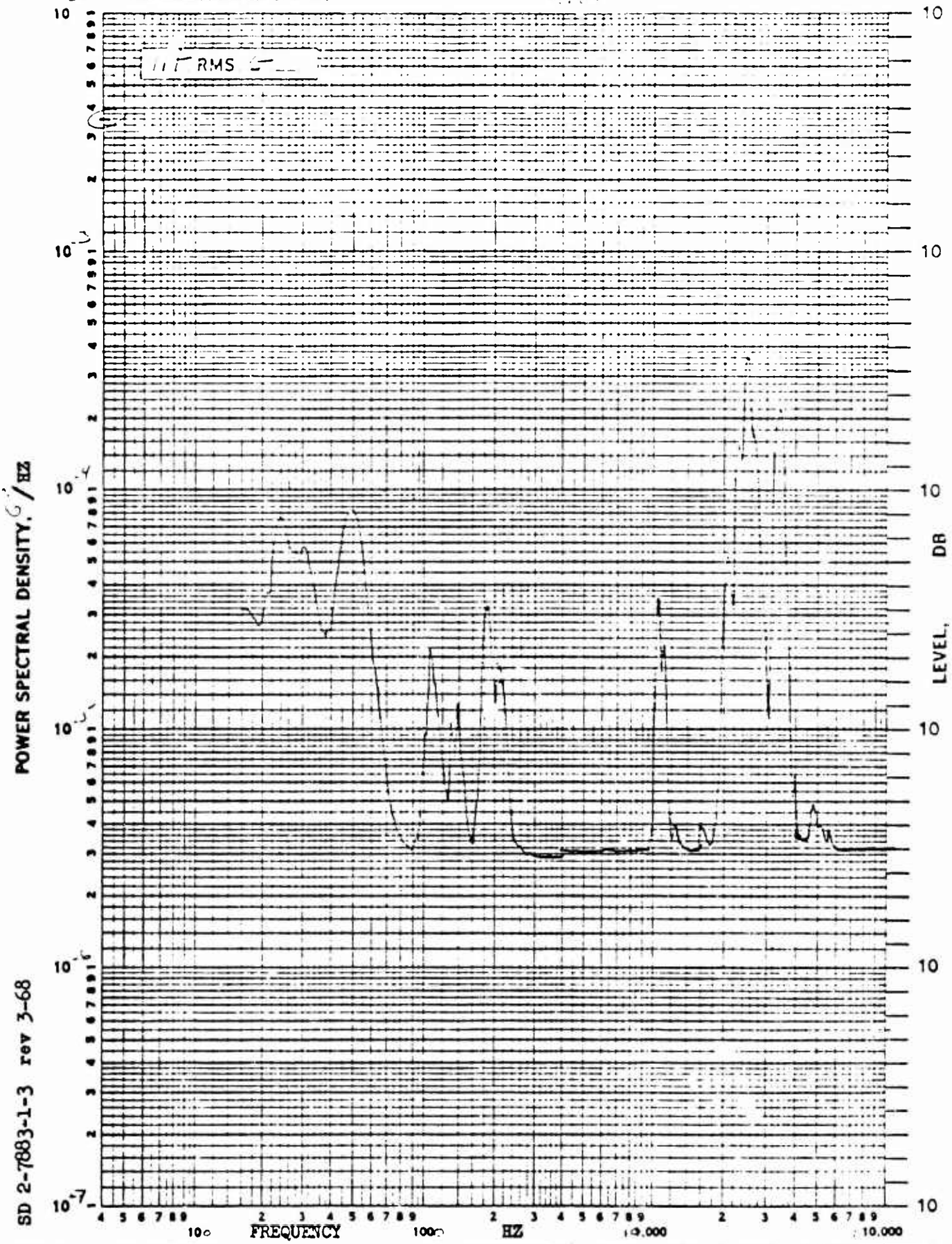

CALC.		D	Bearing #6 New	Figure C-29
CHECK		A		D2-113029-3
APP'D		T	5000 RPM	
APP'D		E		PAGE: 89

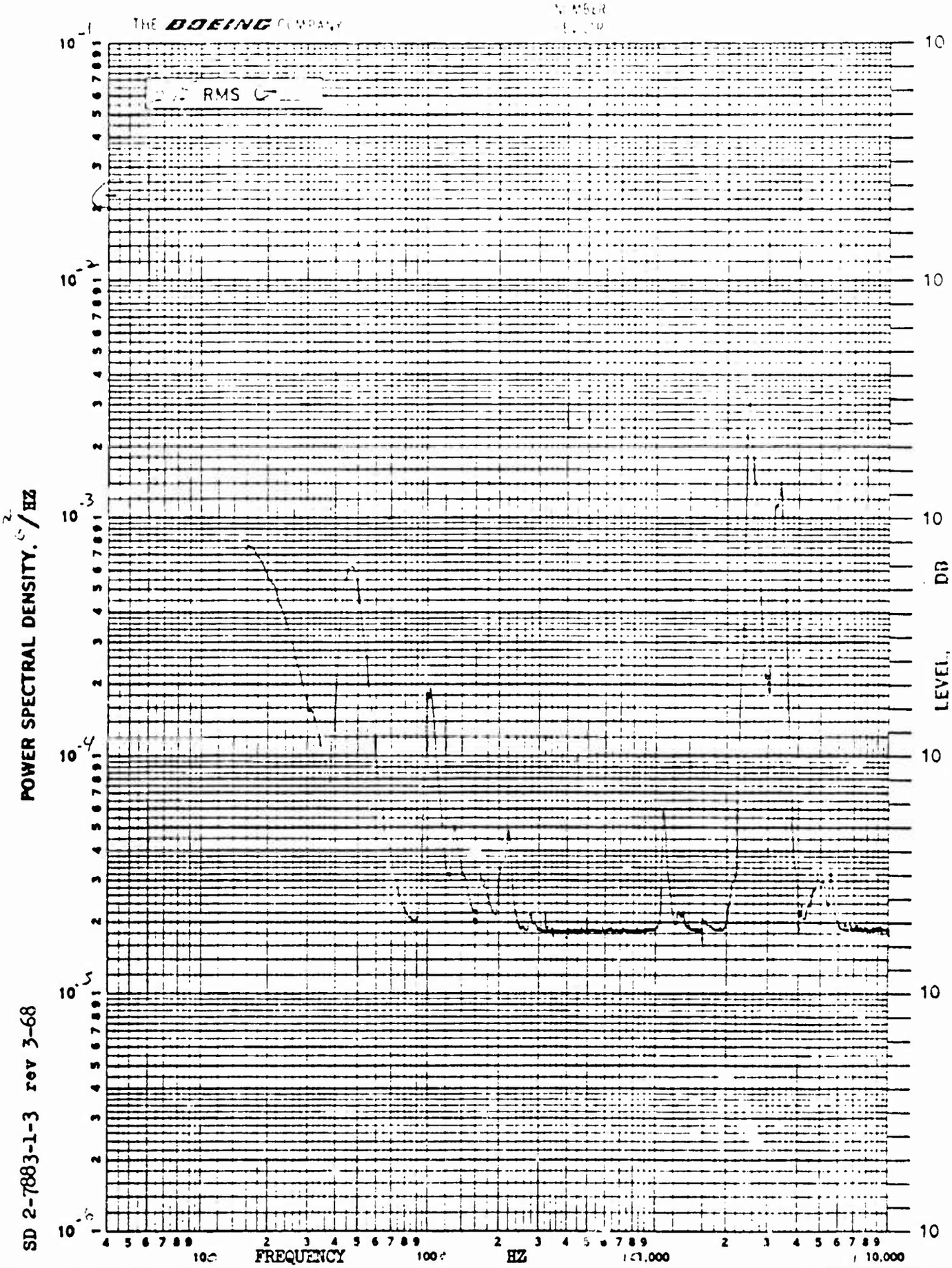

CALC.		D	Bearing #6 NEW	Figure C-30
CHECK		A		D2-113029-3
APP'D		T	10,300 KPM	
APP'D		E		PAGE: 90

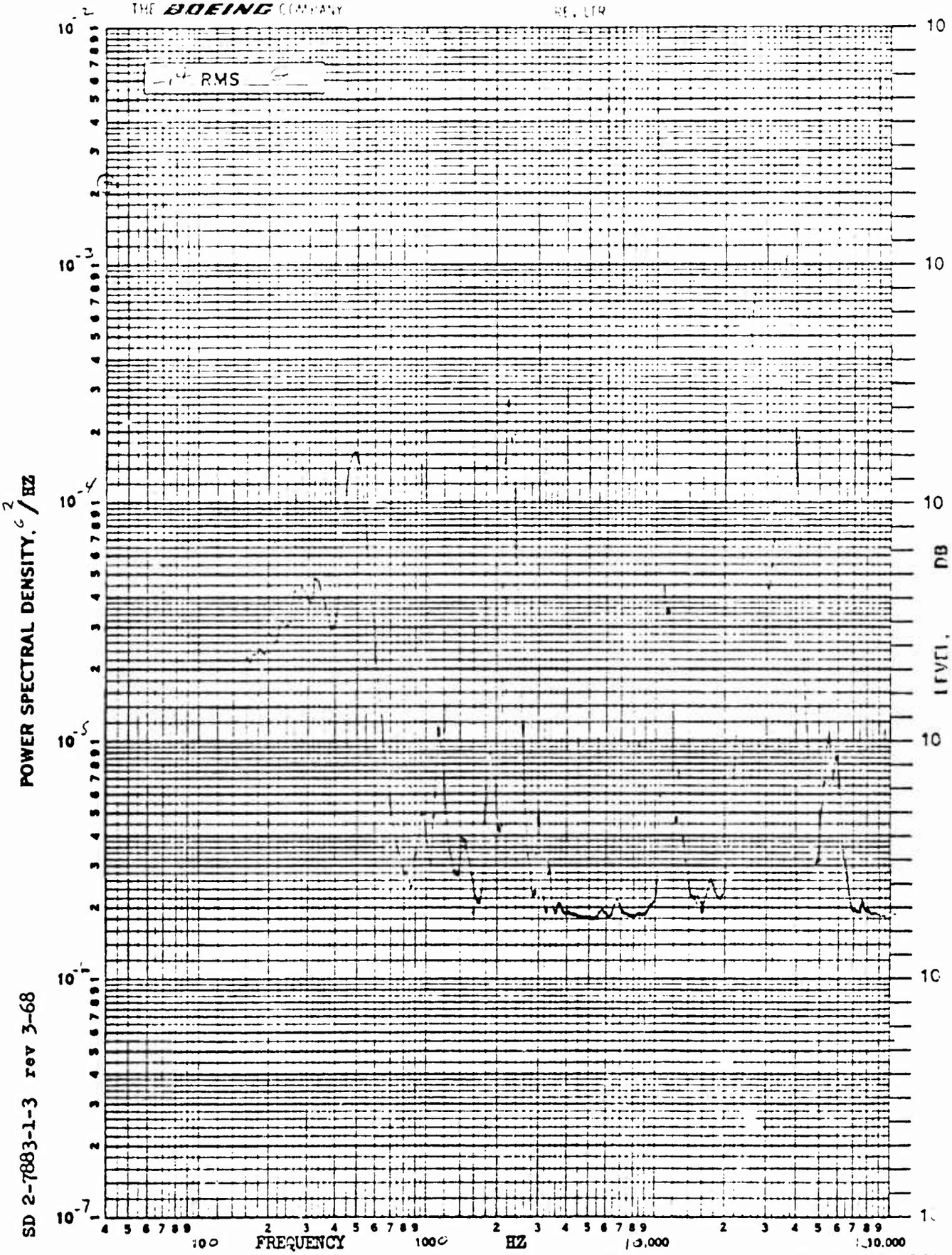

1217-6 -30 dB 1240 VRMS

SD 2-7883-1-3 rev 3-68

CALC.		D	Bearing #6 Fault/inner race 5000 RPM	Figure C-[illegible]
CHECK		A		D2-113029-
APP'D		T		
APP'D		E		PAGE: 91

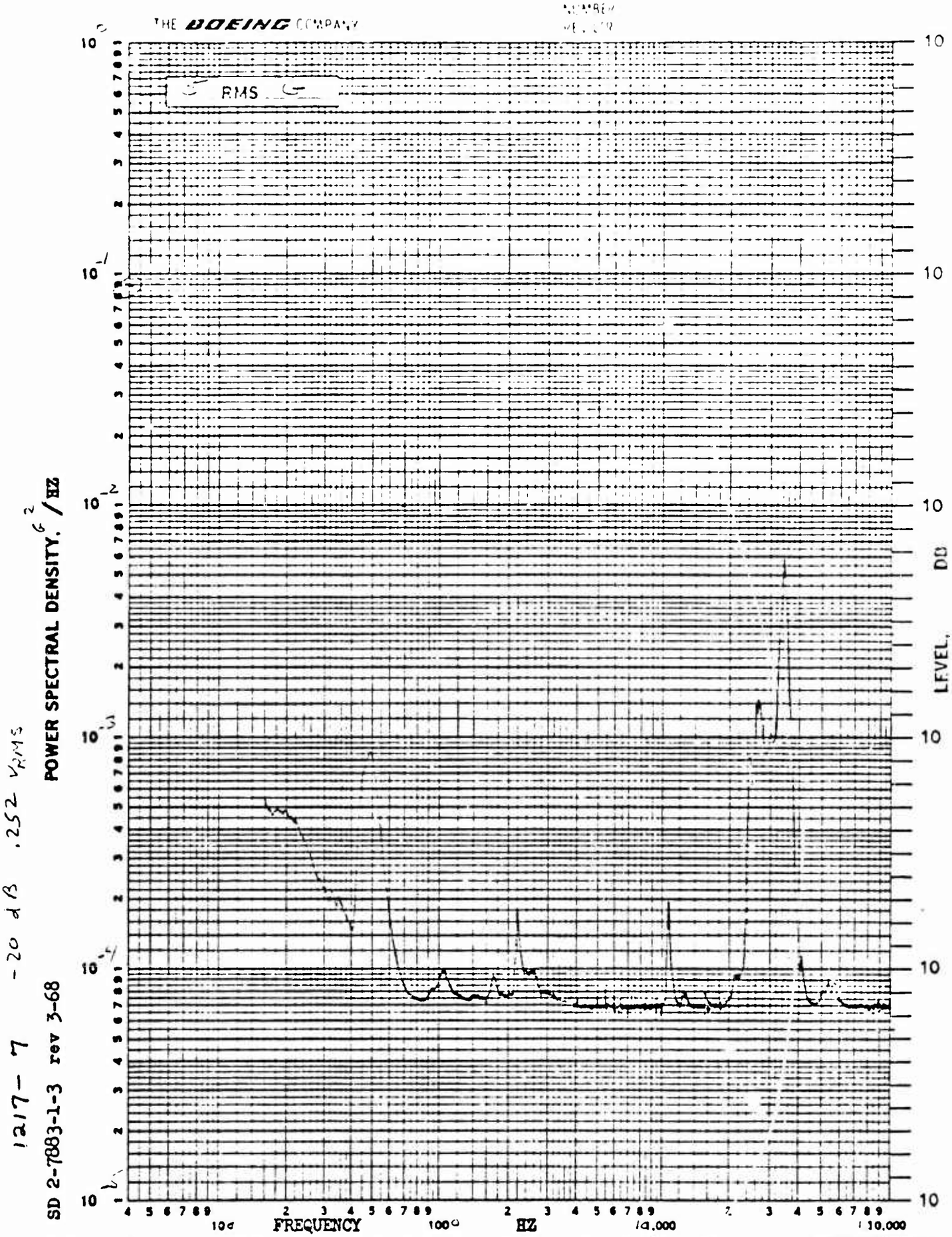

CALC.		D	Bearing #6 FAULT/inner race 10,000 RPM
CHECK		A	
APP'D		T	
APP'D		E	

Figure C-32

D2-113029-3

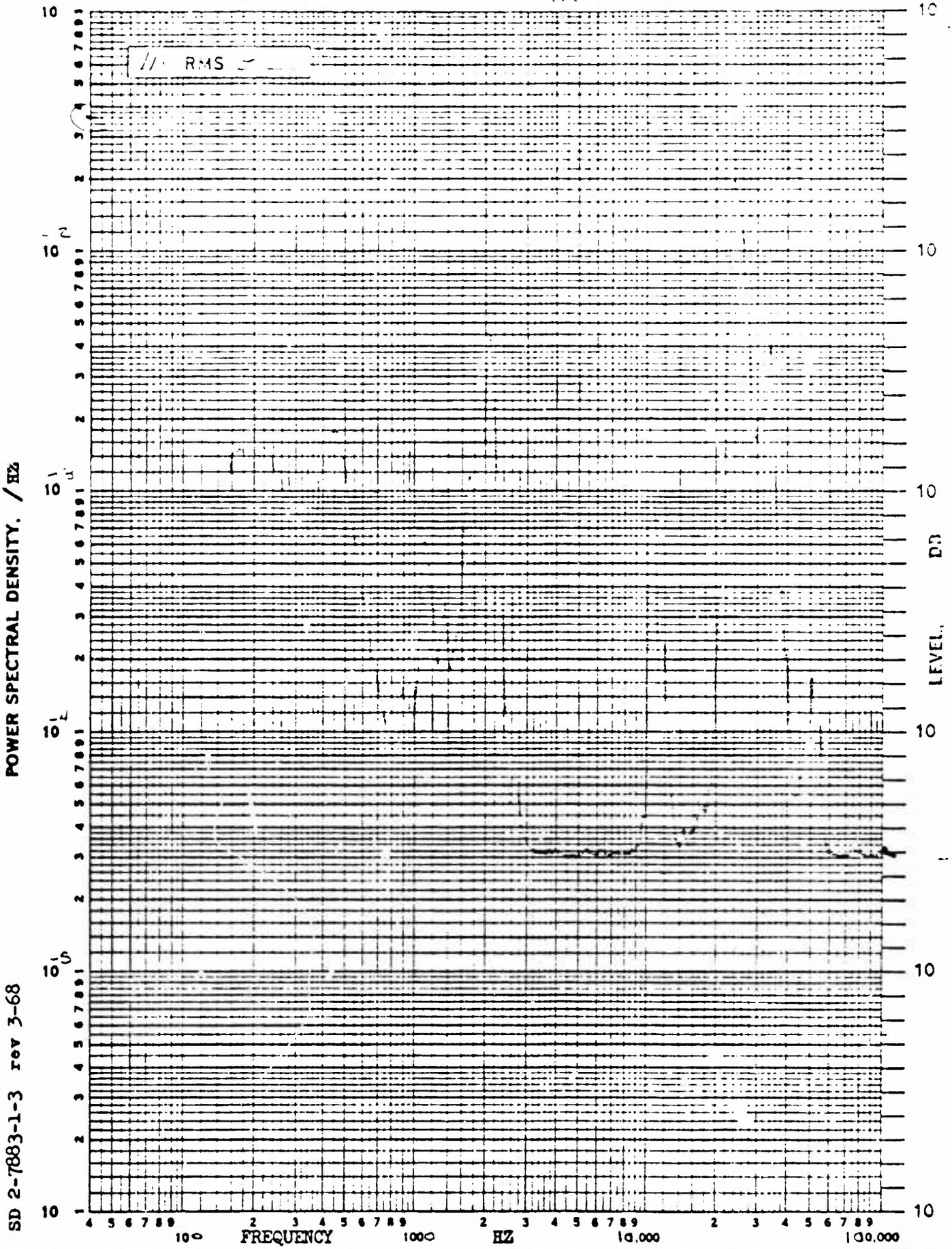

CALC.	DGT	DATE	
CHECK		ATTEST	
APP'D		T	
APP'D		E	

BEARING #6 5000 RPM
ENLARGED PIT IN INNER RACE

Figure C-33
D2-113029-3

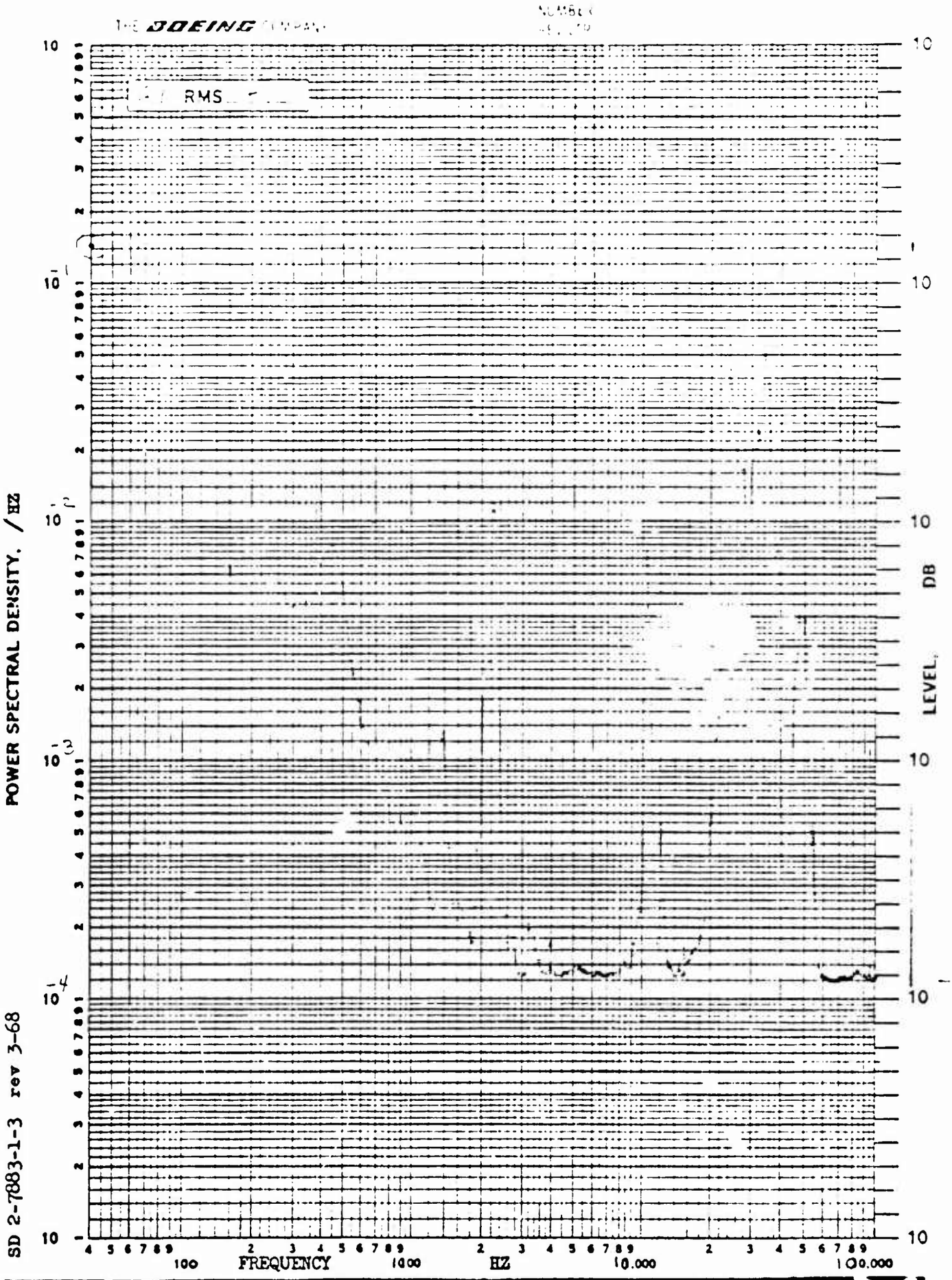

CALC.	DKT	D	
CHECK		A	
APP'D		T	
APP'D		E	

BEARING #6 10,000 R.P.M.
ENLARGED PIT IN INNER RACE

Figure C-34
D2-113029-3

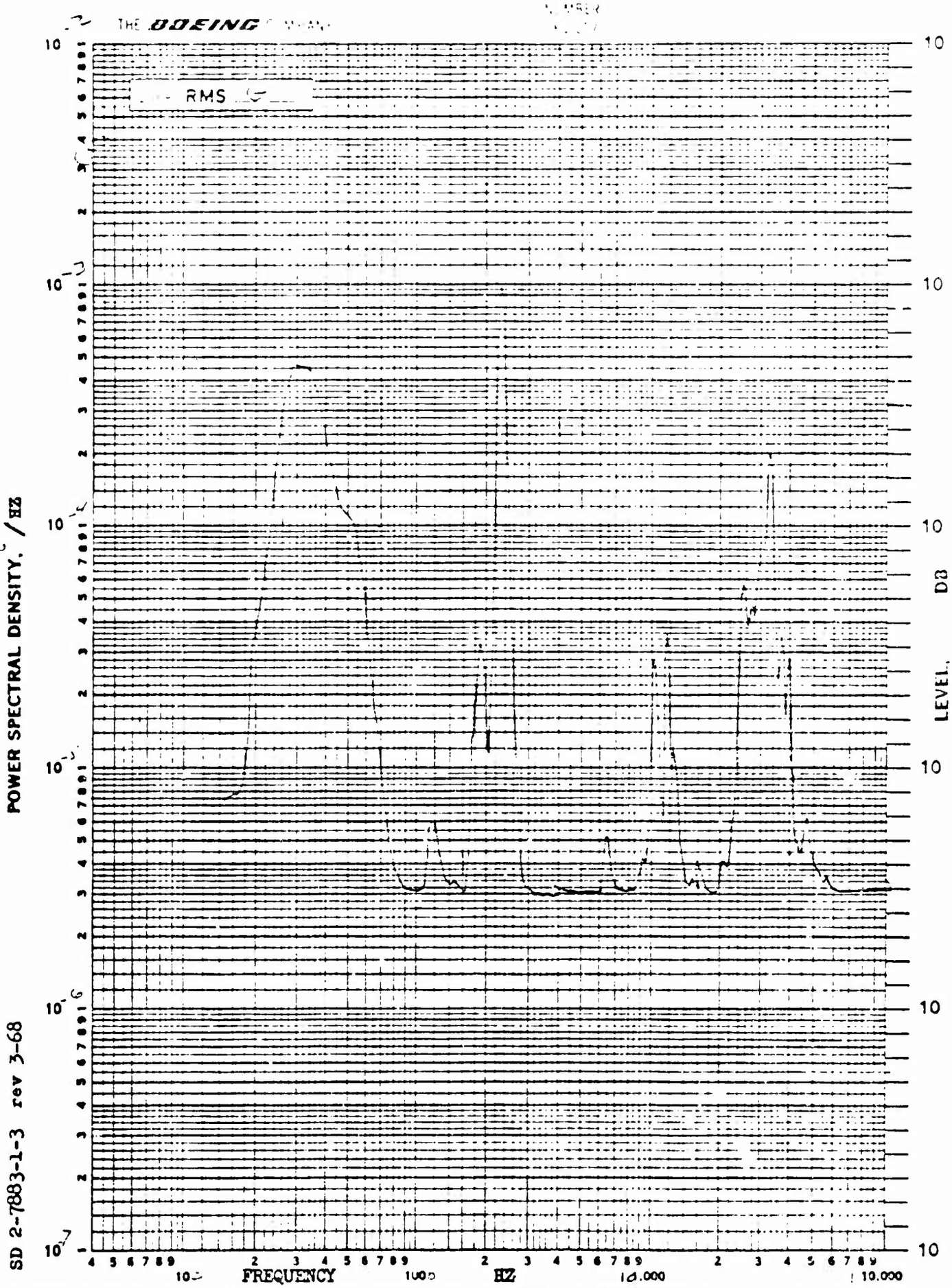

CALC.		D	Bearing # 7 New
CHECK		A	5000 RPM
APP'D		T	
APP'D		E	

Figure C-35
D2-113029-3

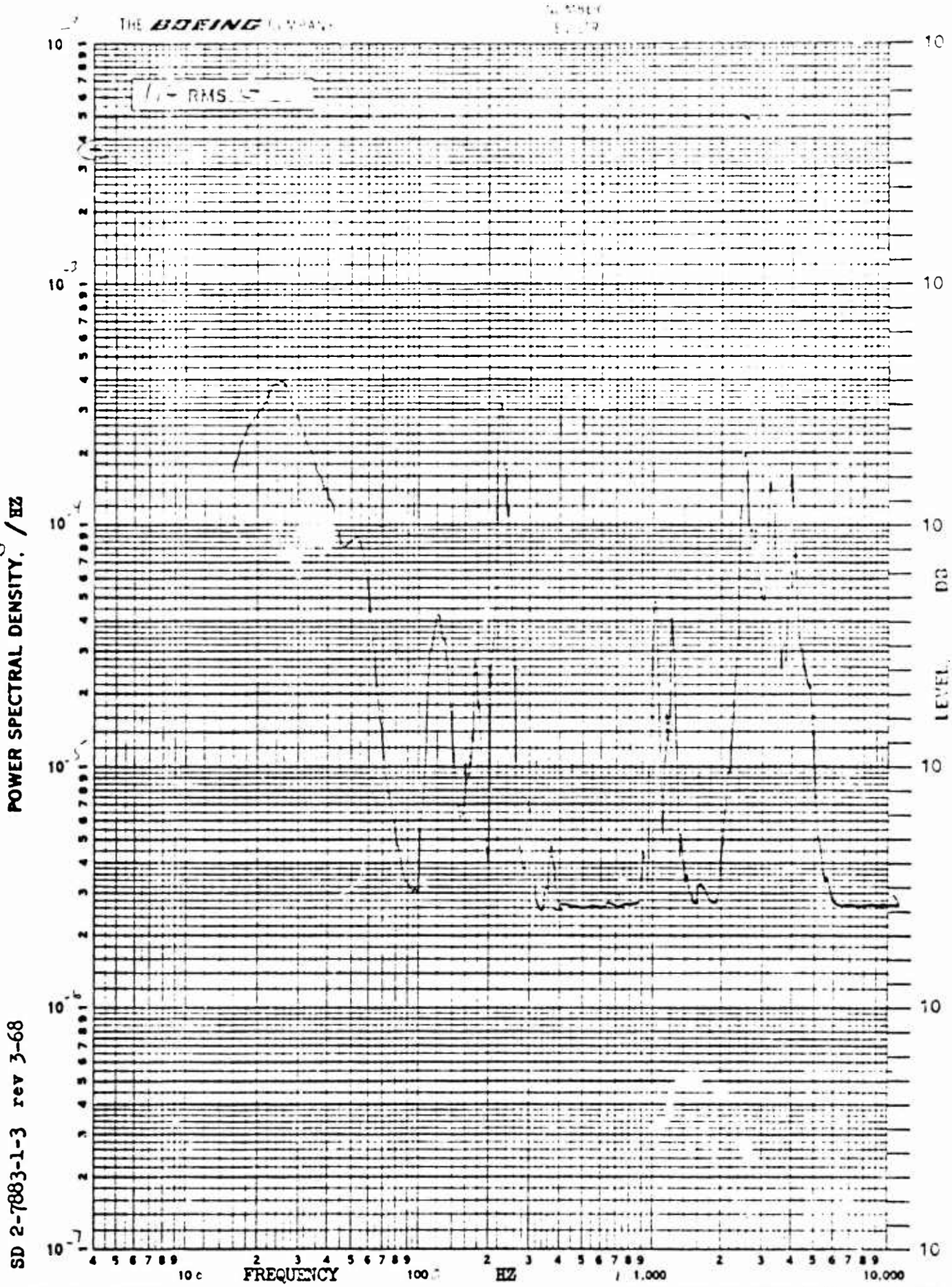

CALC.		D	Bearing # 7 New	Figure C-36
CHECK		A		D2-113029-3
APP'D		T	10,000 RPM	
APP'D		E		PAGE: 96

SD 2-7883-1-3 rev 3-68

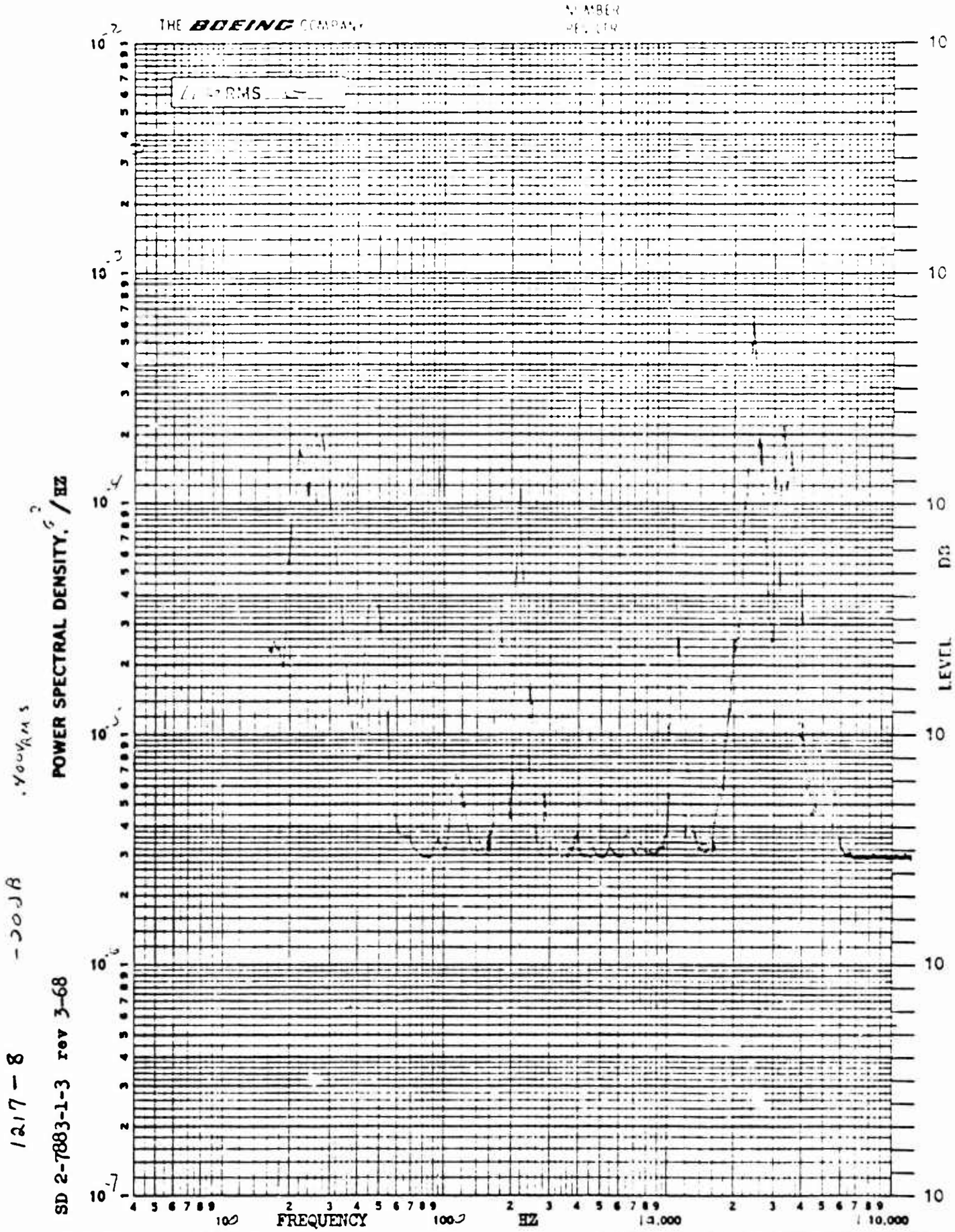

CALC.	WLH	D	Bearing #7 Fault/ball 5000 RPM
CHECK		A	
APP'D		T	
APP'D		E	

Figure C-37
D2-113029-3
PAGE: 97

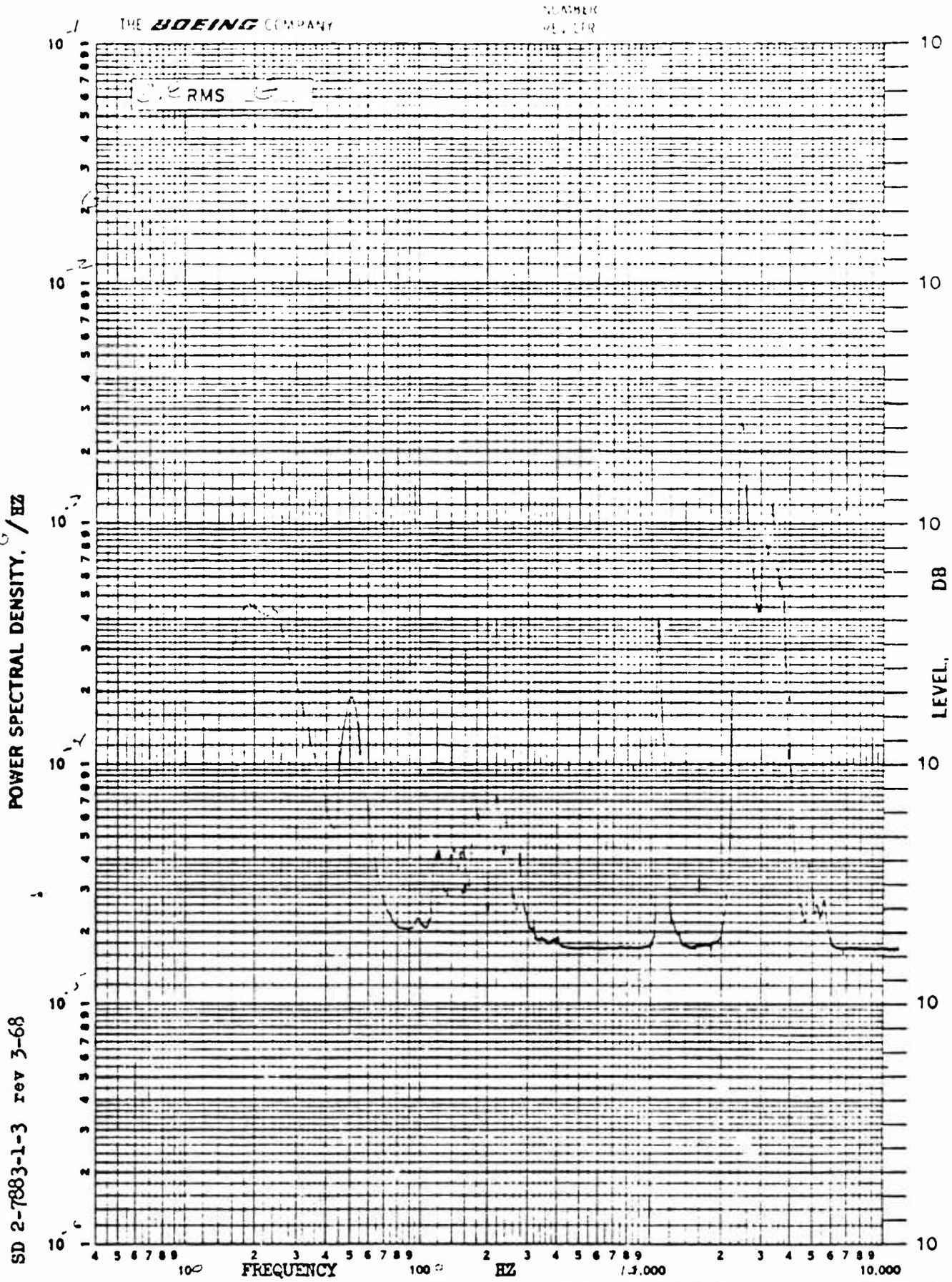

CALC.		D	Bearing #7 FAULT/BALL 10,000 RPM	Figure C-38
CHECK		A		D2-113029-3
APP'D		T		
APP'D		E		PAGE: 98

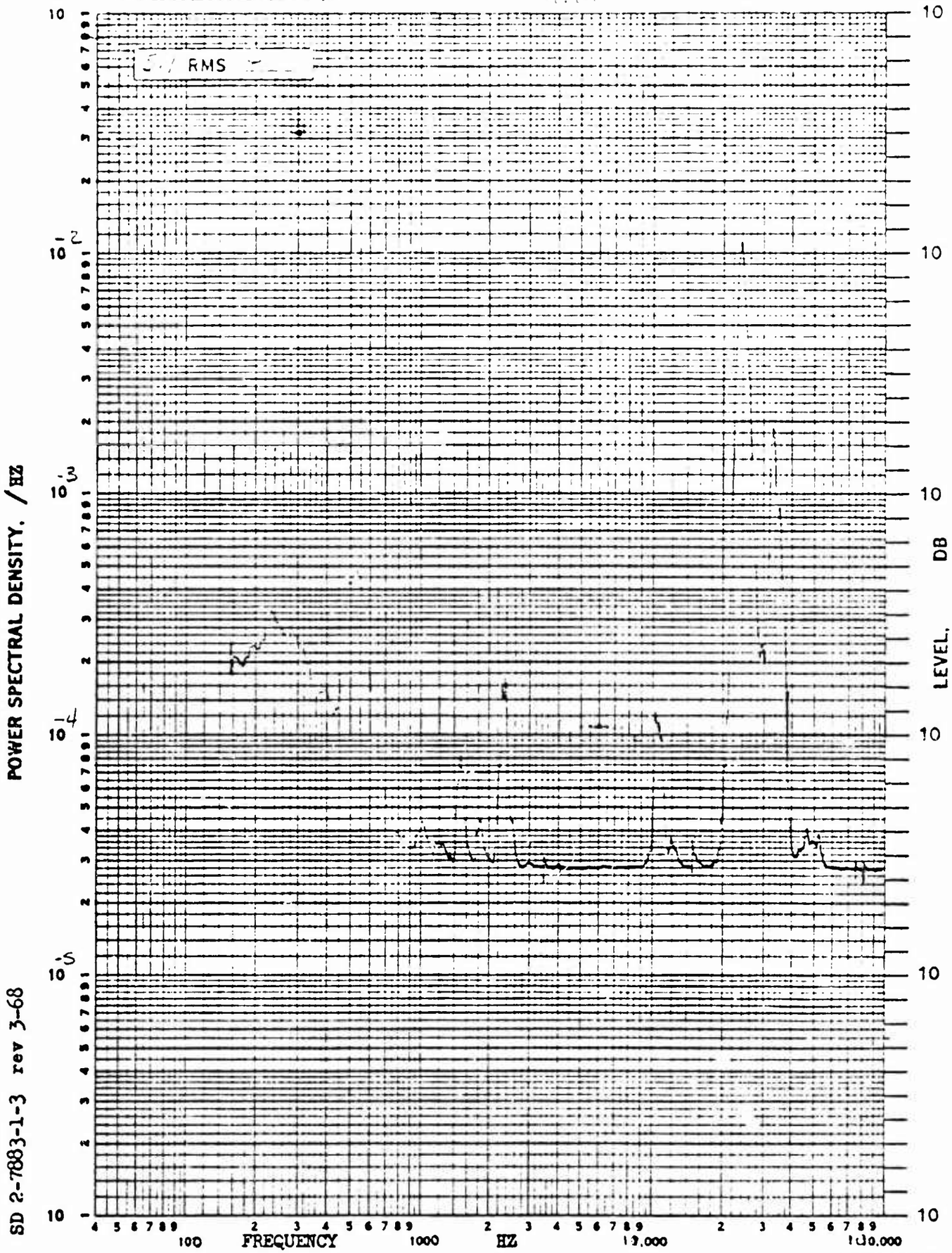

SD 2-7883-1-3 rev 3-68

CALC.			BEARING #7 5000 RPM ENLARGED PIT IN BALL
CHECK		A	
APP'D		T	
APP'D		E	

Figure C-39
D2-113029-3

THE BOEING COMPANY

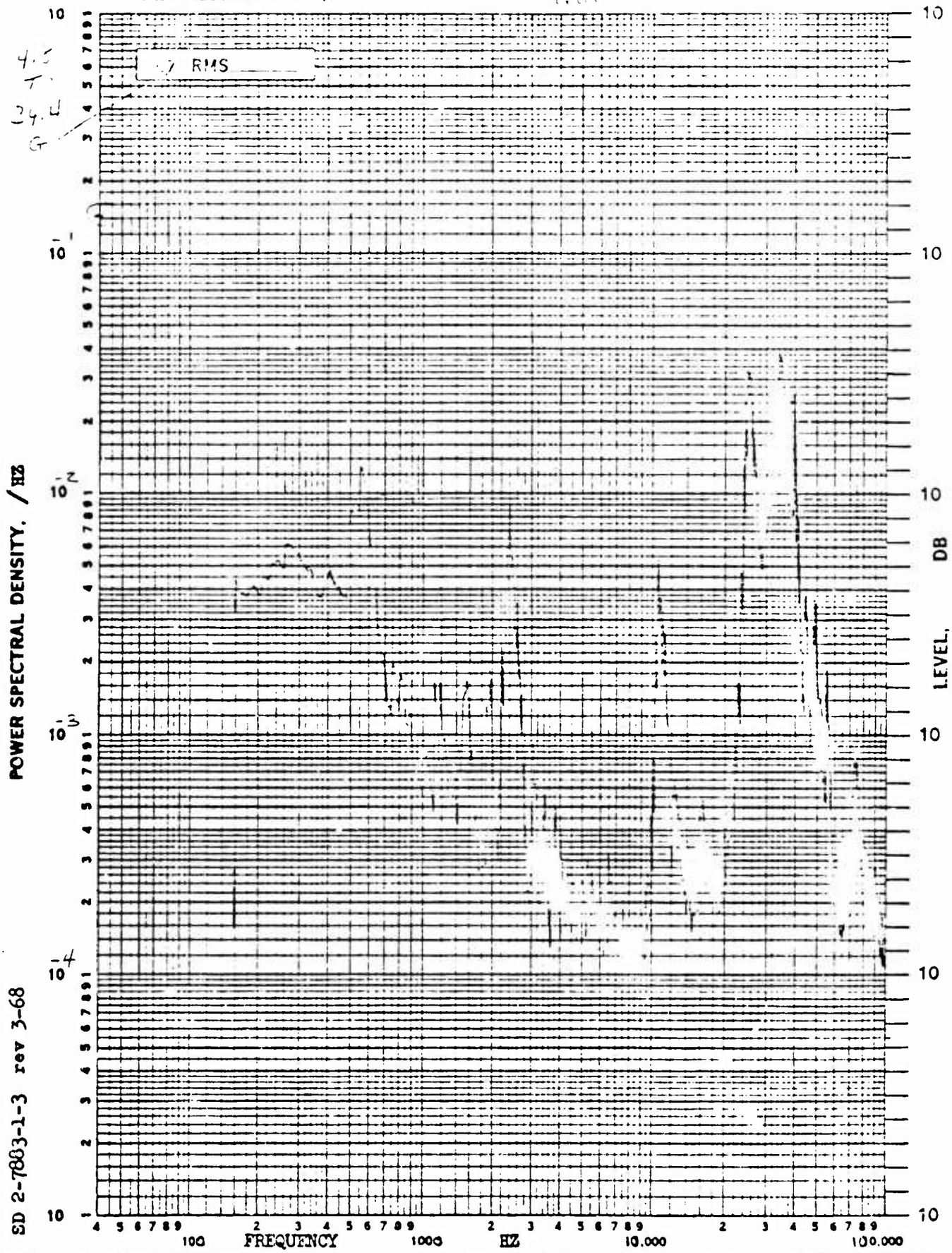

ED 2-7803-1-3 rev 3-68

CALC.			BEARING #7 10,000 R.P.M. ENLARGED PIT IN BALL
CHECK			
APP'D			
APP'D			

Figure C-40
D2-113029-3

PAGE: 100

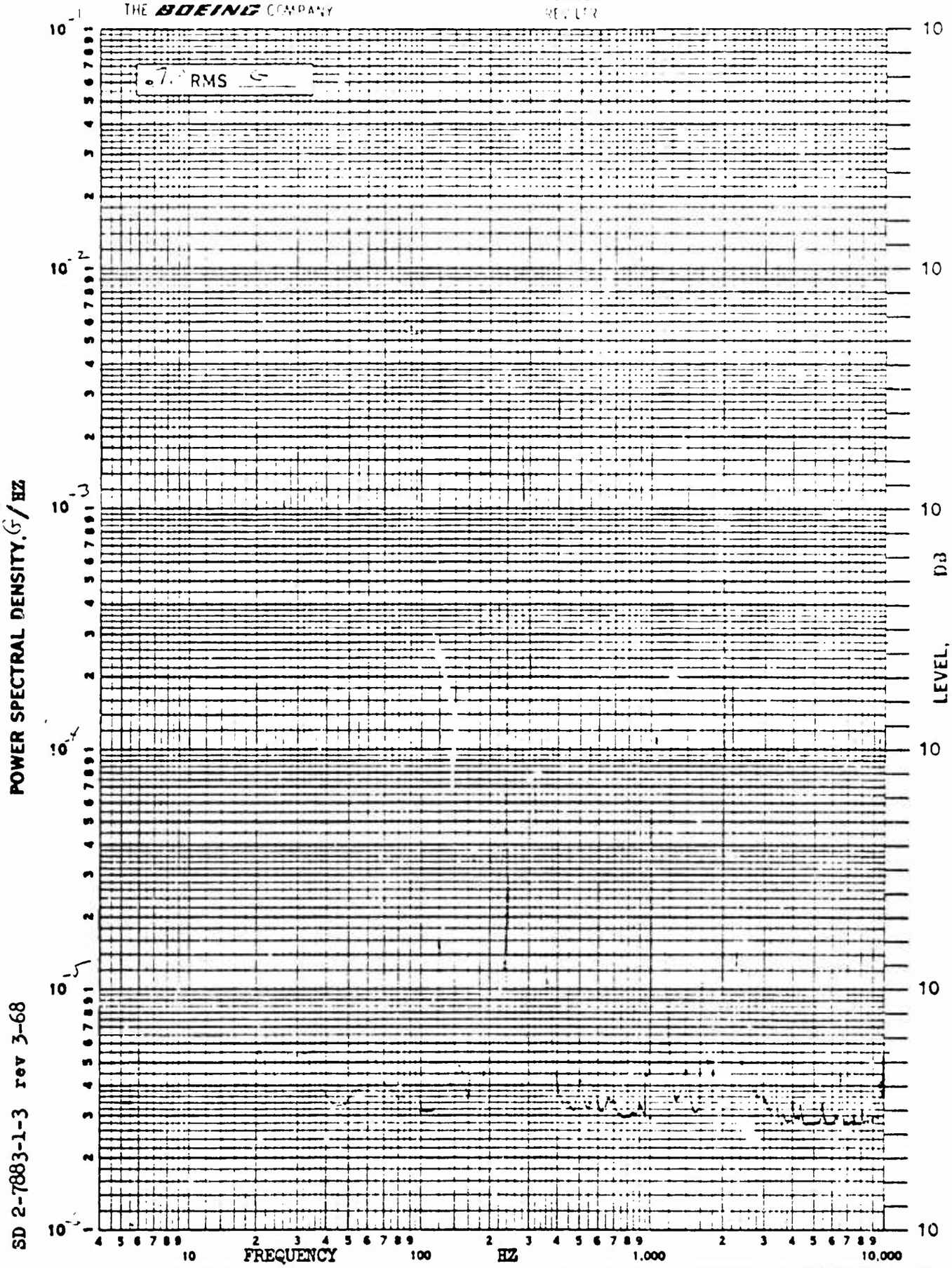

CALC.		D2-	Frequency # 4	Figure C-41
CHECK		A7		D2-113029-3
APP'D		T	5000 RPM	
APP'D		E		PAGE: 101

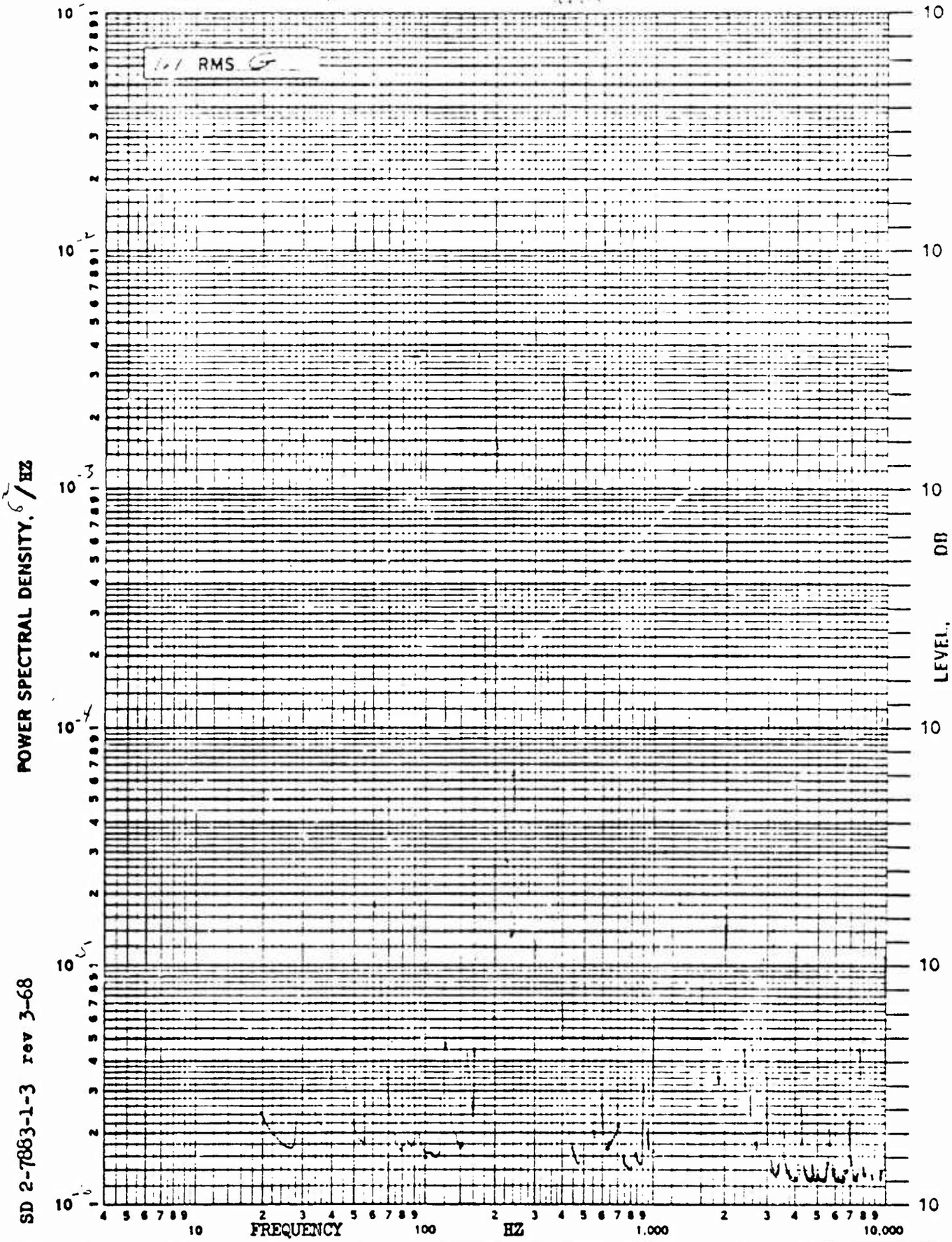

CALC.		DATE	Bearing # 4 Fault/Outer Race	Figure C-42
CHECK		ATTY		D2-113029-3
APP'D		T	10,000 RPM	
APP'D		E		PAGE: 102

THE BOEING COMPANY

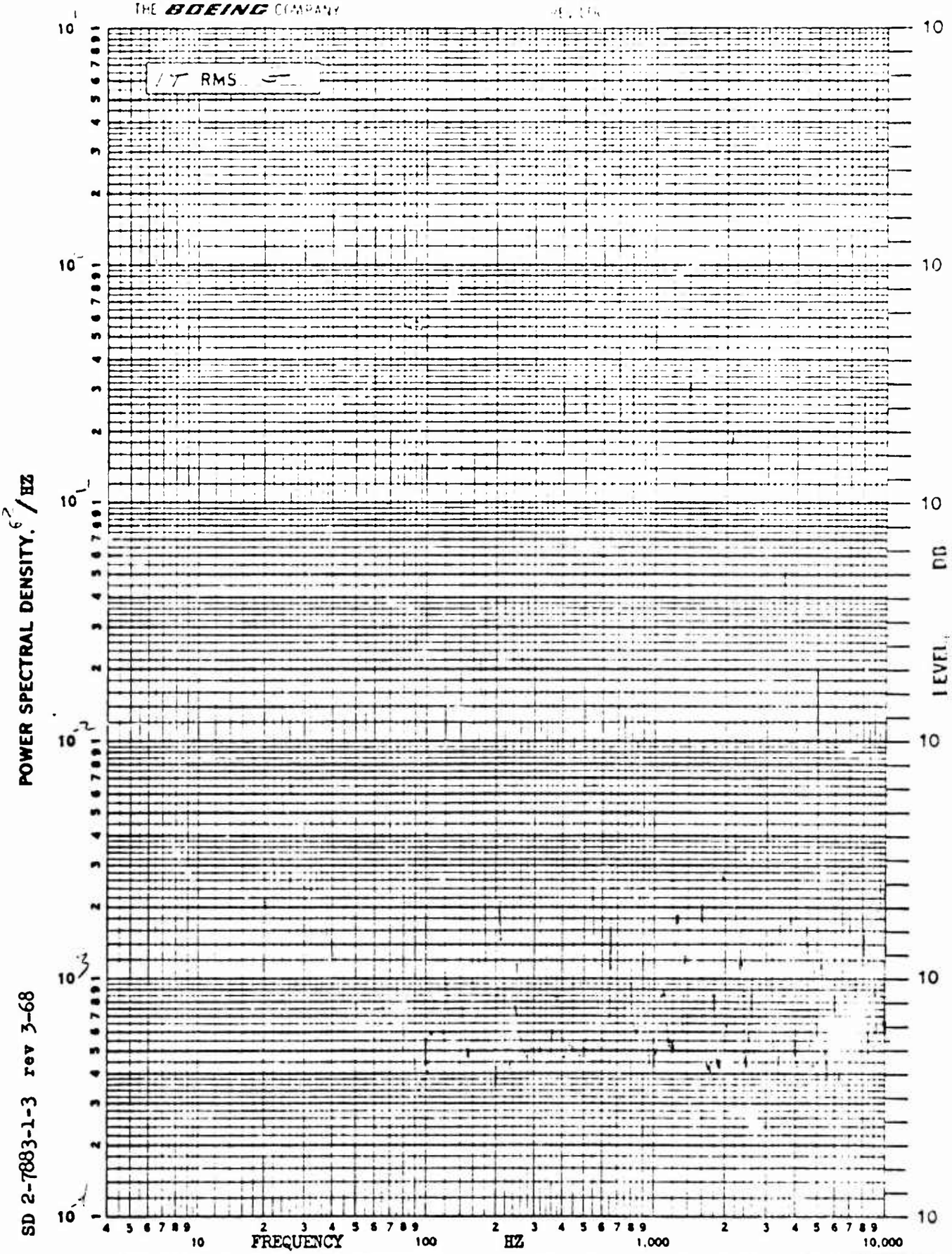

SD 2-7883-1-3 rev 3-68

CALC.		D	Bearing # 4 Enlarged 1T	Figure C-[illegible]
CHECK		A		D2-113029-[illegible]
APP'D		T	10,000 RPM	
APP'D		E		PAGE: 103

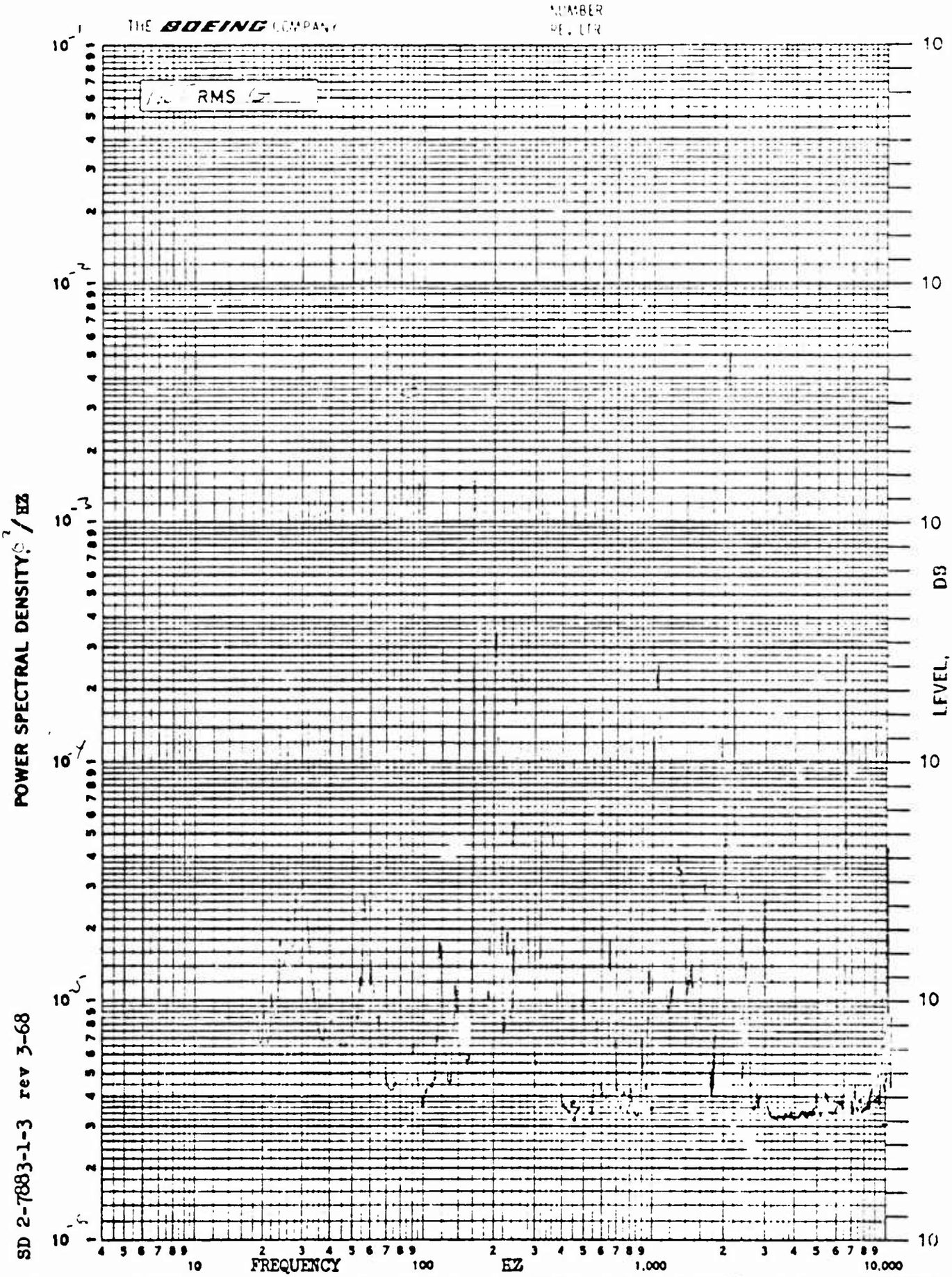

CALC.		D	Bearing # 2 New 10,000 RPM	Figure C-44
CHECK	M.R.	A		D2-113029-3
APP'D		T		
APP'D		E		PAGE: 104

1196-3

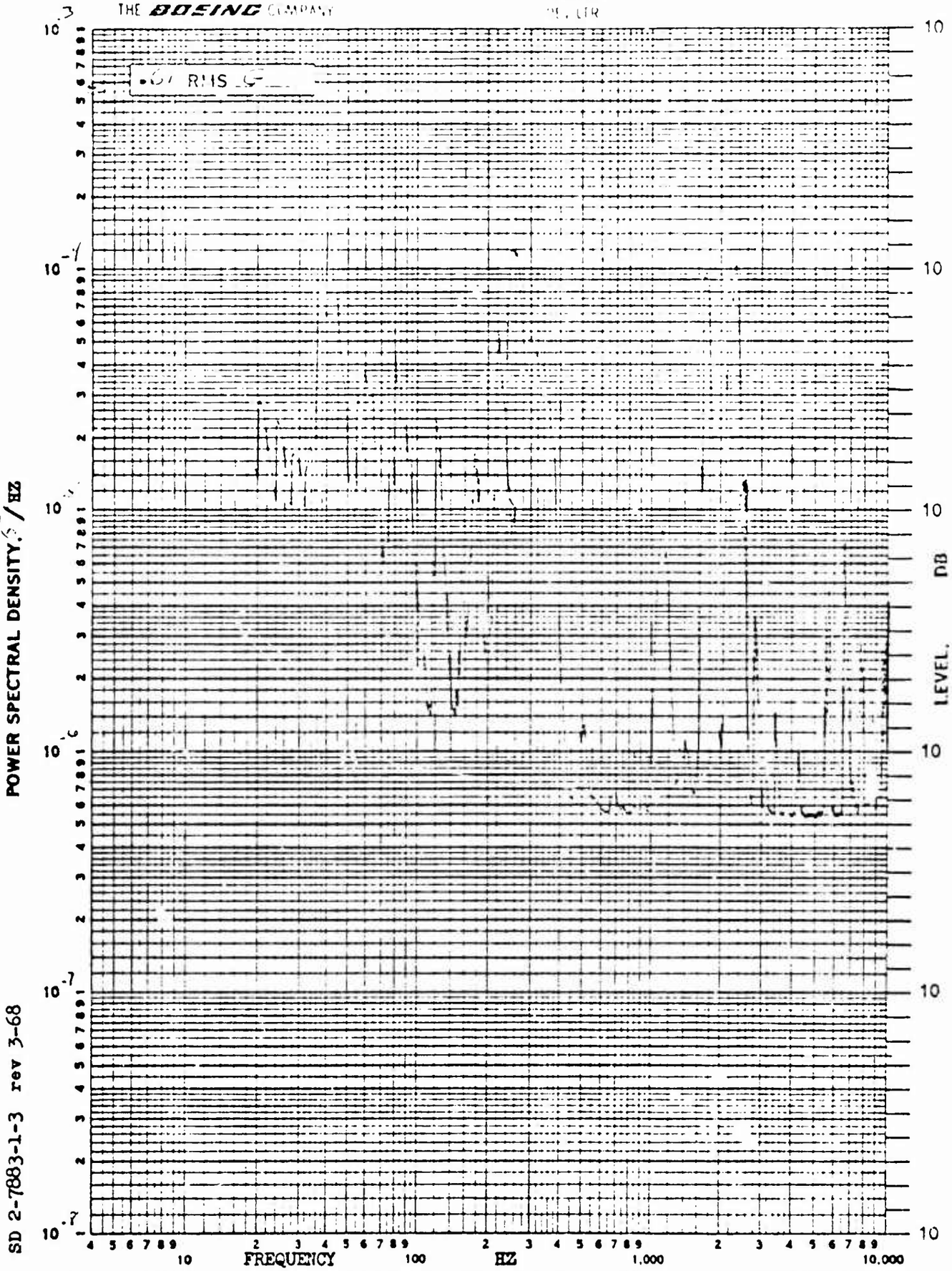

CALC.		D	Bearing #4 FAULT/Outer race 5,000 RPM
CHECK		A	
APP'D		T	
APP'D		E	

Figure C-4

D2-113029-3

NUMBER
REVISION

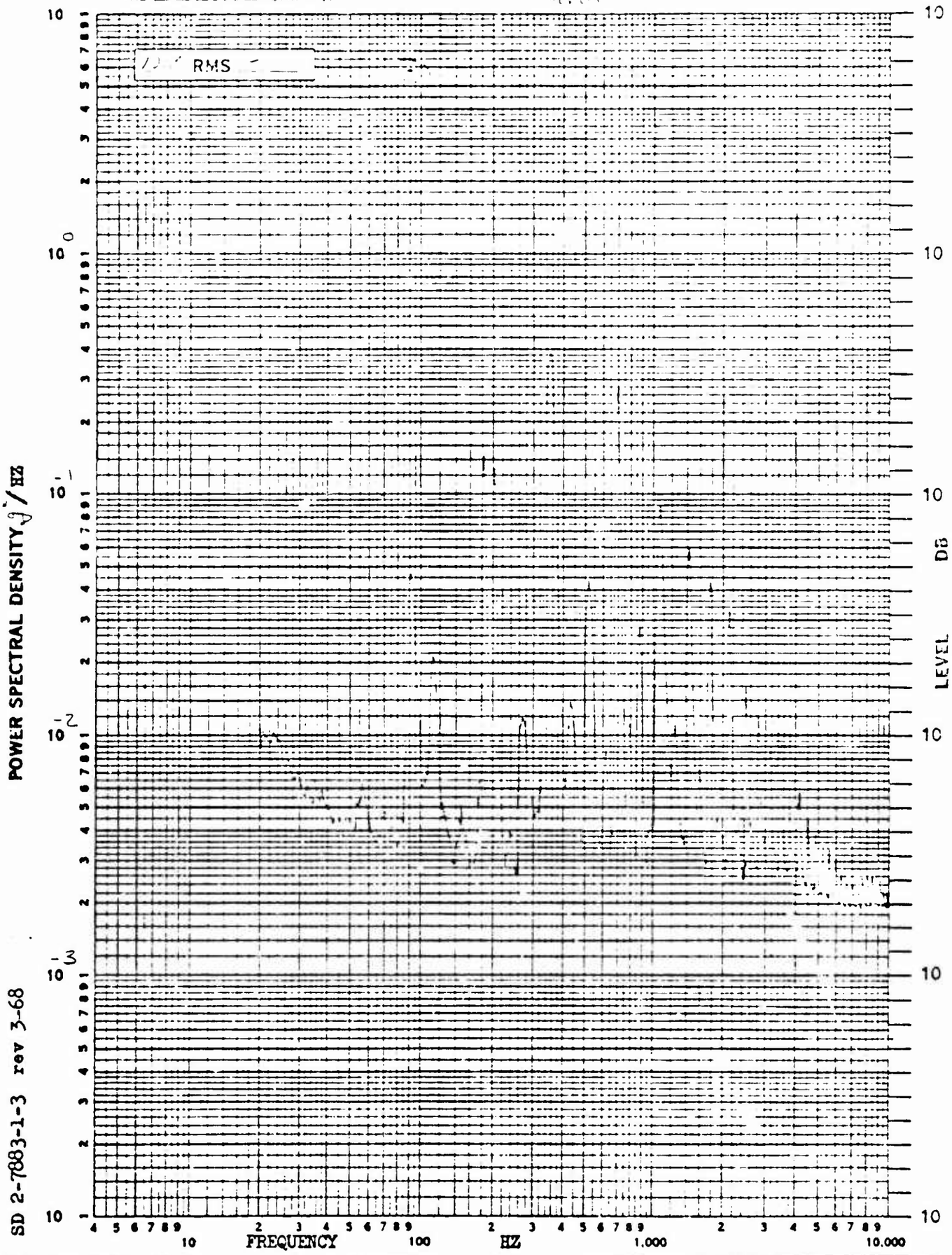

SD 2-7883-1-3 rev 3-68

CALC.	DCT	D	BEARING #4 5000 RPM ENLARGED PIT IN OUTER RACE
CHECK		A	
APP'D		T	
APP'D		E	

Figure C-46
D2-113029-3
PAGE: 106

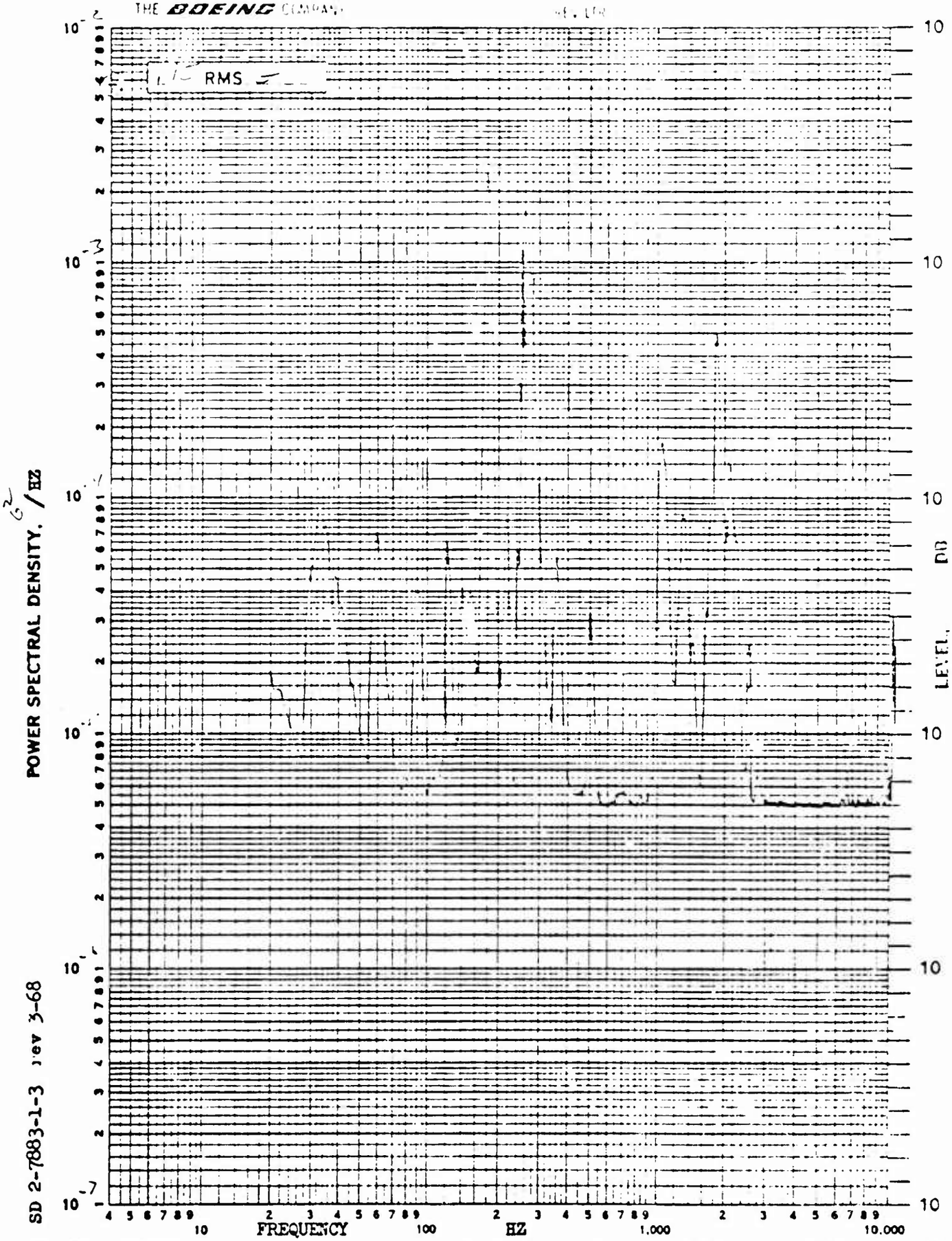

CALC.		DATE	Bearing #6 New
CHECK		ASSY	5000 RPM
APP'D		T	
APP'D		E	

Figure C-47
D2-113029-3

1196-4

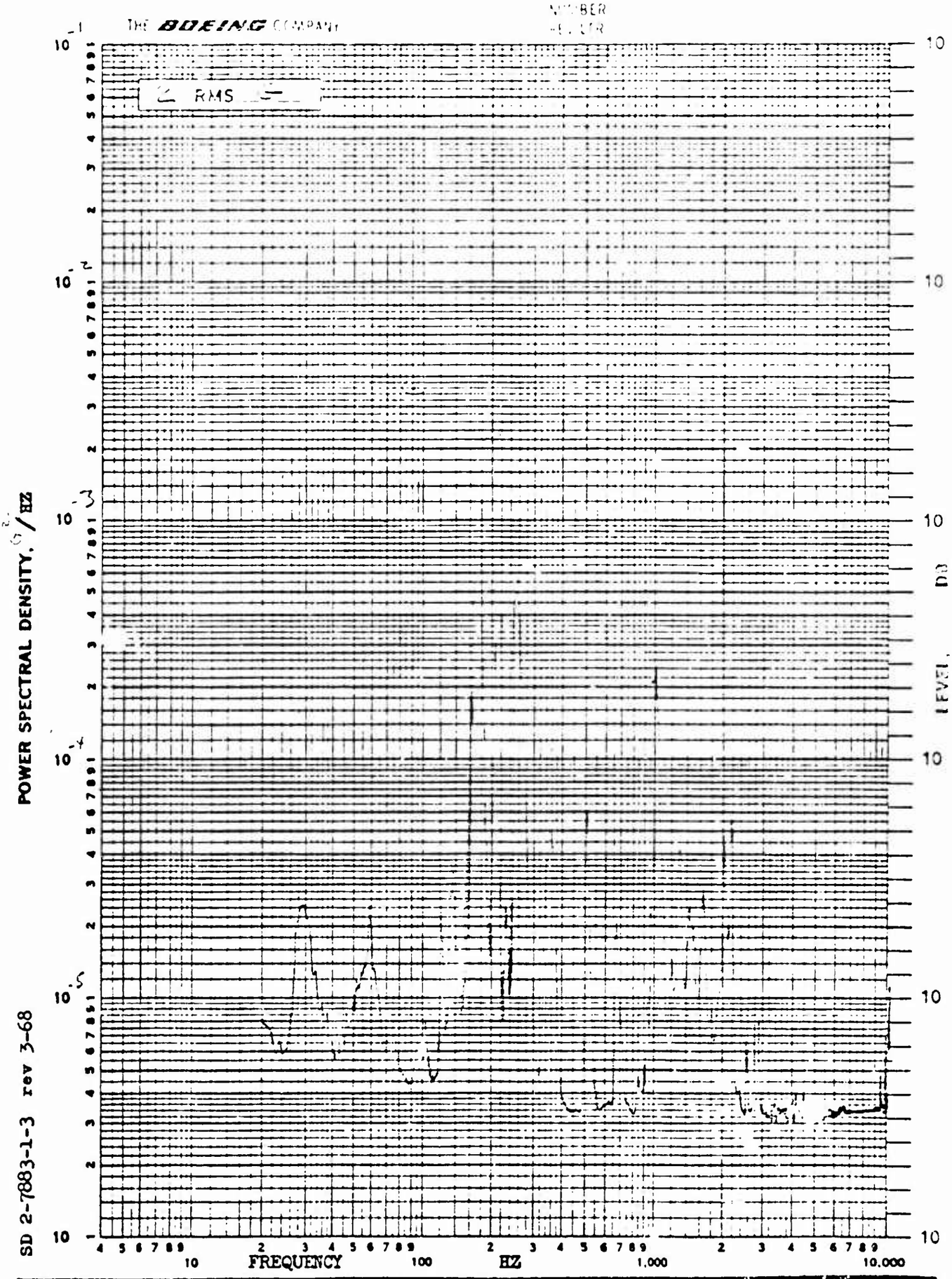

CALC.		D	Engine #6 Now 10,000 RPM
CHECK	MCR	A	
APP'D			
APP'D		E	

Figure C-48
D2-113029-3
PAGE: 108

SD 2-7883-1-3 rev 3-68

1196-5

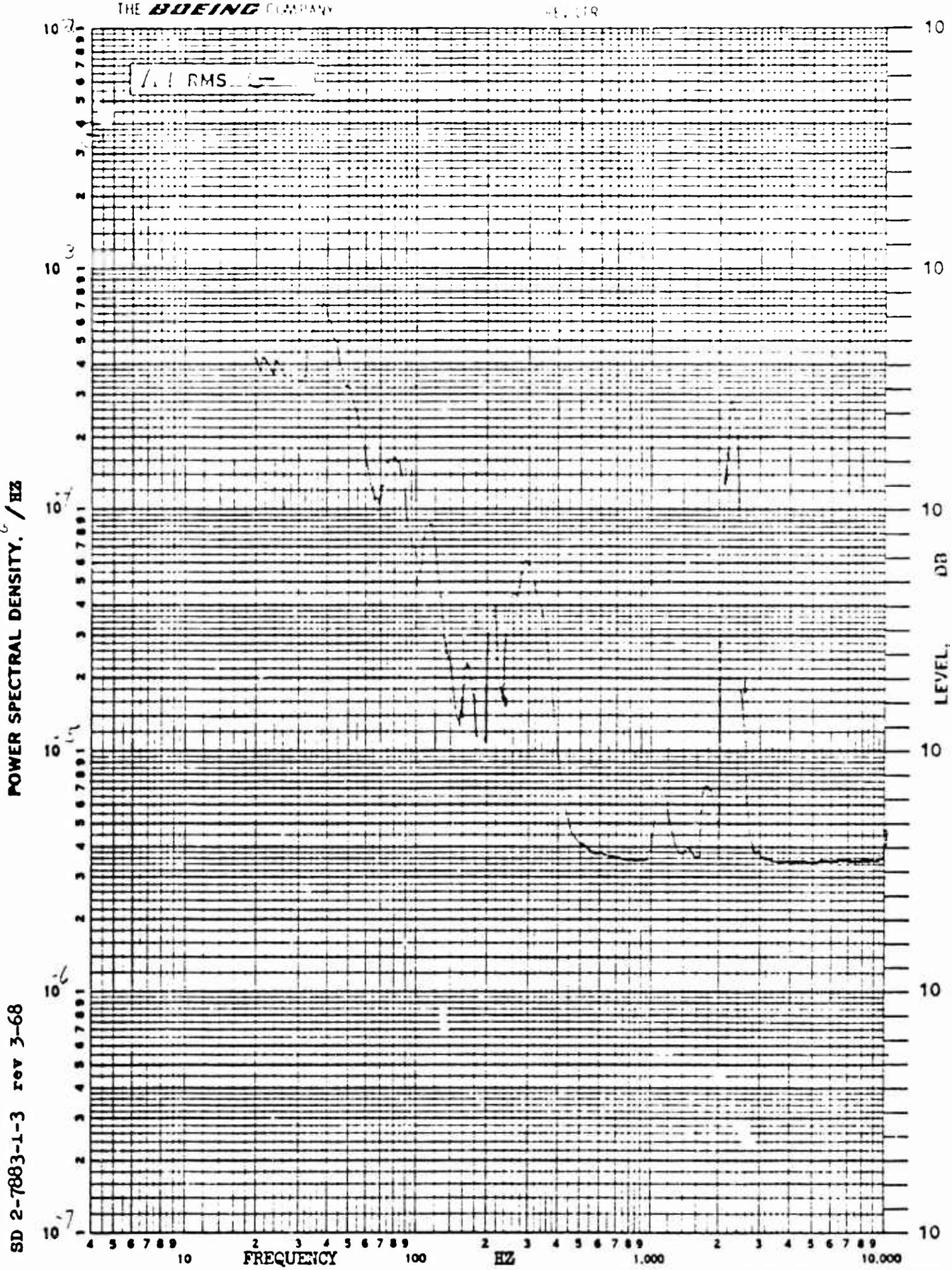

CALC.		D	Bearing #6 Fault/inner race	Figure C-49
CHECK		A	5000 RPM	D2-113029-3
APP'D		T		
APP'D		E		PAGE: 109

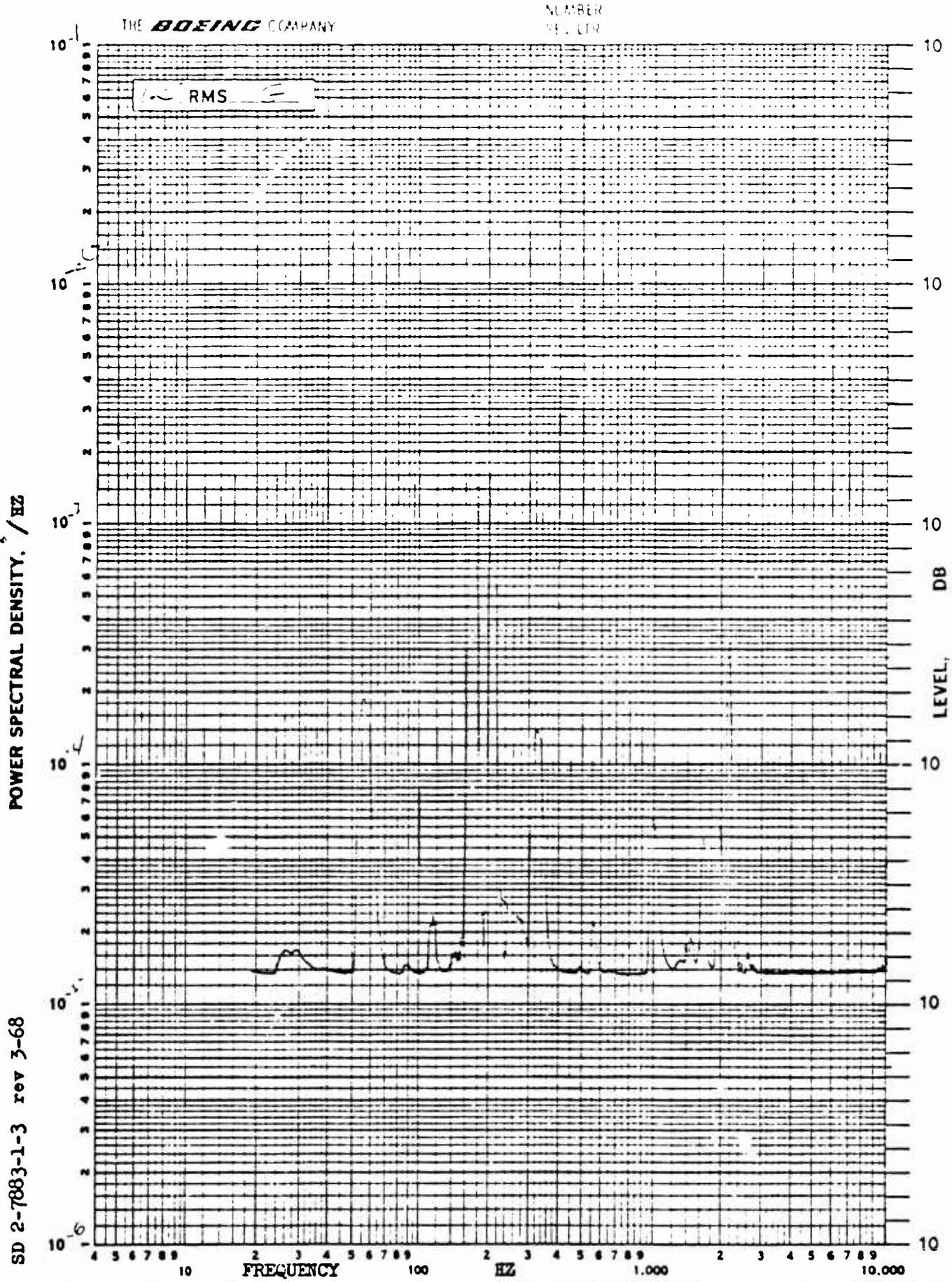

CALC.		D	Battery #6 FAULT/Interface	Figure C-50
CHECK		A	10,000 FPM	D2-113029-3
APP'D		T		
APP'D		E		PAGE: 110

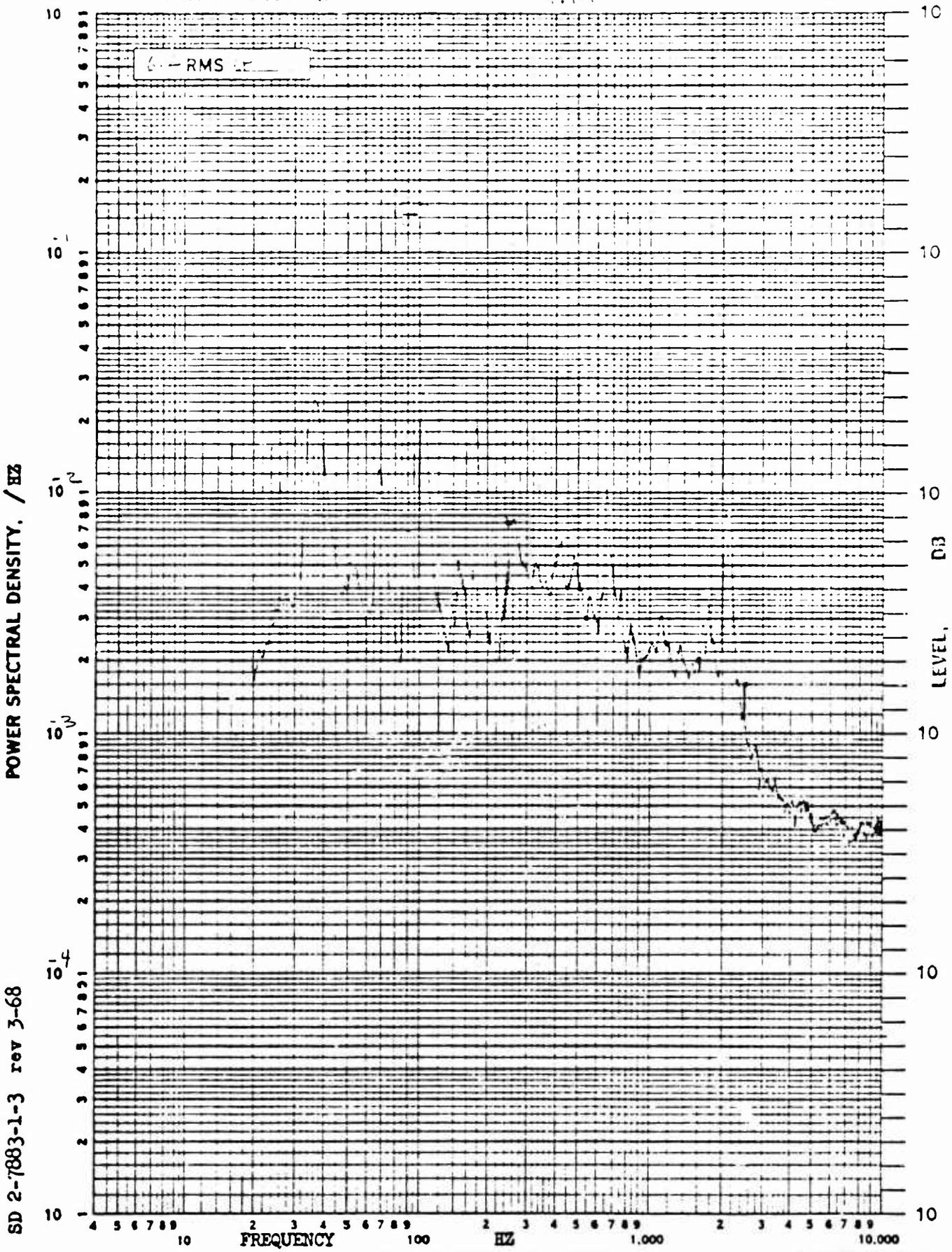

CALC.		DATE	BEARING #6 5,000 R.P.M. ENLARGED PIT IN INNER RACE
CHECK		A	
APP'D		T	
APP'D		E	

Figure C-51
D2-113029-3
PAGE: 111

THE BOEING COMPANY

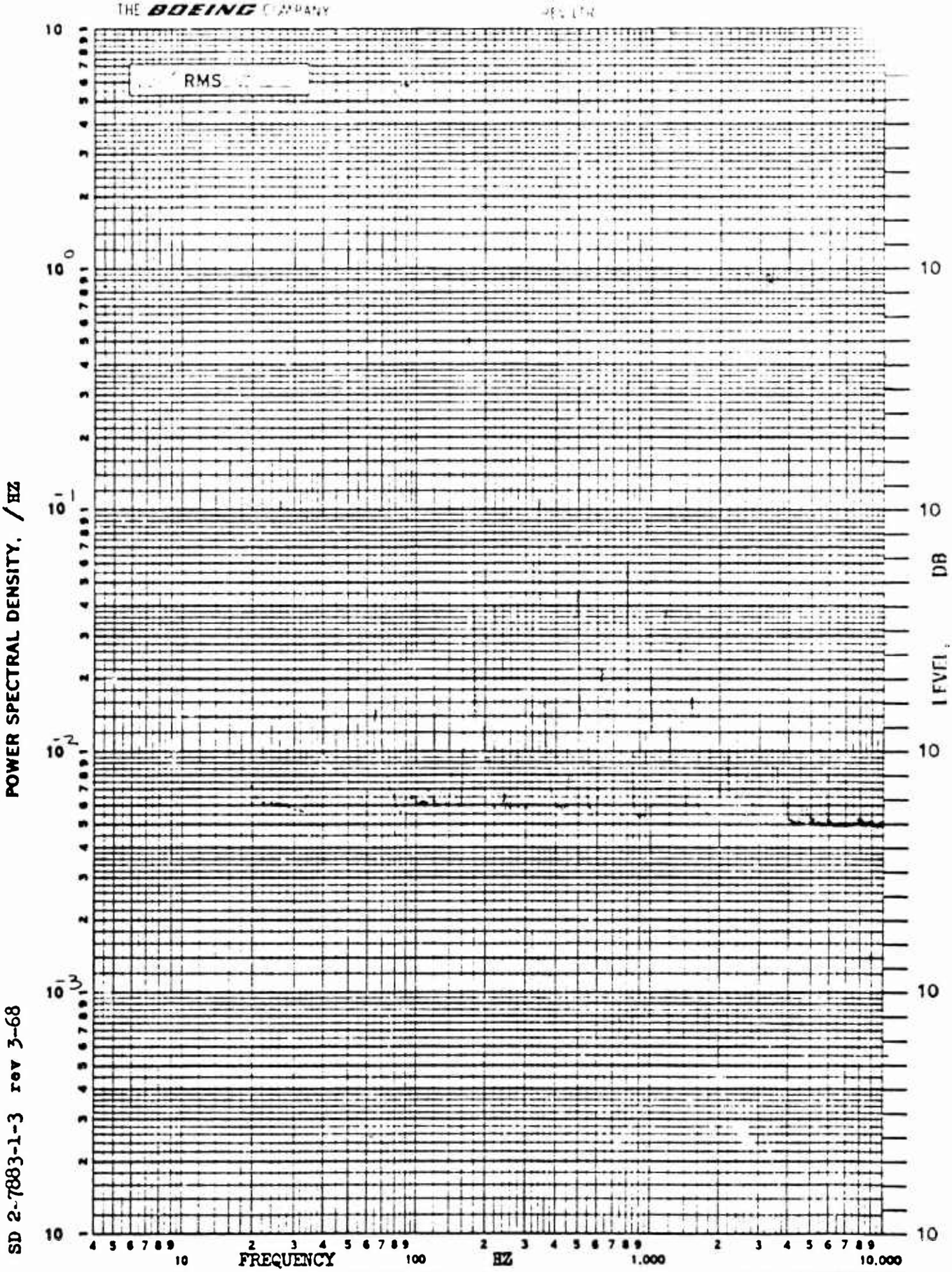

SD 2-7883-1-3 rev 3-68

1329-5 -20 db .320V/FMS

CALC.		D	
CHECK		A	
APP'D		T	
APP'D		E	

BEARING #6 10,000 RPM
ENLARGED PIT IN INNER RACE

Figure C-52
D2-113029-3

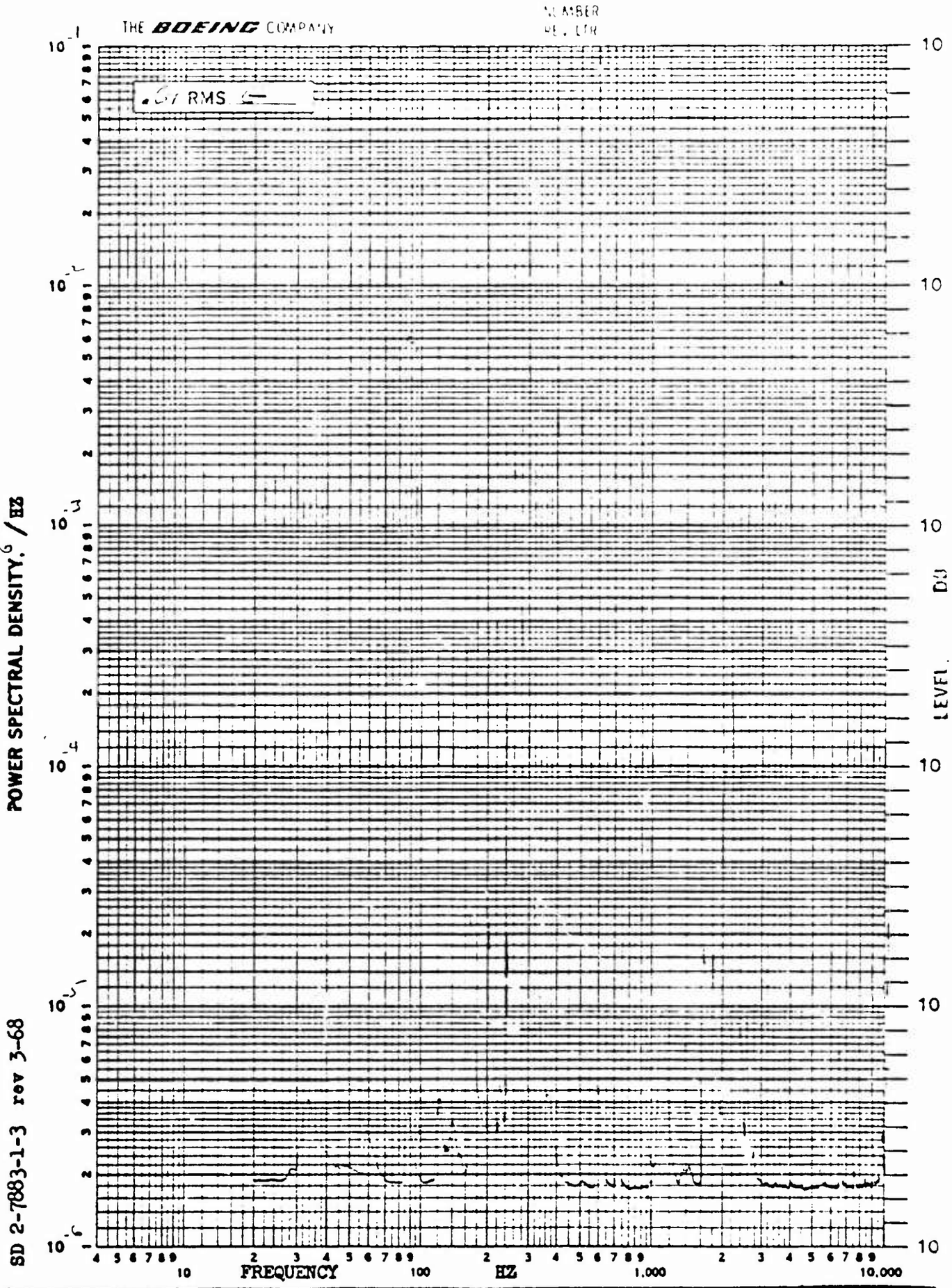

CALC.		D	Bearing # 7 New
CHECK	MCK	A	
APP'D		T	5000 RPM.
APP'D		E	

Figure C-53
D2-113029-3
PAGE: 113

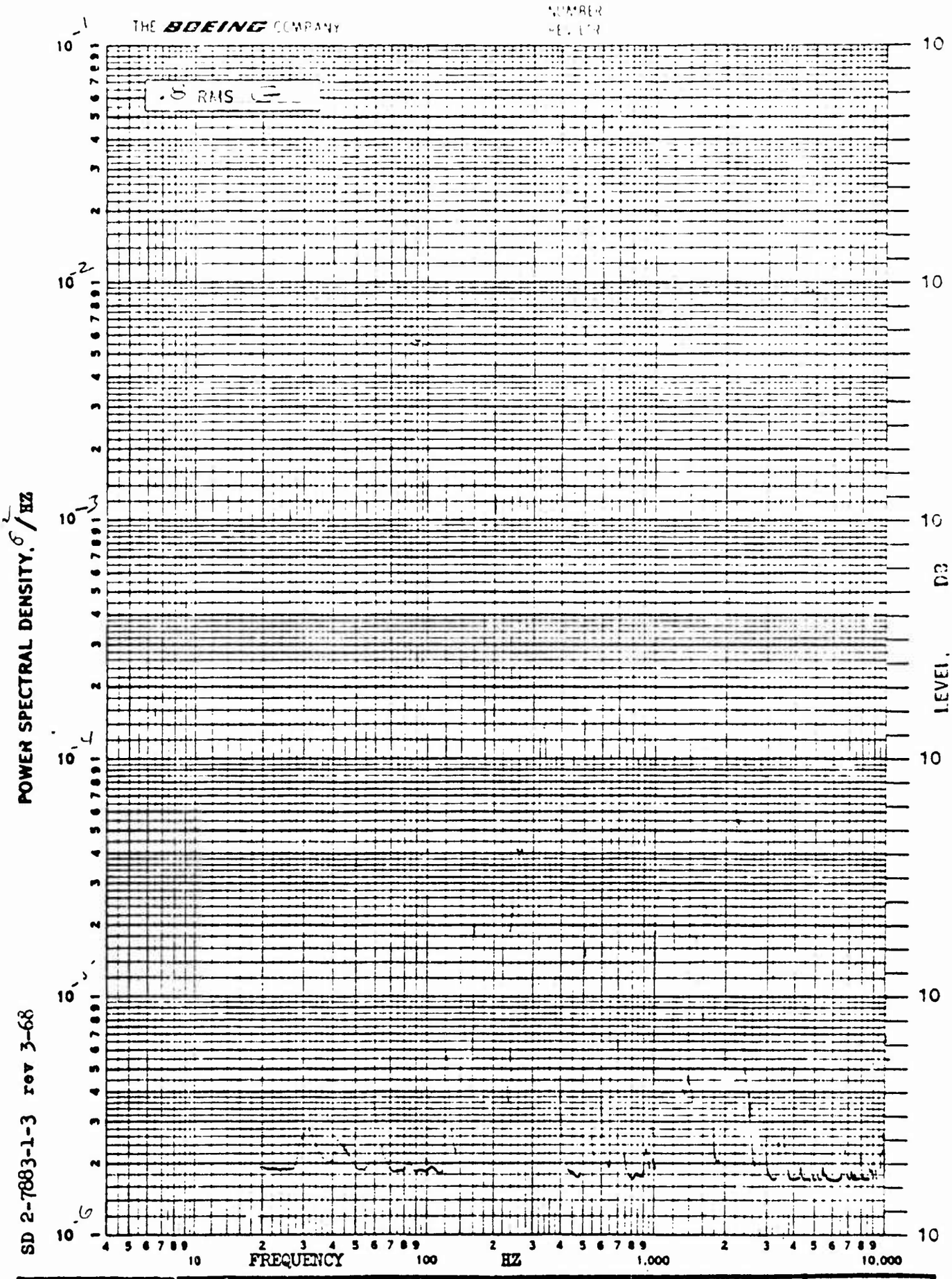

CALC.	[illegible]	D[illegible]	Bearing #7 New	Figure C-54
CHECK	MCR	A[illegible]		D2-113029-3
APP'D		T	10,000 RPM	
APP'D		E		PAGE: 114

SD 2-7883-1-3 rev 3-68

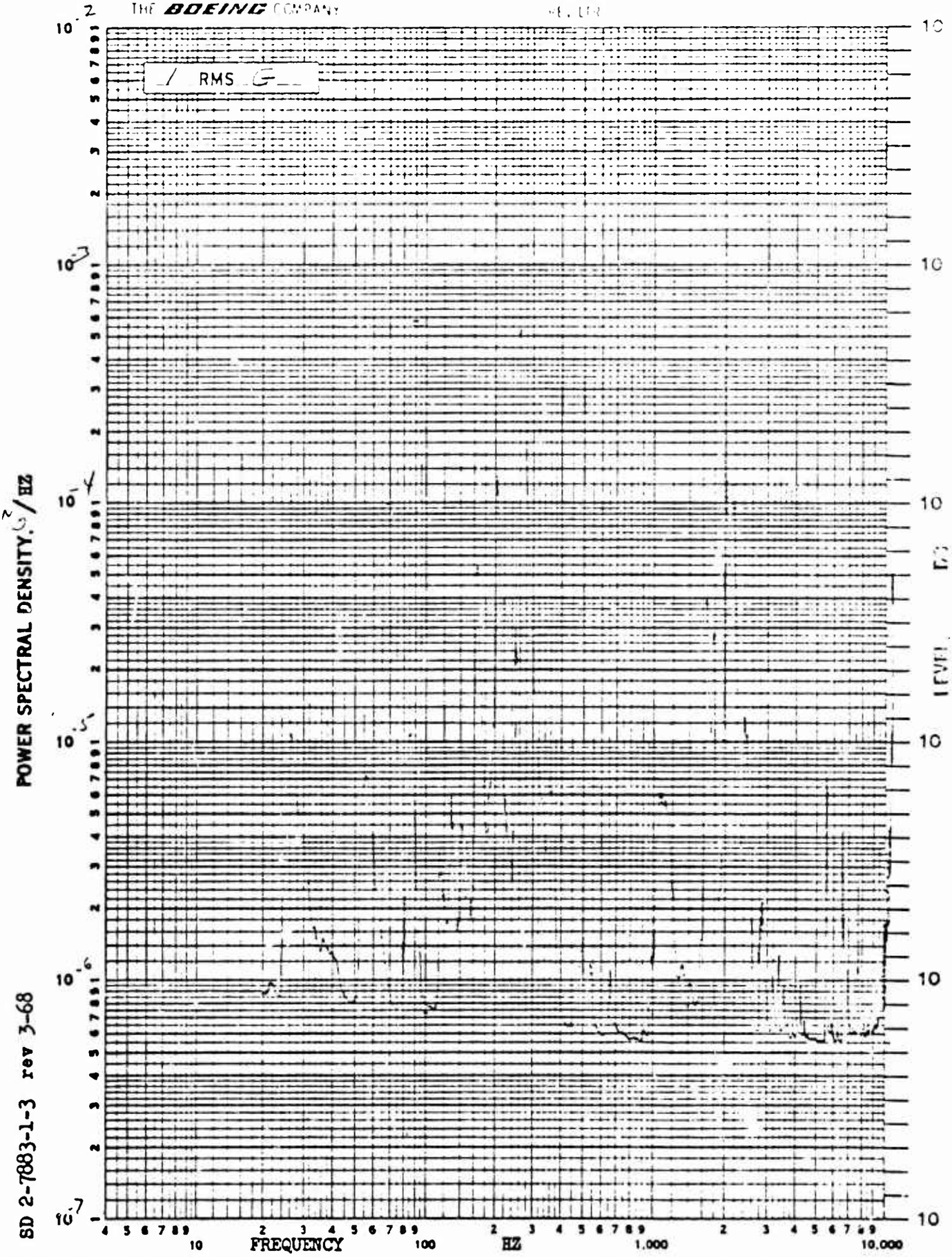

CALC.		D	Earing #7 Fault/Ell	Figure C-55
CHECK		A		D2-113029-3
APP'D		T	5000 RPM	
APP'D		E		PAGE: 115

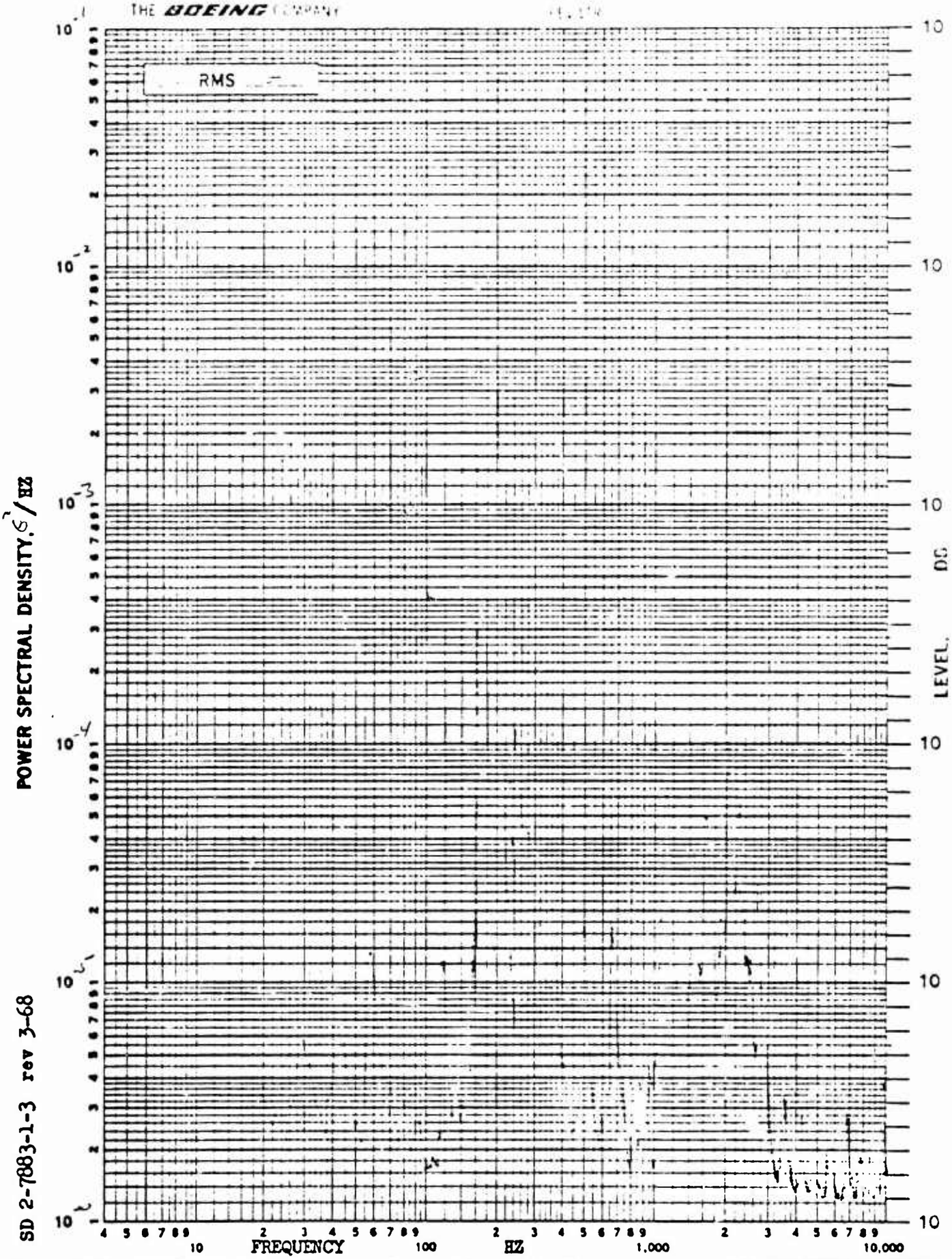

CALC.		D	Boeing 7 Foot/Eff	Figure C-56
CHECK		A		D2-113029-3
APP'D		T	10,000 RPM	
APP'D		E		PAGE: 116

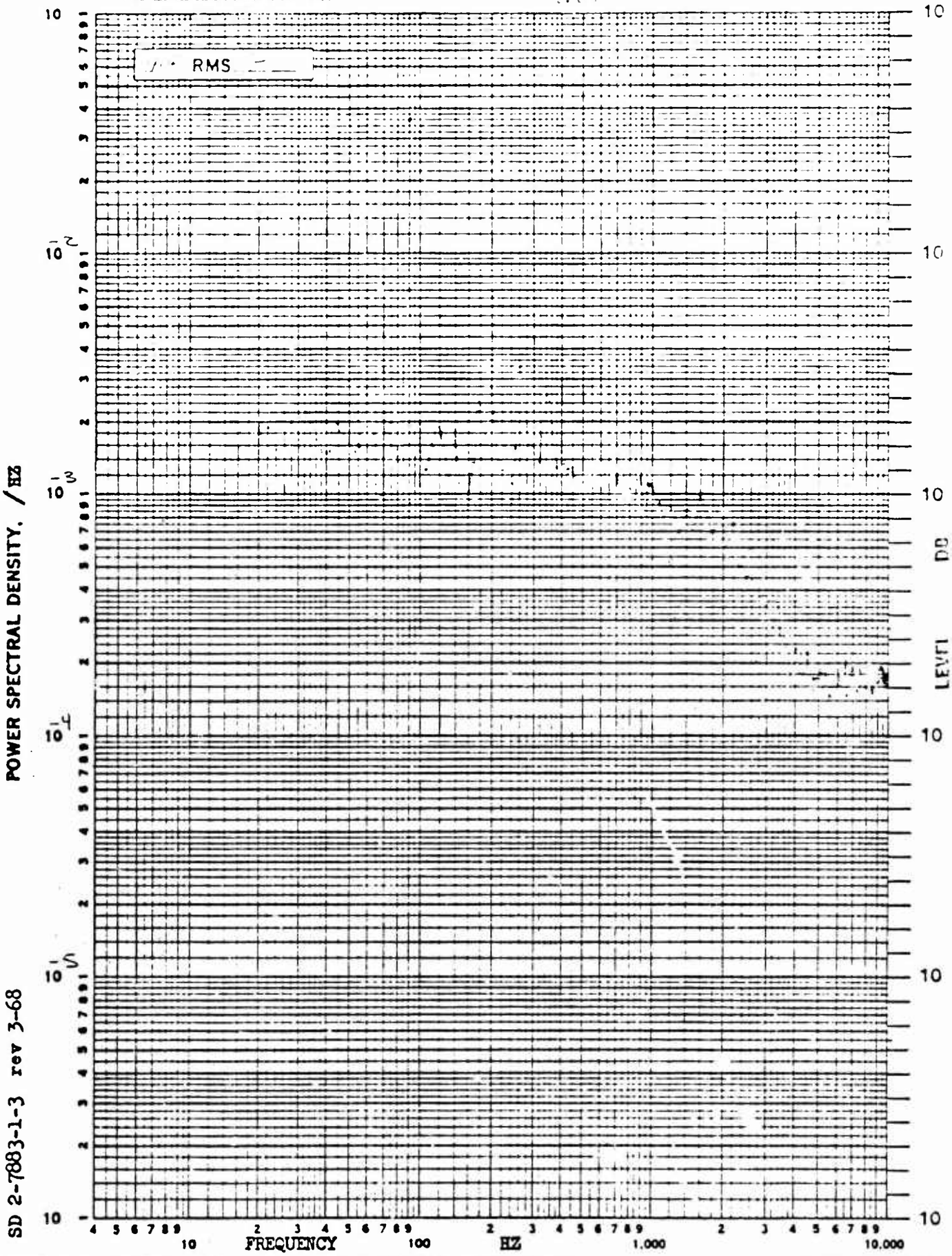

SD 2-7883-1-3 rev 3-68

1324-6 - 30 Nb . 498 V Rms

CALC.	DVT	D	BEARING #7 5,000 RPM ENCLARGED PIT IN BALL
CHECK		A	
APP'D		T	
APP'D		E	

Figure C-57
D2-113029-3
PAGE: 117

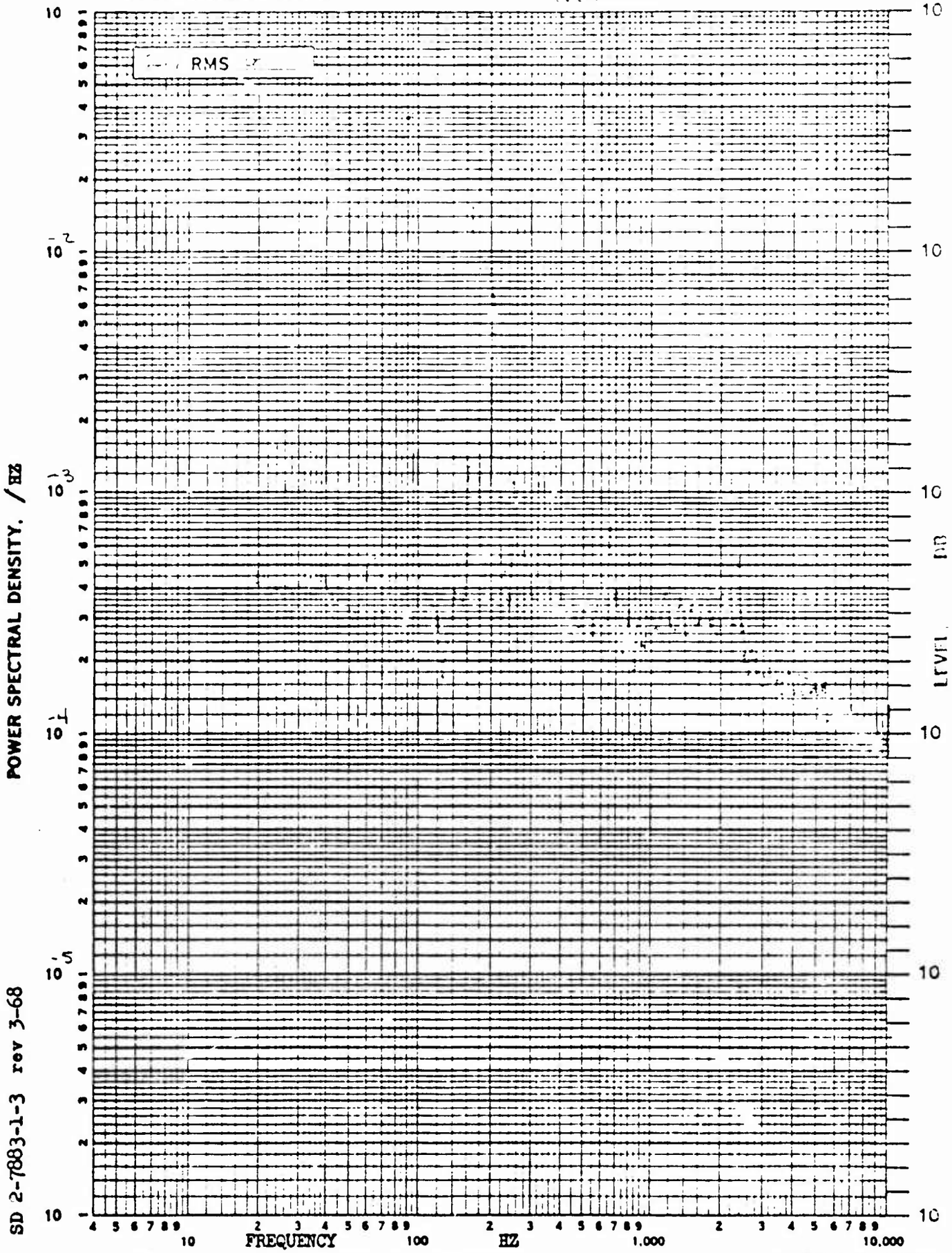

CALC.	DMT	D7-[illegible]	BEARING #7 10,000 R.P.M. ENLARGED PIT IN BALL
CHECK	[illegible]	A[illegible]	
APP'D		T	
APP'D		E	

Figure C-52
D2-113029-3

1329-7 -30.11 .292 V RMS

Unclassified

DOCUMENT CONTROL DATA - R&D

Security classification of title, body of abstract and indexing annotation must be entered when the overall report is classified

1. ORIGINATING ACTIVITY (Corporate author) The Boeing Company, Aerospace Group, Aerospace Systems Division--Kent Facility P. O. Box 3999, Seattle, Wash. 98124	2a. REPORT SECURITY CLASSIFICATION Unclassified 2b. GROUP

3. REPORT TITLE

Incipient Failure Detection: Incipient Failure Detection in Ball Bearings.

4. DESCRIPTIVE NOTES (Type of report and inclusive dates)

Final Report

5. AUTHOR(S) (First name, middle initial, last name)

H. L. Balderston

6. REPORT DATE	7a. TOTAL NO. OF PAGES	7b. NO. OF REFS
August 22, 1969	118	5

8a. CONTRACT OR GRANT NO.	9a. ORIGINATOR'S REPORT NUMBERS
b. nil	D2-113029-3
c. nil	9b. OTHER REPORT NO(S) (Any other numbers that may be assigned this report)
d. nil	

10. DISTRIBUTION STATEMENT All government agencies may obtain copies directly from DDC. DDC is requested to route all other requests to Boeing for approval. Ref. H. F. Eppenstein or J. W. Griswold

11. SUPPLEMENTARY NOTES	12. SPONSORING MILITARY ACTIVITY
Includes a bibliography of ten (10) items.	nil

13. ABSTRACT

This document reports the results of an investigation of incipient failure detection in ball bearings by means of acoustic monitoring techniques. The change of acoustic emanation strength with bearing condition was studied to determine if changes within the frequency spectrum monitored would manifest the onset of a bearing failure. This investigation showed that the acoustic energy emitted from bearings is very sensitive to bearing condition and provides a clear indication of the onset of bearing failure.

FORM DD 1 NOV 65 1473
U3 4802 1030 REV 7/66
PART 1 OF 3

Unclassified
Security Classification

Unclassified
Security Classification

14. KEY WORDS	LINK A ROLE	LINK A WT	LINK B ROLE	LINK B WT	LINK C ROLE	LINK C WT
INCIPIENT FAILURE						
BEARING FAILURE						
FAILURE DETECTION						
ULTRASONIC MONITORING						
BEARING MAINTENANCE						
BEARING INSPECTION						

DD FORM 1 NOV 65 1473
U3 4802 1030 REV 7/66
PART 2 OF 3

Unclassified
Security Classification